University of Stavanger

Faculty of Science and Technology

MASTER'S THESIS

Study program/ Specialization: Industrial economics / Drilling	Spring semester, 2014 Restricted access
Writer: Jone Idsø	…… (Writer's signature)
Faculty supervisor: Helge Hodne External supervisor(s): Laurent Delabroy & Marton Haga, BP Norge	
Thesis title: Addressing zonal isolation challenges and improving 9 5/8'' production liner primary cement jobs across the Valhall field.	
Credits (ECTS): 30	
Key words: Valhall, rock mechanics, hydraulics, ECD, cementing, circumferential cement, SBT log, Valhall case histories, mud systems, displacement efficiency, liner rotation.	Pages: …… + enclosure: …… Stavanger, …….. Date/year

University of Stavanger

BP Norge

Master's thesis

Addressing zonal isolation challenges and improving 9 5/8" production liner primary cement jobs across the Valhall field.

Supervisor BP:
Laurent Delabroy

Supervisor UiS:
Helge Hodne

Author:
Jone Idsø

June 12, 2014

Abstract

Placing cement in the annulus between a casing string and the borehole is essential to obtain compliant zonal isolation. Circumferentially bonded cement provide a hydraulic seal which prevents crossflow between permeable zones, flow to surface and sustained casing pressure during the lifetime of a wellbore. The 9 5/8" production liner primary cement jobs across the depleted Valhall field are challenging. A very tight operating window between the collapse pressure and the fracture gradient is a limitation when designing the cement jobs. A trade-off between dynamic wellbore pressures and industry acknowledged cement guidelines such as high displacement rates, density hierarchy and rheology hierarchy is needed to stay within the pressure limits. Six case histories from the Valhall field are presented and evaluated to determine the most critical elements of a successful primary cement job. All wells have been acoustically logged to evaluate the annular cement bond quality.

Lost circulation events in the deeper parts of the hole section have proven to be the greatest challenge when cementing the 9 5/8" production liner. No common loss zone has been identified, but getting cement above the limestone stringer area in the Intra Late Eocene has proven difficult. ECD (equivalent circulating density) reducing measures such as low density pre-flushes, riser drainage, underreaming and low-rheology mud systems are discussed and quantified by the use of fundamental fluid mechanics. Underreaming the 12 1/4" section to 13" in combination with a carefully designed mud program have been identified as the main contributors to decrease the ECD.

Gelled-up mud, eccentric casing strings and low annular velocities during the cement displacement process increase the risk of cement channeling. Liner rotation has been documented as the most influential parameter in terms of obtaining sufficient intervals of circumferentially bonded cement. Simulations have shown that the ECD effect from liner rotation at low rotational speeds is negligible. An evaluation of three different mud systems and their respective effect upon displacement efficiency is presented.

A subjective evaluation of the main factors affecting the outcome of the 9 5/8" primary cement jobs has been performed. Based upon the evaluation a recommendation aiming to maximize the probability of successful future 9 5/8" liner primary cement jobs across Valhall is presented.

Acknowledgement

This thesis has been written in collaboration with BP Norge and represents the conclusion of my 5 year MSc at the University of Stavanger, Norway.

My supervisors at BP and the University of Stavanger have contributed greatly to the end product of this thesis. First and foremost, I would like to thank my supervisors at BP, Marton Haga and Laurent Delabroy, and the Valhall engineering team for the support and guidance they have provided me from the very start of this project. Furthermore, I would like to thank Arne Asko in MI Swaco, Maxmillian Olsen in Halliburton and Ingve Byberg in Baker Oil Tools for providing simulations and excellent support.

I would also like to thank Tron Golder Kristiansen for the help and feedback he has provided when finalizing this thesis.

Finally, I would like to thank Helge Hodne, my supervisor at the University of Stavanger, for his honest and academic opinions.

Contents

List of Figures

List of Tables

1 Introduction

Primary cementing is the process of pumping cement slurry down the casing/liner and into the annulus between the casing and the exposed formations. The main purpose of the cement is to isolate all zones with a flowing potential. In addition, the set cement supports the casing string and mitigates corrosion from formation fluids [1]. If the cement sheath fails there is a risk of sustained casing pressure (SCP) and unwanted cross flow between permeable formations which may affect the production potential of the well. SCP is defined as "a pressure in any well annulus that is measurable at the wellhead and rebuilds when bled down, not caused solely by temperature fluctuations or imposed by the operator" [2]. Several of the Valhall wells have experienced SCP in one or more annuli. Remedial work is generally extremely expensive and time consuming. Focus should always be to get the cement job right the first time.

Plug and abandonment (P&A) activities are planned to start late 2014 for all 30 wells on the Drilling Platform (DP) in the Valhall field. The operation is expected to last for up to 5 years due to uncertainty regarding casing collapses, SCP and zonal isolation. A successful and documented primary cement job will in many cases remove the need for time consuming and hazardous milling operations to place a permanent barrier which extends across the full cross section of the wellbore. If documented (i.e. logged) that the cement outside a casing string is well bonded to the casing and formation, NORSOK D-010 states that an overlapping cement plug can be set inside the casing string to form a permanent barrier without milling the casing. Sufficient cement quality in wells drilled today will make future P&A work more effective.

After the BP operated Macondo blowout in the Gulf of Mexico in April 2010 new and stricter global requirements in terms of zonal isolation were issued by the BP organization. The global BP zonal isolation regulation, from now on referred to as GP 10-60, defines which criteria a primary cement job needs to fulfill to be classified as satisfactory. If regional standards such as NORSOK provide stricter requirements they are adhered to. In the North Sea Valhall field acoustic logging of the annular casing cement has been initiated to verify sufficient quality of the cement jobs. Several of the logs for the 18 5/8", 13 5/8" and 9 5/8" casing strings have shown a general lack of circumferential cement, initiating very costly remedial work. Especially the 9 5/8" liner cement jobs have caused issues in recent years due to a highly complex geology.

Cementing the 9 5/8" production liner on Valhall is extremely challenging. Depletion and subsidence have affected the pressure regimes in the field and the operating window between the collapse pressure and the fracture pressure is very limited for optimal cement displacement. A thief zone has previously been identified within the Gas Cloud, but natural fractures/faults and heterogeneous formations make the fracture gradient modeling complex and often unpredictable. A lot of time and energy has been spent trying to reduce the equivalent circulating density (ECD) to improve the cementing process. Light weight pre-flushes, drainage of the riser, low rheology mud systems etc. have been applied to optimize cementing within the available mud window. The mud system used to drill the 12 1/4 section is of great focus. Displacing to a less viscous mud system prior to the cement job has been accomplished in some wells with a variable degree of success.

This thesis thoroughly describes the 9 5/8 production liner cement operation, both in terms of equipment, theoretical cementing models and theories behind the process. Recently drilled wells on the Valhall field which have been acoustically logged are analyzed to identify common denominators for successful primary cement jobs. Methods to decrease the ECD are discussed. The overall goal of this thesis was to provide an optimized cement practice which maximizes the probability of future success of 9 5/8 production liner cement jobs in order to achieve zonal isolation and safe, compliant operations.

2 The Valhall Field

The official Valhall discovery was made in 1975. Valhall is an over-pressurized upper Cretaceous chalk reservoir located in the southern part of the Norwegian sector of the North Sea in block 2/8 and 2/11 as shown in Fig. 2.1. Production was started in 1982 with a forecast of 20 years of production. Today the field is expected to produce until 2050. The field is operated by BP Norge AS (35.95 %) with Hess Norge AS (64.05 %) as partner.

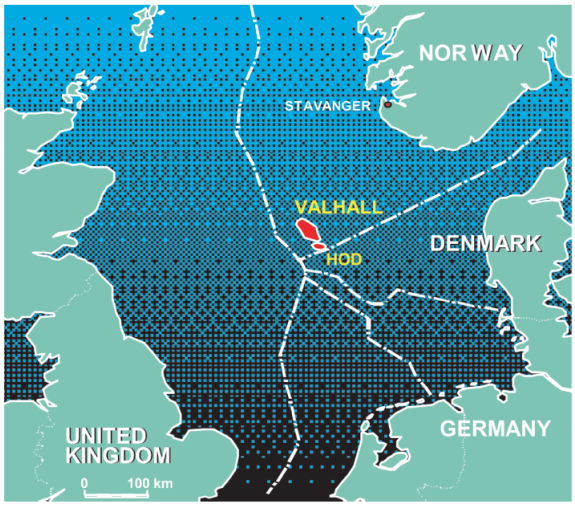

Figure 2.1: Valhall field location [3].

The Valhall complex consists of 6 separate platforms as shown in Fig. 2.2; Quarter Platform (QP), Drilling Platform (DP), Process and Compression Platform (PCP), Wellhead Platform (WP), Injection Platform (IP) and Production and Hotel Platform (PH). In addition there are two, identical, unmanned flank platforms, one at each of the North and South flanks located approximately 6 km away from the field centre. The North and South flank platforms have 16 available well slots each, and were installed in 2003 and 2004 respectively.

The initial Valhall development consisted off three platforms (QP, DP and PCP). In 1996 a fourth platform, the WP, was added to the complex to increase the number of producers. The WP supplemented the 30 already drilled DP slots with an additional 19 slots. The IP was installed in 2003 and consists of 24 well slots which are available both for water injection and production. The PH platform was installed in 2011 and is the latest addition to the field centre. In 2012 the PCP was shut down and the platform will be removed within the next years [4].

Figure 2.2: Valhall field location. The crestal part of the field consists of six platform [5].

Originally production was carried out by pressure depletion with compaction drive. As a result of decreasing reservoir pressure chalk compaction has caused 6-7m of seabed subsidence. Water injection was initiated in January 2004 for pressure support and to improve oil displacement. The rate of subsidence, illustrated in Fig. 2.3, had already decreased when water injection was initiated due to less pressure reduction in the crestal area of the Valhall reservoir.

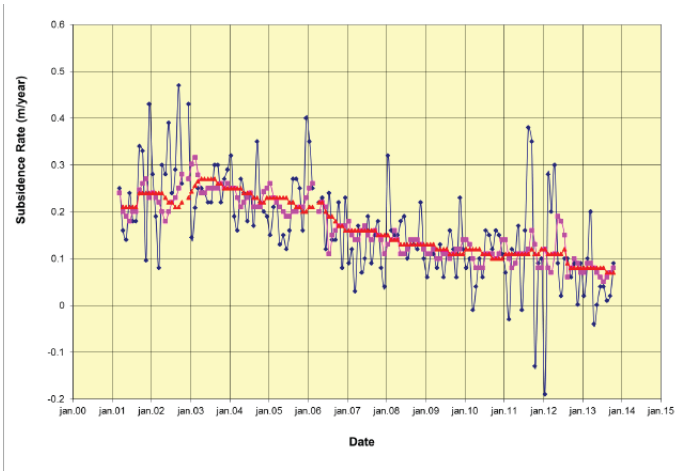

Figure 2.3: Subsidence rate (m/year) plotted against time (2001-2014) at the Valhall crest [6].

Initial estimates of the size of the chalk reservoir were approximately 250 MMBOE (million barrels oil equivalents). Today, 30 years after production start, more than twice the initial estimates have already been produced and the goal is to produce more than 1 000 MMBOE [3]. This corresponds to a recovery factor of more than 40%. The reserves have been adjusted due to better understanding of the Valhall reservoir, improved drilling and completion technology, installation of flank platforms, and reservoir compaction. There are always some uncertainties regarding the ultimate

recovery. Nevertheless, Valhall will continue to be an important asset in the BP portfolio for the foreseeable future [4], [6], [7].

2.1 Geology

The Valhall trap is an asymmetric anticline trending North West−South East. Although the reservoir structure extends over 240 km^2, the productive limits of the field are only about 30 km^2 with the most productive area in the crest of the structure. Black oil is produced from chalk reservoirs in the Tor and Hod formations. The Tor formation is finer grained and contains significant natural fractures which make the fluid mobility higher and more preferable than in the Hod formation. Roughly 2/3 of the oil in place and the majority of the production comes from the Tor formation [4].

2.1.1 Reservoir

The Valhall reservoir is extreme in many respects [6]:

- 50% porosity is not uncommon.
- The chalk has low matrix permeability, despite its high porosities.
- The chalk is characterized by its weakness due to the high porosity.
- Initial reservoir pressure was 6535 psi, whereas today 2000-5500 psi is often observed (although depending on faults, pressure barriers, drainage etc.)

The Tor and Hod reservoirs are part of the geological Shetland group of Cretaceous age. A typical reservoir section is shown in Fig. 2.4. Based on biostratigraphy Tor has been divided into four different zones, Tor-D, Tor-M1, Tor-M2 and Tor-M3+. A very low-porosity "Dense Zone" separates Tor and Hod. Hod itself consists of six members, of which Hod 4 has the best reservoir quality [6].

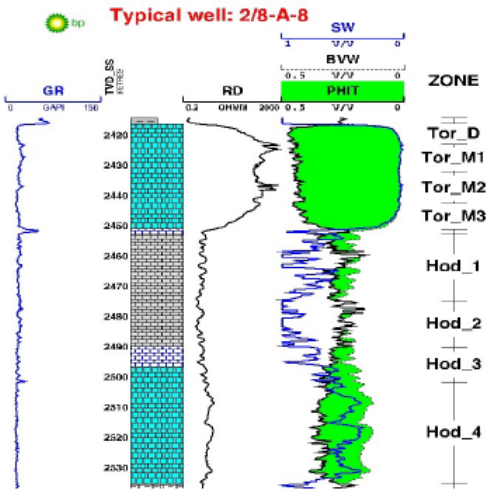

Figure 2.4: A typical reservoir section from well 2/8-A-8 drilled from the DP platform [4].

2.1.2 Overburden

The overburden is a collective term describing all the formations above the reservoir. As seen from Fig. 2.6 the lithology above the chalk reservoir is mainly claystone and mudstone. A total of eight DPZs (distinct permeable zones) are located in the overburden (see Section 2.2). Three main geological groups make up the overburden.

The Rogaland group consists of marl/mudstone from Paleocene to lower Eocene age and is located just above the reservoir. It can be subdivided into Balder, Sele, Lista and Vaale formation as shown in Fig. 2.5. Lista normally overlies the Tor reservoir as Vaale is usually not seen on the Valhall field. As a result of reservoir depletion significant drilling challenges may occur due to high pressure differentials between Tor and Lista, but today this is solved by drilling a liner into the Tor reservoir.

The Hordaland group is mainly composed of marine shales with thin limestone stringers of Eocene to Miocene age. The group can be subdivided into Horda and Lark formation. DPZ 7 and 8 are located in the upper Lark and upper Horda formation, respectively. Both zones are of major importance when cementing the 9 5/8" liner. A hydraulic seal (i.e. cement) must be present between the two zones to avoid cross flow.

The Nordland group extends to surface as seen in Fig. 2.6. Several permeable zones are present in the group. The section is not of particular interest when cementing the 9 5/8" production liner as most of the formations have already been sealed off by previous casing strings [8], [9].

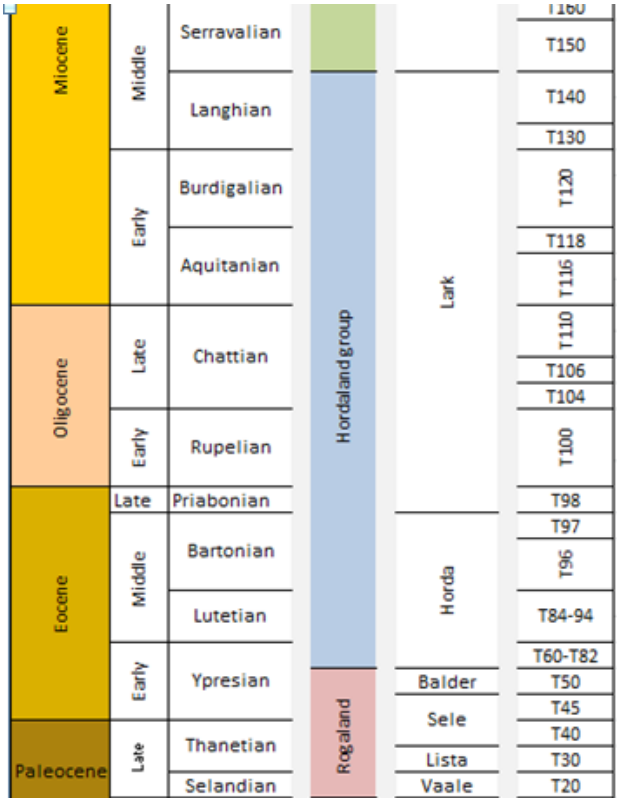

Figure 2.5: Valhall overburden description. Rogaland and Hordaland are of main interest during drilling and cementing of the 9 5/8" production liner [8].

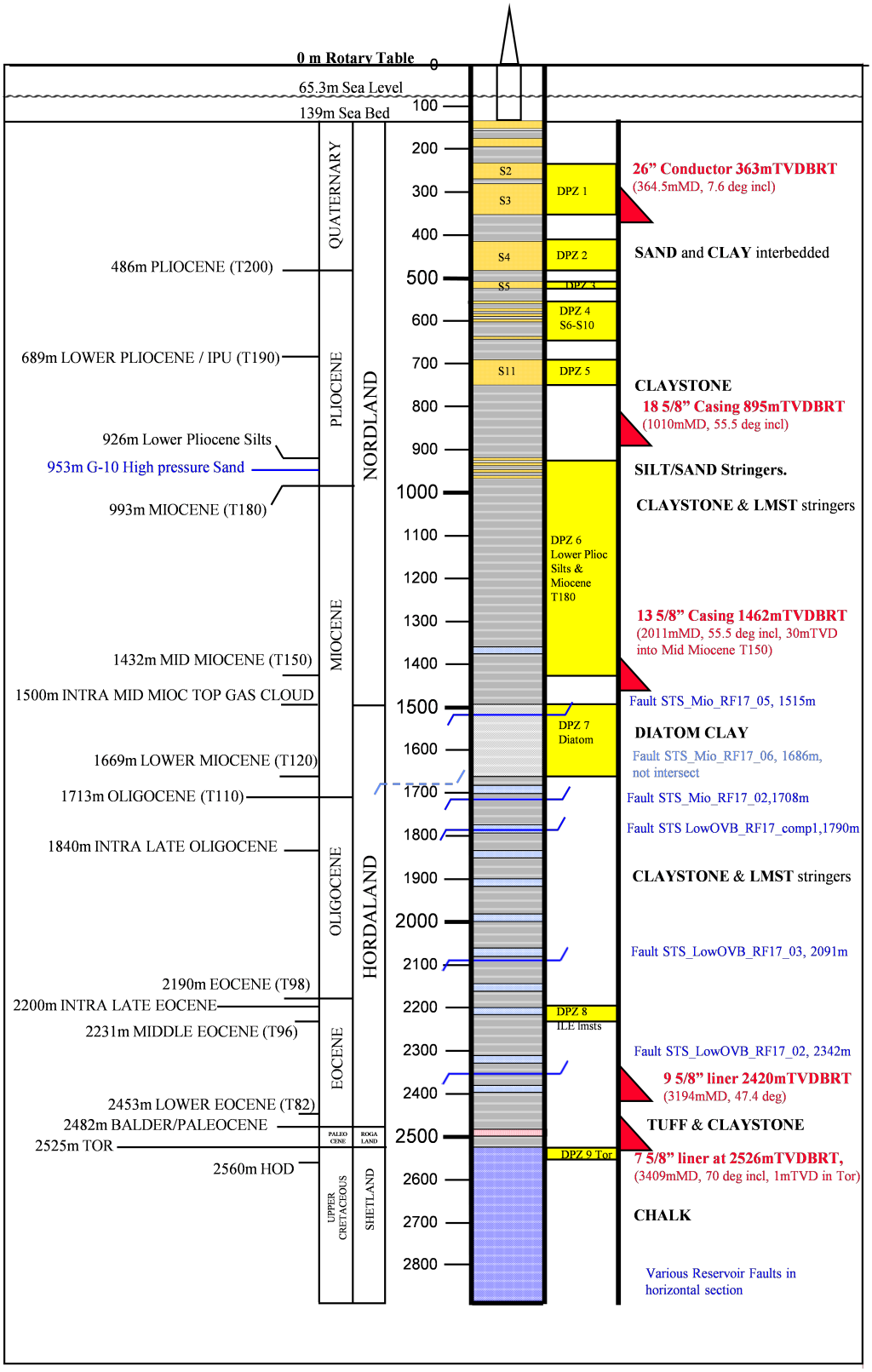

Figure 2.6: Complete stratigraphic description of well 2/8-G-1 Valhall IP (2013). Casing setting depths and lithologies are listed to the right, whereas formation tops and geological ages are given to the left [10].

2.2 Distinct permeable zones

As per BP definition a permeable zone is defined as a "zone with sufficient permeability such that a credible pressure differential would result in the movement of fluids (oil, water or gas) and/or development of SCP". Furthermore, a distinct permeable zone is a "group of permeable zones in which intrazonal isolation is not required for operation or abandonment of the well" [2]. At present there are 10 defined and established DPZs in the Valhall field, including the Tor and Hod reservoirs. The DPZs are the foundation of the zonal isolation requirements. Although all DPZs are an important part of the Valhall overburden, special focus is given to describing DPZ 6, 7 and 8 as these zones are critical for a successful cementation of the 9 5/8" production liner.

All depths given in the following DPZ description is meant as a guidance. Depths and thicknesses will vary across the field, and each well needs to be evaluated separately for precise estimates.

DPZ 1 consists of a package of thick, poorly consolidated sands with some thin associated shale stringers. Typical depths are in the region of 200-370 mTVDBRT (true vertical depth below rotary table). Porosity and permeability are estimated to 38% and 1900mD respectively. Resistivity anomalies since early field life indicate that hydrocarbons could be present at the very top of the zone.

DPZ 2 is a sand zone with thin interbedded shales of approximately 60-75 mTVD thickness. Typical depths are 420-480 mTVDBRT. Measurements from well 2/8-G-4 (2012) indicate a porosity of 34% and a permeability of 1200 mD. Potential gas pockets can be observed from field seismic.

DPZ 3 is a thin sand zone which typically comes in from 500-520 mTVDBRT. Measurements from well 2/8-G-4 indicated a porosity of 34% and a permeability of 295 mD. Gas was mapped out on seismic prior to field start-up.

DPZ 4 is a series of relatively thin sands. Fluid type and flow characteristics are not well understood, but the NMR (nuclear magnetic resonance) log from well 2/8-G-4 indicated a porosity of 28% and a permeability of 10 mD. Typical depths are in the region of 550-650 mTVDBRT, but net sand thickness is only approximately 5-10 mTVD. Marginal over-pressure, 40 psi, was logged in well 2/8-G-3 (2014).

DPZ 5 is a Pleistocene fine sand deposited in a shallow water environment. It is laterally continuous with a thickness of 20-40 mTVD throughout the Valhall (and Hod) structure. The zone is only marginally over-pressured (20-40 psi at the Valhall crest). Top of DPZ 5 is often found at approx. 700 mTVDBRT. Gas was mapped out on seismic prior to field start-up.

DPZ 6 is an interval of mainly shale interbedded with stringers of siltstone. The zone extends approximately 500 mTVD from 950-1450 mTVDBRT. DPZ 6 has been declassified on the South Flank. Porosity and permeability characteristics are not well understood. Porosities in the region of 10% are expected, but not documented. At the start of the Valhall production drilling DPZ 6 was slightly over-pressured. As a consequence of drilling and production induced leak paths, natural fractures and faults the pore pressure has increased over time. Kicks have been taken during

drilling from Valhall IP. Most of the IP wells provide a direct flow path between DPZ 7 and DPZ 6, allowing the pressure to build up (see Section 2.3). The low mobility formation dissipates pressure very slowly within the DPZ. Discussions have been ongoing internally whether the zone should be further split into several DPZs as there is no uniform pressure communication throughout the zone. DPZ 6 will be used as a general term consequently throughout this thesis without any further subdivisions.

DPZ 7 is the most discussed and referred to of all the DPZs from a zonal isolation point of view. However, there is a general lack of understanding regarding its properties and geological characteristics. The zone is often referred to as the Gas Cloud. It is a high porosity and low permeability diatomite of middle Miocene age located in the interval from 1500-1650 mTVD. Porosities of 50-60% are documented, while the maximum permeability is thought to be in the region of 0.1 mD. Its lateral extent and volume are of significant value, and the zone is thought to be heavily faulted across the entire field. Although of high uncertainty, it has been suggested that the Gas Cloud contains a 40m gas column followed by an unknown oil column. The oil (equivalents) in place is estimated to be in the region of 500-700 million barrels. With the technology of today the reserves are considered non-commercial. Analysis of the PPFG (pore pressure & fracture gradient) suggests that an influx from DPZ 7 would fracture DPZ 6, possibly describing how a mostly impermeable zone (DPZ 6) can act as a reservoir (given that the cap rock above DPZ 6 has a higher fracture gradient than the zone itself).

DPZ 8 is a thin and fractured limestone system with interbedded layers of shale. Very limited information regarding pressure and fluid characterisation is available. Seismic can map the zone at the crest and North flank, but the response weakens towards the South flank. The zone typically comes in at approx. 2200 mTVD and extends for 20-30 mTVD. It has caused internal discussions as it is very poorly logged and documented. Some people would argue that the zone is an impermeable, fractured shale system with no flowing potential, but both losses and kicks have been observed within the zone. In terms of 9 5/8" liner cementing, problems have been experienced getting cement above DPZ 8 in some wells due to thief zones below or within the zone.

DPZ 9 and **DPZ 10** are the Tor and Hod reservoirs respectively.

2.3 Casing design

The main function of the casing strings is to seal off above formations to provide a pressure barrier. Hence, the pressure operating window will dictate the boundaries in terms of casing setting depths as shown in Fig. 2.7. After having set and cemented a casing string the MW (mud weight) can be changed (raised) without affecting the already drilled formations. According to NPD (Norwegian Petroleum Directorate) approximately 175 development wells have been drilled on Valhall. Several casing designs have been used and replaced as experience, technology and knowledge have developed throughout the lifetime of the field.

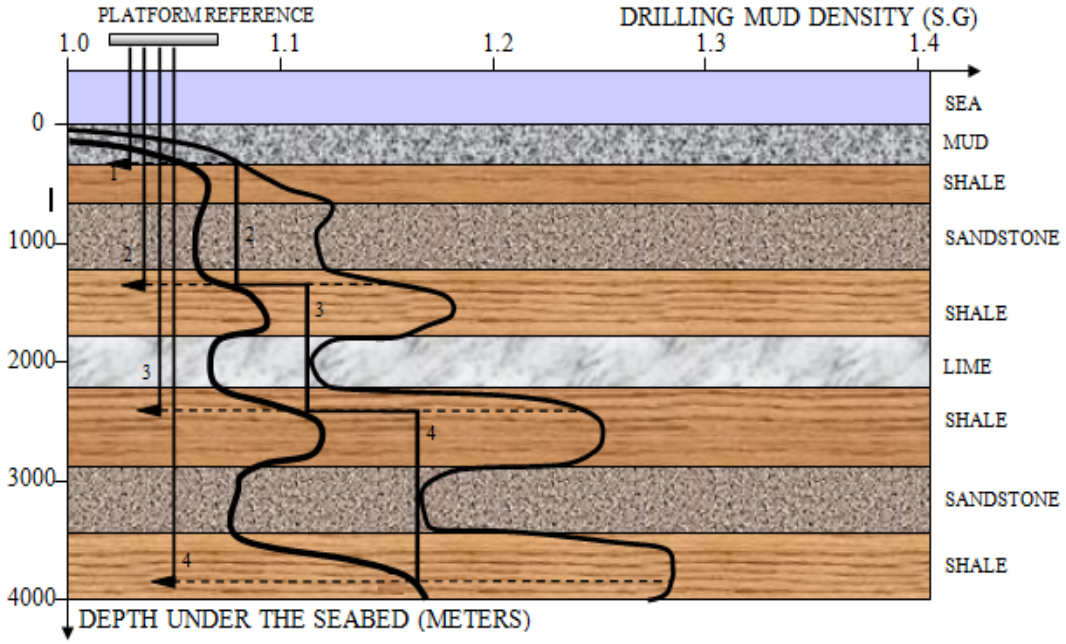

Figure 2.7: Generic figure for picking casing points. Depth below seabed is plotted against pore pressure (left curve), mud weight (middle curve) and fracture gradient (right curve). Casing setting depths are indicated by black triangles (casing shoe) [11].

Mainly two different casing designs have been applied on Valhall IP and the two flank platforms. Drilling on the flanks commenced in 2003, while drilling was initiated on Valhall IP in 2004. The depths listed in Table 2.1 and Table 2.2 are meant as an informative guidance as they vary from well to well. In addition, the reservoir is located deeper on the flanks due to the nature of the anticlinal trap.

The main difference between the original and the current Valhall casing design is the setting depths of the 13 5/8" casing and 9 5/8" liner. The majority of the 17 1/2" sections on Valhall IP have been drilled through DPZ 7 and to TD (total depth) at 2100-2200 mTVD. Due to new requirements, GP 10-60, the 13 5/8" casing setting depth has been moved above DPZ 7. GP 10-60 states that a minimum of 30 mTVD circumferentially bonded cement shall be documented above and below each DPZ. The original Valhall IP design leaves both DPZ 6 and 7 exposed after drilling the 17 1/2" hole section. Acoustic logs have proven it to be extremely difficult to get any cement above DPZ 7 due to weak formations (losses). This effectively leaves the

interval between DPZ 6 and DPZ 7 free of cement. Hence, the 13 5/8" setting depth has been changed to above DPZ 7 as seen in Fig. 2.6.

Originally the 9 5/8" liner was drilled into the reservoir as shown in Table 2.1. This was accomplished by drilling a 12 1/4" hole to just above the reservoir, pulling the drill string and running a 9 5/8" liner with a casing shoe similar to a drill bit. The remaining distance is then drilled by the casing shoe. As a result of the decision to move the 13 5/8" casing point above DPZ 7, the remaining casing design also had to be modified. Today the 12 1/4" hole section is drilled to just above the Tor reservoir (20-50 mTVD) and the 9 5/8" liner is run and cemented traditionally (i.e. not drilled into the reservoir). Finally, a 7 5/8" drilling liner is drilled into the Tor reservoir prior to drilling the 6 1/2" horizontal reservoir section. A drilling liner is necessary due to the high pressure differential between the cap rock and the depleted reservoir.

The original Valhall Flank North and South design differs to some extent from Valhall IP. The 18 5/8" casing was dropped, and replaced by extending the 13 3/8" and 9 5/8" casing strings. In addition the 12 1/4" section could (can) be drilled into the less depleted parts of the reservoir. Three wells were drilled on the North Flank in the period 2012-2013. The first two wells followed the original Valhall IP design shown in Table 2.1, while the most recent well was drilled according to Table 2.2 to fulfil the requirements of GP 10-60.

The current 9 5/8 cement job has two main objectives [12]:

1. Act as a primary and secondary barrier against a re-pressurized reservoir for eternity.

2. Isolate between DPZ 7 and DPZ 8, and DPZ 8 and DPZ 9.

Whether or not the current casing design is optimized in terms of zonal isolation is difficult to address. Even though the casing design has been changed to adhere to GP 10-60 several primary cementing challenges need to be solved. It has proven extremely difficult to cement the 9 5/8 production liner as per requirements. The 12 1/4" section is typically a relatively long, deviated section which needs to be cemented in a very narrow operating window.

Table 2.1: Original casing design Valhall IP [6].

Hole size	Start [mTVD]	TD [mTVD]	Casing
32"	139	370	26" conductor
21-24"	370	900	18 5/" casing
17 1/2"	900	2100-2200	13 3/8"-13 5/8" casing
12 1/4"	2100-2200	2510	9 5/8" drilling liner
8 1/2"	2510	2550	5 1/2" reservoir liner

Table 2.2: Current casing design Valhall IP [6].

Hole size	Start [mTVD]	TD [mTVD]	Casing
32”	139	370	26” conductor
23 1/2”	370	900	18 5/8” casing
17 1/2”	900	1450	13 5/8” casing
12 1/4”	1450	2450-2500	9 5/8” liner
8 1/2”	2450-2500	2520	7 5/8” drilling liner
6 1/2”	2520	2550	4 1/2” reservoir liner

3 Rock mechanics

During the lifetime of Valhall hundreds of millions of barrels of oil have been produced, significant subsidence has been experienced, water has been injected, and drilling has been ongoing for more than 30 years. All of which have to some extent affected the pressure regimes and stresses in the field, not only in the reservoir, but also in the overburden. Modelling and simulation of the geomechanics are extremely complex. It is not the purpose of this chapter to go into details regarding the rock mechanics, but rather to introduce some basic theories and concepts which are important to understand the challenges associated with cementing the 9 5/8" production liner.

3.1 Definitions

Stress is defined as force divided by area as given in Eq. (3.1) and can be decomposed as normal stress, σ, and shear stress, τ. Within the field of rock mechanics compressive stresses are defined as positive.

$$\sigma = \frac{F}{A} \tag{3.1}$$

$$\sigma = \begin{bmatrix} \sigma_x & \tau_{xy} & \tau_{xz} \\ \tau_{xy} & \sigma_y & \tau_{yz} \\ \tau_{xz} & \tau_{yz} & \sigma_z \end{bmatrix} \tag{3.2}$$

If an object is oriented relative to a reference system within a given stress state the individual stress components will change. The reference system may be oriented such that all shear stress components equal zero. In this situation the three existing normal stresses are referred to as the principal stresses. The mathematical definition of principal stresses is given in Eq. (3.3).

$$\sigma = \begin{bmatrix} \sigma_1 & 0 & 0 \\ 0 & \sigma_2 & 0 \\ 0 & 0 & \sigma_3 \end{bmatrix} \tag{3.3}$$

As per definition $\sigma_1 > \sigma_2 > \sigma_3$ independent of stress direction.

Three principal in-situ stresses exist in the formation, minimum horizontal in-situ stress, σ_h, maximum horizontal in-situ stress, σ_H, and the vertical in-situ stress, σ_v, often referred to as the overburden in-situ stress. The overburden stress is mainly a result of the weight of the overlying rocks, but other geological features could also influence the overburden stress. As a result of the compressive overburden stress a horizontal stress state is created as shown in Fig. 3.1. The magnitude of the horizontal stresses are dependent on rock properties such as the Poisson ratio (a measure of a material's lateral to axial strain in response to an axial load). The greater the Poisson ratio of a rock the greater the ability to expand laterally, and hence the greater the horizontal stress required to prevent lateral movement. As a result sandstones and carbonates tend to have a lower fracture gradient than shales and salts, since they have a lower Poisson ratio. Several methods to measure the in-situ stresses exist. The most accurate method is analysis of extended leak-off tests (XLOT) [13], [14].

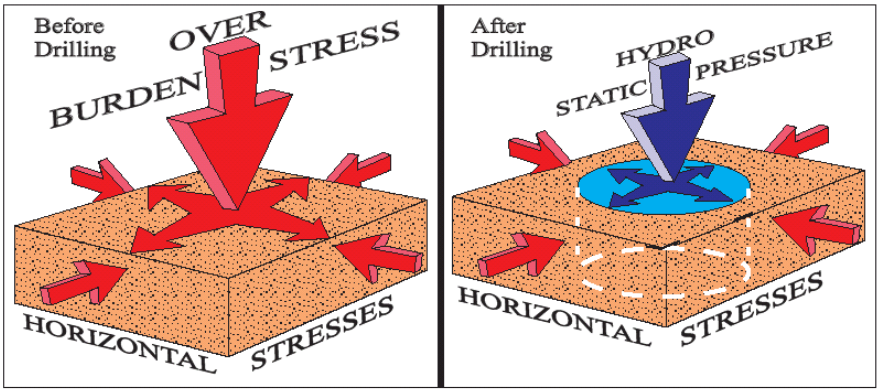

Figure 3.1: The left figure illustrates the stress state in a rock segment before drilling, while the right figure shows the stresses after a wellbore has been drilled and a drilling fluid introduced to the system [15].

Drilling a hole and applying a pressure from a drilling fluid will create stresses around the wellbore. Stresses around a wellbore are described in terms or radial stress, tangential stress (hoop stress) and axial stress, represented by σ_r, σ_θ and σ_z in cylindral coordinates respectively. Fig. 3.2 illustrates the stress state. The stresses describe the near wellbore stress state of the rock. Formation stability management is about balancing these stresses to prevent the formation from fracturing or collapsing.

Within a rock some of the load is carried by the pore pressure. The effective principal stress, $\sigma^{'}$, is defined as the difference between principal total stress and pore pressure, P_o, as shown in Eq. (3.4). All rock failure models apply the concept of effective stresses [3], [13].

$$\sigma^{'} = \sigma - P_o \tag{3.4}$$

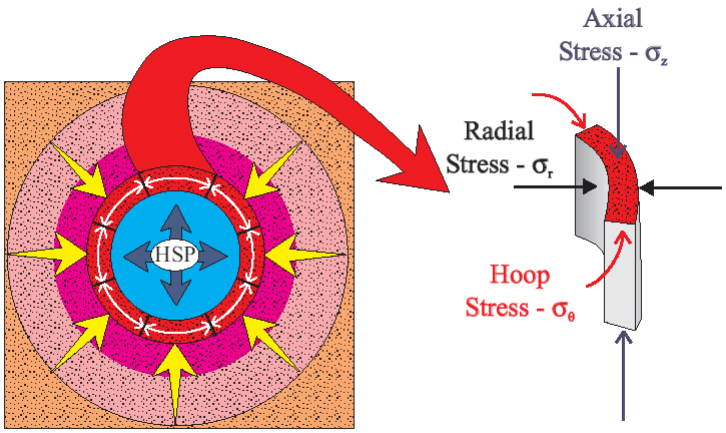

Figure 3.2: Stresses around a wellbore. HSP represents the hydrostatic pressure of the drilling fluid. Decreasing the HSP will increase the hoop stress, while increasing the HSP will decrease the hoop stress [15].

3.2 Pore pressure

Formation pore pressure is the pressure of the natural occuring fluid(s) within the pores of a rock [15]. As per definition, normally pressurized formations follow the pressure gradient (density) of water and over-pressurized formations have a pressure gradient greater than water. At Valhall the formations are normally pressurized down to approximately 500 mTVD and over-pressurized for the remaining formations down to and including the reservoir. Measuring the pore pressure in permeable formations is relatively straight forward, but direct measurements in impermeable shale sections are not easily done, and is in most cases estimated. The pore pressure defines the absolute minimum allowable mud weight for normal drilling in order to avoid kicks.

3.3 Formation fracturing

Formation fracturing is a tensile failure occurring at too high hydrostatic or circulating pressure of the drilling fluid. A qualitative illustration of the gradual lost circulation sequence is shown in Fig. 3.3. If the wellbore pressure is continuously increased the hoop stress will decrease and the rock stress will eventually change from compression to tension. When the hoop stress becomes lower than the tensile strength of the rock a tensile fracture will occur. Through the initiated formation fracture losses of drilling fluids to the surrounding formation will commence. If faults or natural fractures exist within the formation it is normal to assume that the rock has a tensile strength equal to zero. This will decrease the fracturing pressure. Another important phenomenon is that the fracture will form and propagate along the direction of the largest in-situ stress.

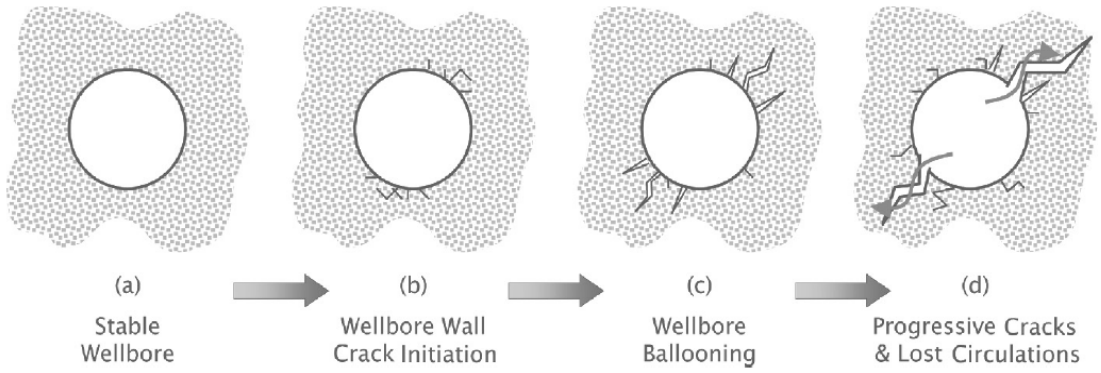

Figure 3.3: Typical fracture and lost circulation sequence. As the wellbore pressure is gradually increased from a) to d) a fracture is initiated and eventually propagated, effectively leading to lost circulation [13].

The initial fracturing pressure has been observed to be dependent on wellbore inclination as illustrated in Fig. 3.4. Generally, the initial fracturing pressure close to the wellbore wall will decrease with inclination. The required pressure to propagate a fracture away from the wellbore is independent of inclination and needs to be larger than the minimum in-situ horizontal stress [13], [16], [17].

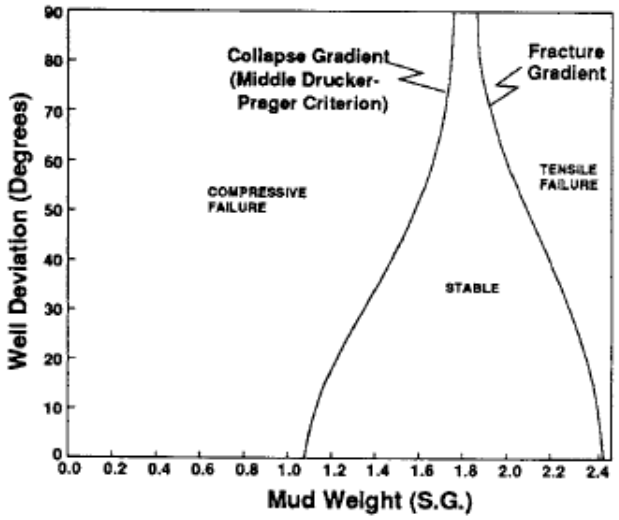

Figure 3.4: For a given failure criteria the collapse and fracture gradient is plotted against wellbore inclination. Although dependent on criteria, McLean et al. (1990) showed that the tested criteria decreased the mud window when inclination was increased [17].

The fracture gradient trend seen in Fig. 3.4 can be shown using the Kirsch equations. A simplified fracture pressure, assuming that the wellbore is aligned with the maximum horizontal in-situ stress, can be written as [13],

$$P_{wf} = 3\sigma_y - \sigma_x - P_o. \tag{3.5}$$

A case where all shear stresses equal zero is defined as a symmetric case. By observation of the entire set of transformation equations [13, p. 161] it is seen that the shear stresses equal zero when the wellbore is aligned with either one of the horizontal stresses. The cartesian stress components in Eq. (3.5) can be expressed by the in-situ stresses and the wellbore inclination, γ.

$$\sigma_x = \sigma_H cos^2\gamma + \sigma_v sin^2\gamma \tag{3.6}$$

$$\sigma_y = \sigma_h \tag{3.7}$$

The fracture pressure can now be written as,

$$P_{wf} = 3\sigma_h - (\sigma_h cos^2\gamma + \sigma_v sin^2\gamma) - P_o. \tag{3.8}$$

The in-situ stresses and pore pressure for well 2/8-G-3 at approximately 2000mTVD are given as $\sigma_v = 16.82$, $\sigma_H = 16.21$, $\sigma_h = 15.44$ and $P_o = 13.67ppg$. A correlation between the fracture initiation gradient and wellbore inclination can now be obtained. The correlation is shown in Fig. 3.5.

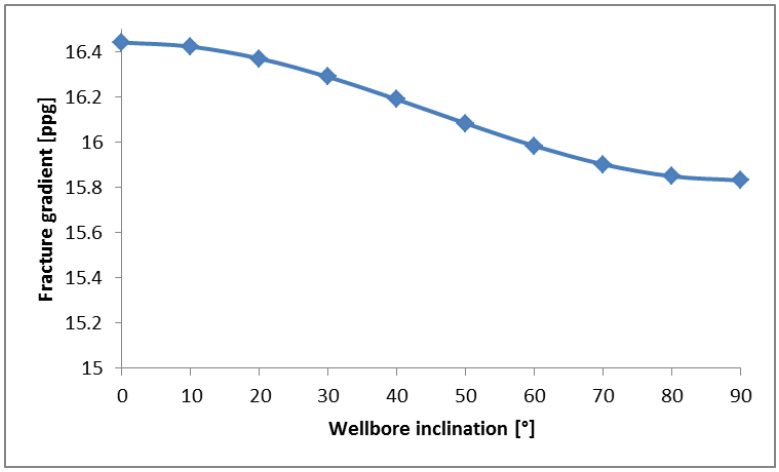

Figure 3.5: Correlation between fracture initiation gradient and wellbore inclination derived from simplified Kirsch equations.

Equation 3.8 is not of sufficient accuracy to develop a fracture gradient, but it may be helpful as an indication. In addition, it proves that by carefully planning the well trajectory it is possible to optimize critical parts of the mud window. The fracture gradient used today for the Valhall field have been measured from LOTs, XLOTs and lost circulation events for over more than three decades.

3.4 Formation integrity test / Leak-off test

Pressure testing of the formation is a very important measure to establish the formation fracture gradient and the in-situ stresses. In addition, a FIT (formation integrity test) or LOT (leak-off test) is necessary to assure that the planned mud weight can be used drilling the next section without fracturing the formation and introducing well integrity risks. FITs and LOTs are very similar, and the only difference is in terms of how much pressure is applied. When multiple fracture cycles (including fracture propagation) are performed the test is referred to as an XLOT (extended LOT). The different formation pressure testing methods are shown in Fig. 3.6. During a FIT the strength of the formation is never exceeded, while during a LOT the applied pressure initiate a small fracture into which a small volume of drilling fluid is lost. The operational sequence is quite straight forward. A FIT or LOT is performed after a casing string is set. Usually the cement and 3-5m of new formation is drilled out and the well shut in (i.e. closing the annular or pipe ram). Low flow rates of mud are pumped down the drill string (often using the cement pump unit for enhanced accuracy) while reading the surface standpipe pressure. As the well is shut in, mud is pumped into a closed volume, effectively increasing the bottom hole pressure. When the pressure reaches the strength of the formation a fracture will occur. The LOT data provide the upper mud weight allowable for drilling the next section.

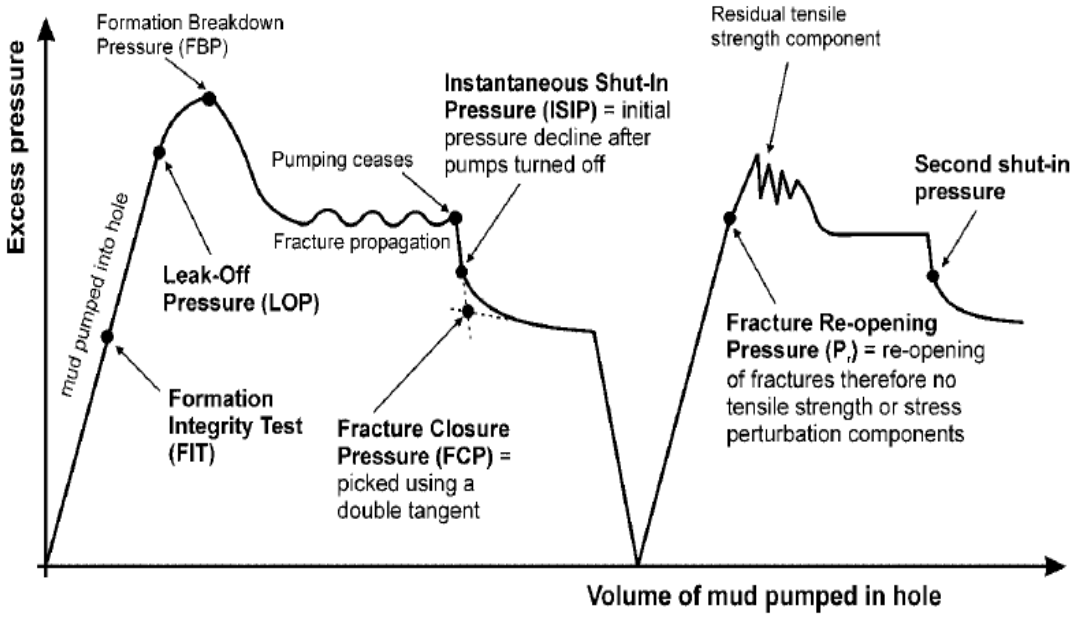

Figure 3.6: Idealized XLOT of two fracturing cycles. Surface pressure is plotted against time or volume mud pumped. During a FIT the applied surface pressure never exceeds the linear part of the curve. Hence, using only FIT data will underestimate the true fracture gradient. When the slope of the curve breaks from linear mud starts leaking to the formation. This is defined as the leak-off pressure. Increasing the pressure further will eventually break down the formation. The fracture will propagate at a pressure lower than the breakdown pressure, and the fracture will close when the pressure decreases below the fracture closure pressure [18].

Several important concepts related the cement job can be explained through the XLOT cycle. Firstly, once the formation has been broken down the fracture will propagate at a lower pressure than the breakdown pressure. Secondly, to close the fracture the pressure must be decreased below the fracture closure pressure which is equal to the minimum horizontal stress. Finally, the rock strength is weakened after the first fracture as the rock loses its tensile strength. This is clearly illustrated in Fig. 3.6 where the fracture reopening pressure is lower than the LOT. Hence, inducing a fracture during drilling of the 12 1/4" section may reduce the strength of the formation in front of running and cementing the 9 5/8" liner. StressCage is one method applied by BP to artifically increase the fracture resistance (hoop stress) in permeable formations above the minimum horizontal stress by introducing sized particles to the mud system [15]. The concept of StressCaging is illustrated in Fig. 3.7. Furthermore, Okland et al. [19] state that if given enough time a fracture may naturally heal. WBM (water-based mud) is thought to have better healing capabilities than OBM (oil-based mud) [19].

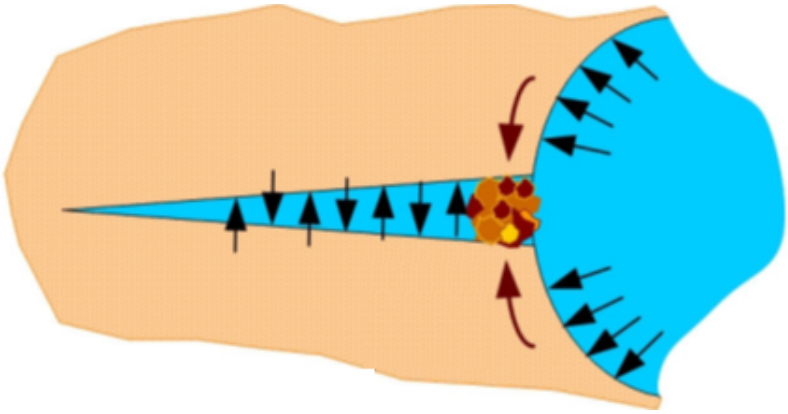

Figure 3.7: The StressCage model describes how fracture resistance can be increased by introducing sized particles to the drilling fluid system. The particles form a bridge at the mouth of the fracture, effectively choking the flow of mud into the fracture. As the fluid pressure drops, a high compressive stress is transfered to the bridge making it more resistant to re-opening of the already induced fracture [15].

3.5 Formation collapse

Formation collapse is a shear failure occurring at too low drilling fluid pressures. When the wellbore pressure is decreased the radial stress decreases correspondingly, effectively increasing the hoop stress. A large shear stress develops due to the significant difference between the hoop stress and the radial stress. At a critical limit the borehole will collapse [13]. The collapse pressure can be both higher and lower than the pore pressure, but at the Valhall field it is generally higher. In a normally faulted stress regime, one where the vertical in-situ stress is the largest, the collapse resistance will decrease with inclination as illustrated in Fig. 3.4. As the wellbore turns from vertical to horizontal the full effect of the vertical in-situ stress is felt, resulting in a less stable wellbore [15]. Field experience has also shown that wellbore collapse is a function of time. The longer an open hole is left exposed the higher is the risk of cavings, pack-offs and losing the well in general. Some of the time aspect can probably be explained by the loss of weight material in the drilling fluid, barite sag, but when a hole section has been drilled it is considered good practice to run the casing as soon as the drill string is out of the hole. Documented mechanisms of the time aspect are pressure diffusion, temperate changes and chemical changes which leads to stress changes [20].

Aadnøy and Looyeh [13] showed that the collapse pressure, P_{wc}, for a symmetric case where $\sigma_x > \sigma_y$ could be written as,

$$P_{wc} = \frac{1}{2}(3\sigma_y - \sigma_x)(1 - sin\phi) - \tau_o cos\phi + P_o sin\phi. \tag{3.9}$$

The internal angle of friction, ϕ, and the cohesive rock strength, τ_o, are rock dependent strength parameters which can be established in the lab from the Mohr-Coulomb failure model [13].

3.6 Valhall subsidence and compaction

The seabed has subsided approximately 6.5m during the lifetime of Valhall due to reservoir compaction. However, the top of the reservoir has been compacted more than 10m, indicating that there is extension in the overburden which affects the field stress state. A simulated shear stress development across the Valhall field just above the Balder formation due to reservoir compaction is given in Fig. 3.8. Seismic data have shown that the stresses in the lower part of the Rogaland Group are mostly influenced. Fractures and faults are often seen in the formations just above the reservoir [9]. Thus, picking the setting depth of the 9 5/8 production liner could be the difference between a success and failure in terms of cementing. If the liner is set too deep in an extensively fractured and faulted formation significant wellbore challenges affecting the liner cement job may occur.

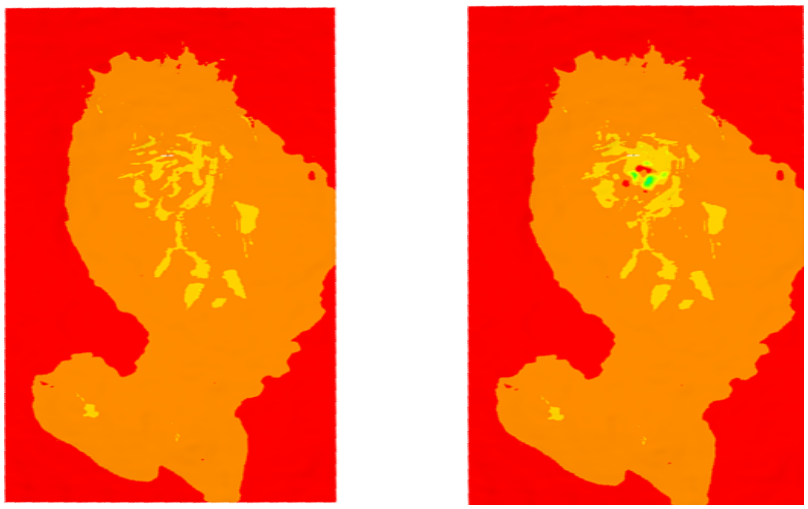

(a) 1982 **(b)** 1986

(c) 1997 **(d)** 2007

Figure 3.8: Shear stresses just above the Balder formation at the Valhall field from start of production in 1982 to 2007. Areas of high shear stresses are labelled red. Reservoir compaction has resulted in a complex stress state which complicates drilling and cementing operations on the field. The simulations have been made applying a finite element model of 3 million elements [20].

Compaction is also beneficial as it maintains reservoir pressure. When the pore pressure decreases more of the overburden stress needs to be taken up by the rock matrix according to Eq. (3.4). At some point the rock matrix is too weak to support the overburden and is compacted. This will reduce the porosity of the rock and the gross thickness of the reservoir. Due to depletion the pore pressure in the Valhall field has decreased by approximately 3-4000 psi. Aadnøy and Looyeh [13] stated that the subsequent decrease of fracture pressure was a function of the Poisson ratio.

3.7 Valhall operating window

The operating or mud window is the difference between the fracture pressure and the maximum of the pore pressure and collapse pressure. On Valhall this will be the collapse pressure. A typical Valhall overburden pressure plot is shown in Fig. 3.9. From 1400 mTVD the window decreases quite significantly due to increasing pore and collapse pressure in the Gas Cloud (DPZ 7). The 12 1/4" section is often drilled from approximately 1450-2450 mTVD. This leaves an operating window from 14.6-15.5 ppg available for the 9 5/8" liner cement job which is extremely narrow for ideal cement displacement conditions. All guidelines of a succesful cement job cannot be met on Valhall today, and a trade-off is necessary to stay within the mud window.

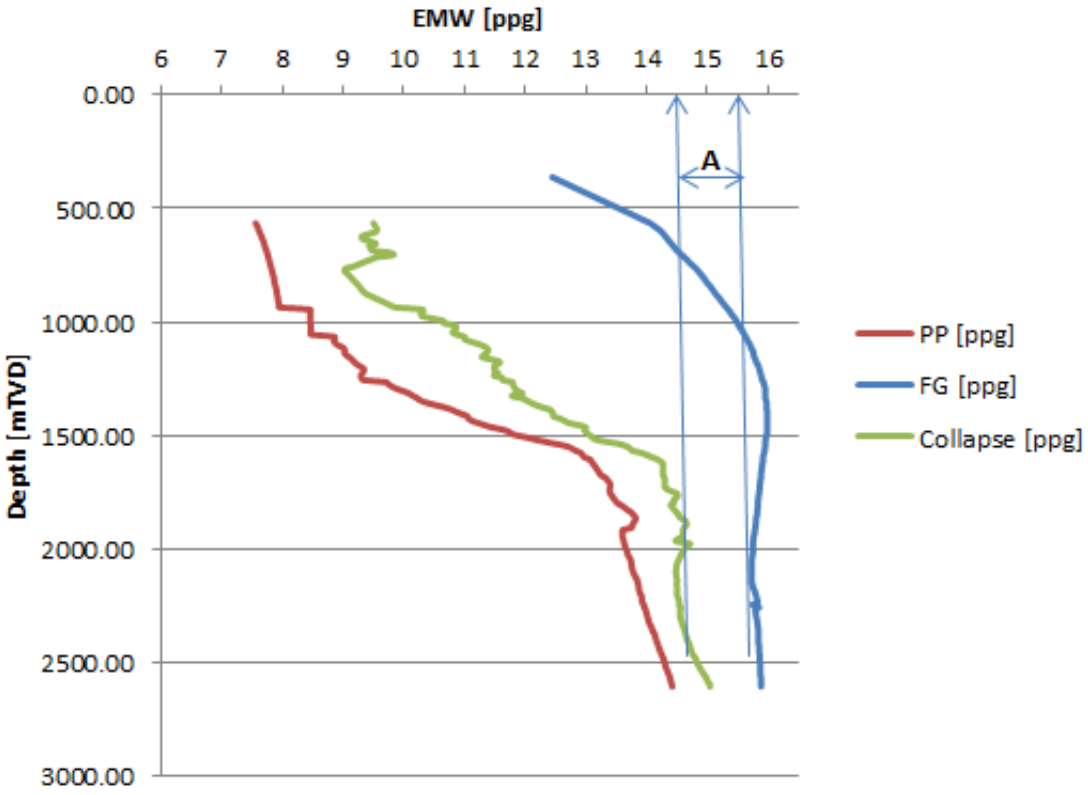

Figure 3.9: Pore pressure (PP), fracture pressure (FG) and collapse pressure expressed by equivalent mud weight (EMW) for well 2/8-G-1 (2013). The operating window available when cementing the 9 5/8" production liner is indicated by the range A.

4 Hydraulics

Understanding fluid properties and how different flow parameters affect the wellbore is crucial when designing a cement job. The 9 5/8" liner on Valhall is cemented in a very narrow operating window which restricts flow rates, densities and viscosities. Flow regimes, displacement efficiencies, hole cleaning, annular velocities and so-fort are all a part of fluid mechanics. Non-centralized casing strings and varying annular geometry complicate the cementing simulations. All of which will be discussed in the following, with a special focus on how to understand and analyze annular frictional pressure drop during a cement job.

4.1 Definitions

The viscosity, μ, of a fluid is defined as its resistance to shear or angular deformations. An important property is that the viscosity of most liquids decreases with increasing temperature. The opposite is true for gases [21]. Mathematically the viscosity can be expressed by the shear stress, τ, and shear rate, $\dot{\gamma}$, as given by Eq. (4.1).

$$\mu = \frac{\tau}{\dot{\gamma}} = \frac{\tau}{du/dy} \tag{4.1}$$

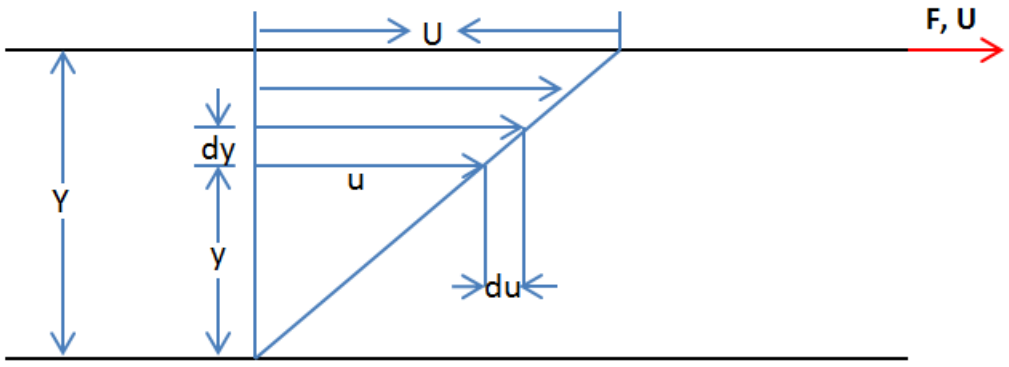

Figure 4.1: Viscosity defined using two plates of which the lower plate is held stationary. A force, F, is applied to the upper plate, effectively moving it at a velocity U. The moving plate will drag the fluid located between the plates and create a velocity profile. The viscosity is directly related to the slope of the velocity profile and the force per area (shear stress).

When describing flow in cylindrical geometries the term hydraulical diameter, D_H, is often introduced. It is a quantity which measures the ratio between the fluid flowing area, A_L, and the total fluid wetted circumference, S_L, as shown in Eq. (4.2). The idea behind the hydraulic diameter is to transform a flow conduit to an equivalent circular pipe. Directly from Eq. (4.2) it can be shown that for pipe flow the hydraulic diameter is simply the diameter of the pipe. Similarly, for flow in annuli between two circular pipes the hydraulic diameter is defined as the diameter of the larger pipe minus the diameter of the smaller pipe [22].

The average fluid volumetric velocity, U, is given by the flow rate, Q, divided by the cross sectional area, A, as shown in Eq. (4.3).

$$D_H = \frac{4A_L}{S_L} \tag{4.2}$$

$$U = \frac{Q}{A} \tag{4.3}$$

4.2 Rheological models

All derivations in Chapter 4 have been based upon two standard assumptions when describing fluid mechanics.

1. Incompressible flow (i.e. the fluid density is independent of pressure).
2. Steady-state flow (i.e. all flow conditions are independent of time).

Different rheological models describe how fluid shear stress changes with shear rate. The slope of the curve is per definition equal to the fluid viscosity. ECD simulations prior to drilling and cementing operations specify the rheological model thas has been applied as the choice of model will affect the outcome of the simulation algorithm. Drilling fluids and cement slurries are mainly assumed to follow the characteristics of a Bingham plastic, Power-law or Herschel-Bulkley fluid.

Fluid shear rate and shear stress are determined using a Fann viscometer which consists of a rotating outer cylinder and a stationary inner cylinder. A standard Fann viscometer is presented in Fig. 4.2. When rotating the outer cylinder in presence of a liquid between the cylinders a force will act on the inner cylinder due to the fluid viscosity. The force is proportional to the cylinder surfaces, the distance between them and the angular velocity of the outer cylinder. Measurements of the shear stress is made in terms of degrees, θ, which is converted to the desired system of units. The shear stress is measured at different angular velocities which are converted to shear rates. Measurements are typically taken for 3, 6, 100, 200, 300 and 600 rpm [23].

It is common to separate Newtonian from non-Newtonian fluids. Both drilling fluids and cement slurries are considered non-Newtonian. The non-Newtonian fluids can be further split into plastic, pseudoplastic and dilatant fluids. Plastic and pseudoplastic fluids are shear thinning (i.e. the viscosity decreases with increasing shear rates). In addition, the plastic fluids have a yield point. Dilatant fluids are shear thickening, but they are not of particular interest from a drilling and cementing perspective [23]. All fluids discussed in this thesis will be within the plastic and pseudoplastic groups.

Figure 4.2: Fann viscometer is the most common apparatus used to measure rheological properties. Rheological properties are measured both onshore and offshore to assure that the mud/cement is within specifications [24].

4.2.1 Newtonian fluids

Newtonian fluids are characterized by a linear relationship between shear stress and shear rate that goes through the origin as shown in Eq. (4.4). The viscosity is independent of the shear rate as shown in Fig. 4.3. Unless stated otherwise, Newtonian properties have been assumed in Section 4.3-4.4 as several of the simplified derivations also hold for non-Newtonian fluids.

$$\tau = \mu\dot{\gamma} \tag{4.4}$$

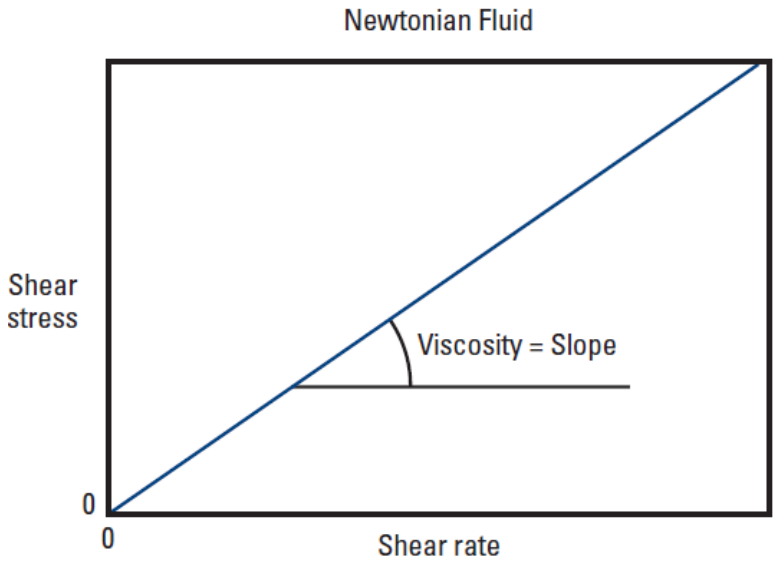

Figure 4.3: Relationship between shear stress and shear rate of a Newtonian fluid. The slope of the line is constant and equal to the fluid viscosity [25].

4.2.2 Bingham-plastic fluids

Bingham plastic fluids have a linear shear stress – shear rate relationship, but needs to overcome a minimum yield stress to flow as shown in Fig. 4.4. Shear yield stress, τ_y, and the slope of the line, μ_p, need to be determined to quantify the relationship between the shear stress and shear rate shown in Eq. (4.5). The slope of the line is known as the fluid plastic viscosity. As the model is based upon just two readings from the Fann viscometer it is not optimal for pressure drop calculations [23].

$$\tau = \tau_y + \mu_p \dot{\gamma} \tag{4.5}$$

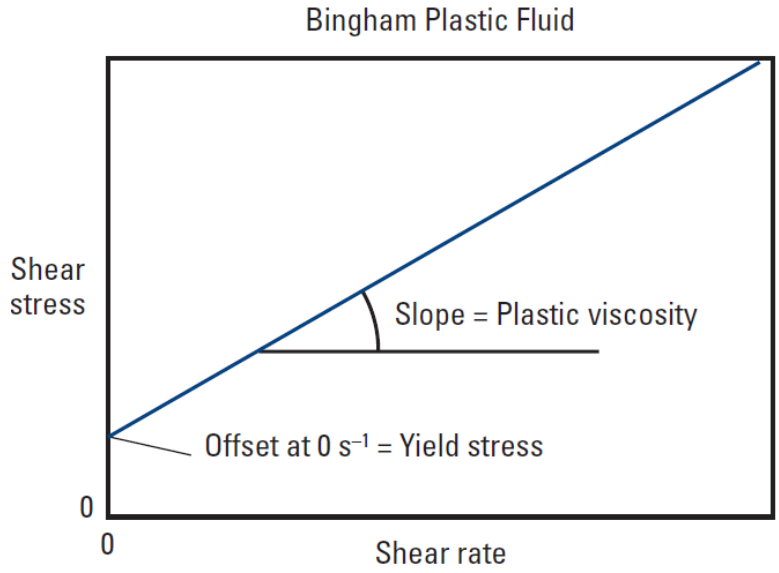

Figure 4.4: Shear rate plotted against shear rate for a Bingham plastic fluid. A minimum pressure gradient is needed to initiate flow represented by the yield stress. Once the yield stress has been reached a linear relationship exists [25].

4.2.3 Power-law fluids

The power-law model gives an accurate description of the shear stress – shear rate relationship in pseudoplastic fluids, especially at low shear rates. As opposed to Bingham plastic fluids, power-law fluids flow immediately once a pressure gradient is applied as shown in Fig. 4.5. The non-linear relationship between shear stress and shear rate is described through two parameters. A power-law index, n, and consistency index, K, are determined from the Fann-viscometer readings. The consistency index K is closely related to the fluid viscosity at low shear rates. At high shear rates the index is a measure of the solids content in the mud.

$$\tau = K\dot{\gamma}^n \tag{4.6}$$

Considering Eq. (4.6) it can be observed that for,

- $n = 1$: Newtonian fluid.
- $n > 1$: Dilatant fluid.
- $n < 1$: Pseudoplastic fluid

It should be noted that as the power-law model does not include a yield stress it will tend to underestimate the shear stress at low shear rates [23].

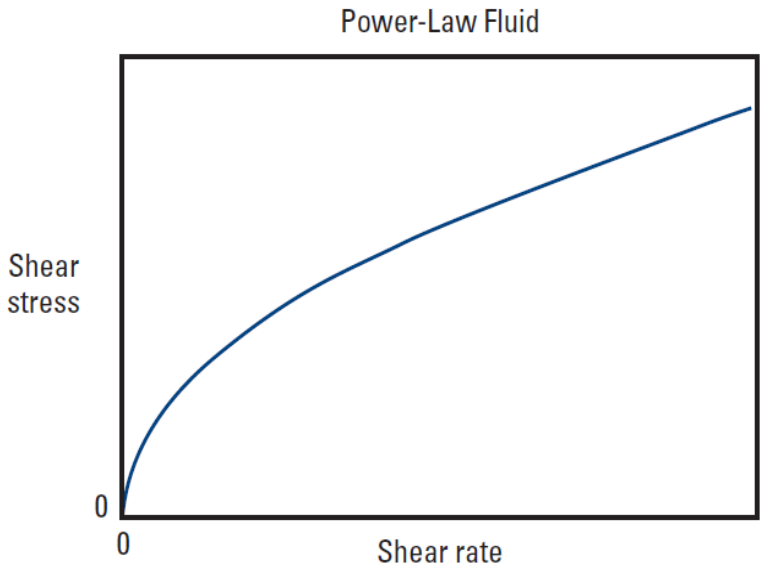

Figure 4.5: The relationship between shear stress and shear rate of a power-law fluid is generally non-linear. The curve is plotted for a pseudoplastic fluid ($n < 1$) [25].

4.2.4 Herschel-Bulkley fluids

Herschel-Bulkley fluids share some characteristics with both Bingham plastic and power-law fluids as illustrated in Fig. 4.6. A yield stress needs to be exceeded before flow commences, but at shear stresses exceeding the yield stress the model follows the power-law relationship. The model normally represents the Fann-readings with high accuracy.

$$\tau = \tau_y + K\dot{\gamma}^n \tag{4.7}$$

Equation (4.7) is valid for shear stresses exceeding the yield shear stress. Pressure simulations are generally based on the assumption that the drilling fluids and cement slurries follow the characteristic of a power-law or Herschel-Bulkley fluid.

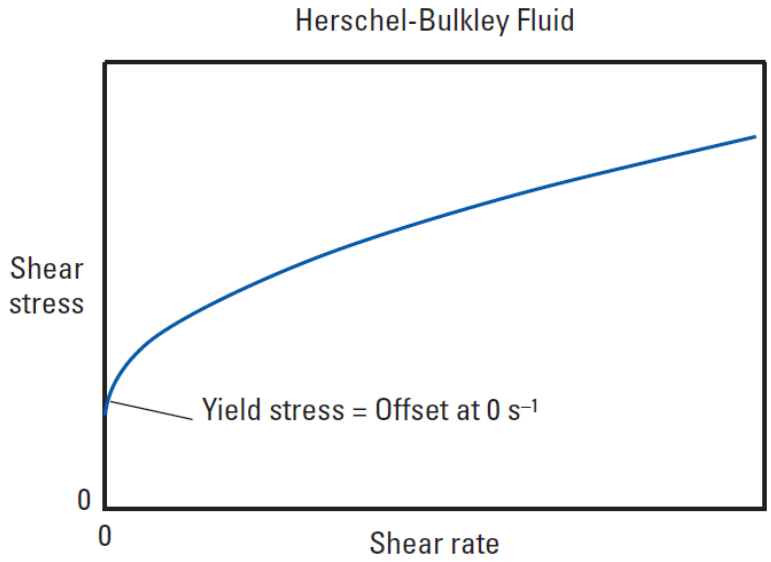

Figure 4.6: The relationship between shear stress and shear rate for a Herschel-Bulkley fluid is generally non-linear. The curve is plotted for a pseudoplastic fluid ($n < 1$). To move the fluid a pressure gradient exceeding the yield stress must be applied [25].

4.3 Flow regimes

Fluids generally flow in either laminar or turbulent flow. The flow regimes are characterized by different velocity profiles, frictional pressure drops and mixing of transported materials. A poorly understood and quantified transition zone exists between the two flow regimes. To determine the fluid flow regime the dimensionless Reynoldsnumber is applied. The quantity expresses the ratio of inertia forces to viscous forces, as shown in Eq. (4.8) where ρ symbolizes the fluid density.

$$Re = \frac{\rho U D_H}{\mu} \tag{4.8}$$

Different cut-offs are used to determine the fluid flow regime. Time [22] states that for

- $Re < 2000$ Laminar flow.
- $2000 < Re < 4000$ Transitional flow.
- $Re > 4000$ Turbulent flow.

Correlations including the power-law index have been proposed for power-law and Herschel-Bulkley fluids to determine the flow regime borders [22], [25]. Unless specified otherwise, the cut-offs presented by Time will be applied throughout this thesis.

4.3.1 Laminar flow

Laminar flow is characterized by fluids flowing in streamlines parallel to the pipe axis. There is no lateral component of the velocity vector. The laminar velocity profile in a circular pipe of a Newtonian fluid is illustrated in Fig. 4.7. It can be expressed by the distance, r, away from the centre of the pipe as shown in Eq. (4.9) [26].

$$u(r) = u_{max}\left(1 - (\frac{r}{R})^2\right) \tag{4.9}$$

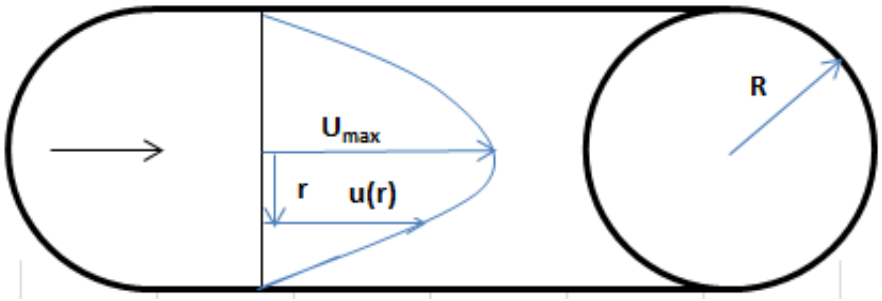

Figure 4.7: A parabolic velocity profile exists for laminar flow of Newtonian fluids (e.g. water). The velocity is symmetrically decreasing from maximum velocity at the centre of the pipe to zero at the pipe walls.

The average velocity, U, is found by averaging $u(r)$ over the cross sectional area, A.

$$U = \frac{1}{A}\int_0^R u(r)dA = \frac{1}{A}\int_0^R u_{max}\left(1 - (\frac{r}{R})^2\right)dA \tag{4.10}$$

Inserting for $dA = 2\pi r dr$ and solving the integral yields,

$$U = \frac{1}{2}u_{max}. \tag{4.11}$$

Equation (4.11) shows that the centerline velocity is twice the average flow velocity. Most of the 9 5/8" liner cement jobs on Valhall are performed within a laminar flow regime due to ECD restrictions (see Section 5.4.5). The velocity profile will in reality be different from fluid to fluid, depending on its rheological properties. Generally, the velocity profile of power-law fluids tends to flatten as the power-law index decreases [25]. The importance of fluid velocity profiles is further discussed in Chapter 5.

4.3.2 Turbulent flow

Turbulent flow is highly complex and characterized by velocity fluctuations at all points. The flow pattern changes with time and there is no exact way to predict the time variation. To graphically describe the velocity profile a time-average is plotted as indicated by Fig. 4.8. While laminar flow is parallell to the pipe axis, the particles in turbulent flow travels both laterally and axially. From an engineering point of view the most important characteristic of turbulent flow is a significant increase in pipe friction due to the steep change in velocity near the pipe wall [26].

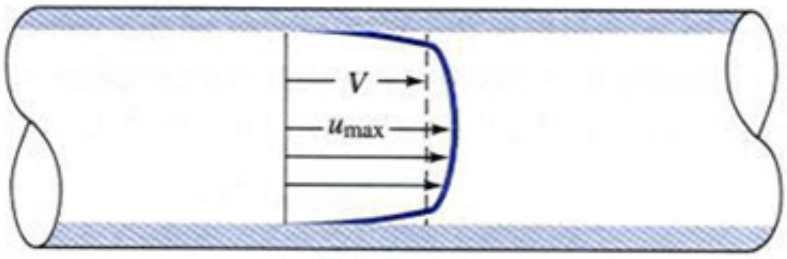

Figure 4.8: The turbulent velocity profile is flattened as compared to the laminar velocity profile. As a result the average velocity is closer to the maximum velocity. The blue layer illustrates a very thin laminar layer which is present at the pipe wall.

In turbulent flow it is common to express the velocity profile as [26],

$$u(r) = u_{max}\left(1 - \frac{r}{R}\right)^n. \tag{4.12}$$

The index n ranges from 1/5 in weak turbulence to 1/7 in strong turbulence [26]. It should be noted that numerous empirical velocity profiles exist and the best choice will depend upon the fluid and application. Similarly as for laminar flow the average velocity is found averaging Eq. (4.12) with respect to the area. After some manipulation the average velocity can be written as,

$$U = \frac{2u_{max}}{R^{n+2}} \int_0^R (R - r)^n r dr. \tag{4.13}$$

The remaining integral is solved using the laws of partial integration.

$$U = \frac{2u_{max}}{(n+1)(n+2)} \tag{4.14}$$

Inserting for n=1/7 the average velocity profile is approximately $0.82u_{max}$ which is significantly higher than for laminar flow. This is one of the obvious reasons why turbulent flow often is preferred for cement displacement and circulation activities in front of the cement job.

Another important concept in turbulent flow is that a laminar sublayer exists very close to the pipe wall. The velocity profile given in Eq. (4.12) is not valid in this region as it can be shown that the velocity profile yield an infinitely large wall shear stress. The physics behind the laminar sublayer are not fully understood and practical problems are often solved using empirical correlations [26]. As a result no exact solution to the frictional pressure drop in turbulent flow exists.

4.4 Fluid pressure drop calculations

The dynamic fluid pressure is composed of three main components as shown in Eq. (4.15). Hydrostatic, kinetic and frictional pressure all contribute to the total pressure in a dynamic fluid. Pressure, P, is often given as a gradient along the direction of flow.

$$\left(\frac{dP}{dx}\right)_{tot} = \left(\frac{dP}{dx}\right)_{hydr} + \left(\frac{dP}{dx}\right)_{kin} + \left(\frac{dP}{dx}\right)_{fric} \tag{4.15}$$

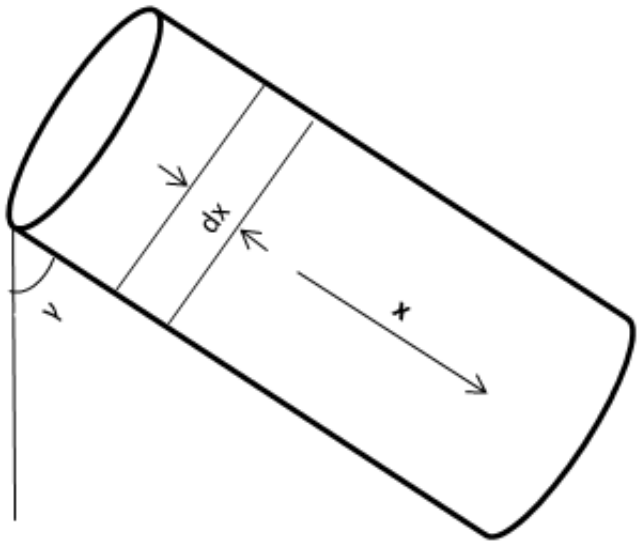

Figure 4.9: The total fluid dynamic pressure is given as a gradient where the x-direction is aligned with the flow direction. Wellbore inclination is represented by γ.

In drilling the dynamic pressure at a certain point in the wellbore is referred to as the ECD. ECD can be defined as "the effective density exerted by a circulating fluid against the formation that takes into account the pressure drop in the annulus above the point being considered" [27]. Prior to drilling and cementing operations simulations are performed to assure that the ECD is below the formation fracture pressure given the planned flow rates. During drilling a pressure sub is installed in the BHA (bottom hole assembly) which transmits real-time ECD readings. However, when running and cementing a casing string there is no pressure logging tool available on the market. Although the pump pressure can be used as an indication, one is highly dependent upon accurate simulations.

4.4.1 Hydrostatic pressure gradient

The hydrostatic pressure gradient can be expressed as,

$$\left(\frac{dP}{dx}\right)_{hydr} = \rho g cos\gamma. \tag{4.16}$$

For practical purposes, neglecting fluid compressibility and temperature effects, the hydrostatic pressure gradient is simply equal to the mud weight.

4.4.2 Kinetic pressure gradient

Kinetic pressure or pressure gradient is a result of changes in geometry and hence fluid velocities. From a drilling perspective this would include tapered drill strings, collars, liner hangers, bit nozzles etc. The kinetic pressure gradient is derived from the Bernoulli equation, Eq. (4.17), assuming incompressible steady-state flow and no friction.

$$P + \frac{1}{2}\rho U^2 = constant \tag{4.17}$$

Differentiating Eq. (4.17) yield the kinetic pressure gradient,

$$\left(\frac{dP}{dx}\right)_{kin} = -\rho\frac{dU}{dx}. \tag{4.18}$$

Equation (4.18) proves an important characteristic of the kinetic pressure gradient. If a fluid travels from a wide section, A, to a narrow section, B, the associated change in kinetic pressure is positive ($P_A > P_B$). The setup is illustrated in Fig. 4.10. As a result, narrow annular restrictions in a wellbore such as liner hangers will increase the ECD at all points below the restriction.

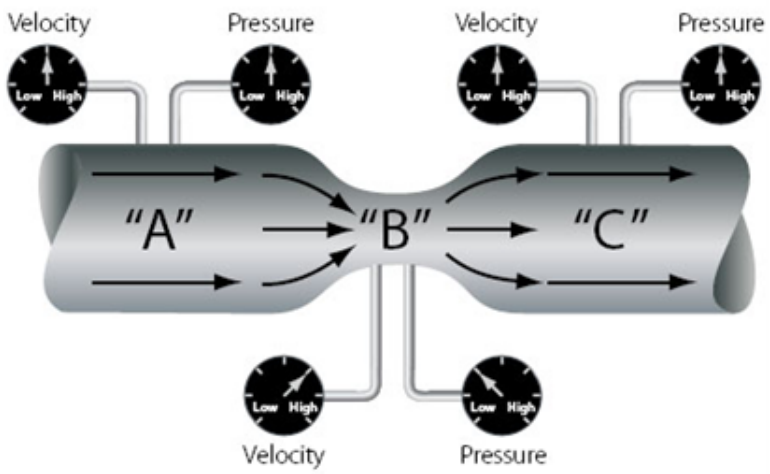

Figure 4.10: The Bernoulli principle shown by a venturi. In the wide sections of the venturi (point A and C) the fluid moves at low velocity, but at high pressure. When the fluid travels through the narrow side of the venturi (point B) the pressure is converted into energy by increasing the velocity of the fluid, effectively decreasing the pressure at point B [28].

4.4.3 Frictional pressure gradient

From a cementing perspective understanding the frictional pressure drop is of high importance. The frictional pressure drop is a function of the characteristic pipe (or annular) diameter, flow velocity, fluid viscosity and fluid density. As the ECD is a function of the remaining frictional pressure drop in the flow conduit, the annular friction drop is of most interest. Firstly, looking at incompressible, steady-state flow

in a circular pipe with diameter D is useful as several important concepts can be derived and mathematically justified.

A simple balance of forces in a horizontal pipe, as symbolized in Fig. 4.11, is used to derive the relationship between shear stress, τ_w, and frictional pressure gradient.

$$\tau_w S dx = (P_1 - P_2)A \tag{4.19}$$

Inserting for the pipe circumference, S, and the cross sectional area, A

$$\left(\frac{dP}{dx}\right)_{fric} = \frac{4}{D}\tau_w = \frac{4}{D}\mu\frac{du}{dy}. \tag{4.20}$$

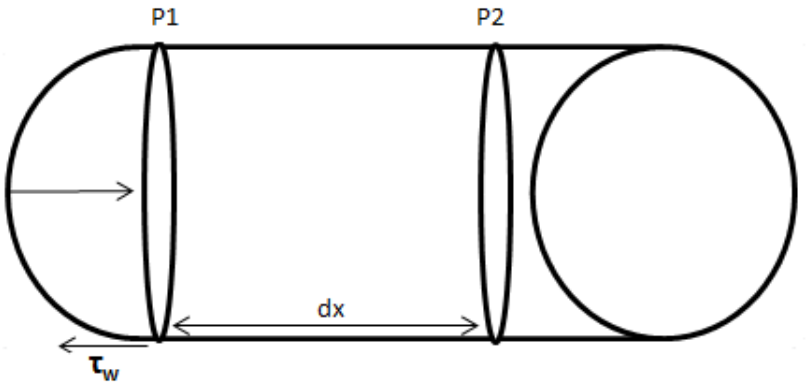

Figure 4.11: Balance of forces in a horizontal pipe. The pressure drop from P_1 to P_2 is due to shear stress/friction at the pipe wall, τ_w.

Equation 4.20 is valid both for laminar and turbulent flow. Assuming laminar flow and applying the symbols defined in Fig. 4.1 the laminar velocity profile can be expressed by the distance from the pipe wall to the point of interest, $y = R - r$. Differentiating the velocity profile yield an important result for laminar flow,

$$\frac{du}{dy} = u_{max}\left(\frac{2}{R} - 2\frac{y}{R^2}\right). \tag{4.21}$$

As per definition the fluid friction takes place near the pipe wall where y approaches zero.

$$\left.\frac{du}{dy}\right|_{y=0} = u_{max}\frac{2}{R} \tag{4.22}$$

Substituting Eq. (4.22) into Eq. (4.20) yields the general expression for laminar frictional pressure drop of Newtonian fluids,

$$\left(\frac{dP}{dx}\right)_{fric} = \frac{32}{D^2}\mu U = \frac{2}{D}\frac{16}{Re}\rho U^2 \tag{4.23}$$

The term $16/Re$ is the Fanning friction factor, f_F, for laminar flow. A general expression for the frictional pressure gradient independent of flow regime is given by,

$$\left(\frac{dP}{dx}\right)_{fric} = \frac{2}{D}f_F\rho U^2 \tag{4.24}$$

Finally, expressing the frictional pressure gradient given in Eq. (4.23) by the flow rate indicates that the pressure drop is highly dependent upon pipe diameter as shown in Eq. (4.25). If the pipe diameter is doubled, and everything else assumed constant, the frictional pressure drop will correspondingly decrease by a factor of 16.

$$\left(\frac{dP}{dx}\right)_{fric} = \frac{128}{\pi}\frac{Q\mu}{D^4} \tag{4.25}$$

For turbulent pipe flow the friction factor is dependent on wall roughness, ϵ, and the Reynolds number. Several attempts have been made to analytically quantify the turbulent friction factor, but they remain empirical correlations with varying accuracy [22], [26].

4.4.4 Frictional pressure gradient in concentric annuli

The annular frictional pressure drop is of main interest during both drilling and cementing as it is the only one that affects the ECD. Pipe friction only affects the pump pressure. Several of the same concepts as described for pipe friction can be applied in the annuli between two pipes or between pipe and formation. However, the equations and derivations quickly become more complex. It should be stressed that Eq. (4.24) holds for annular frictional pressure drop if D is replaced by hydraulic diameter and the friction factor calculated for annular flow. When calculating the annular frictional pressure drop it is common to approximate the annulus by an equivalent slot to simplify the equations. Fig. 4.12 describes the analogy behind the model. The slot approximation is increasingly accurate the narrower the annulus becomes. Guillot [25] showed that the error is less than 2.5% for a diameter ratio (d_{inner}/d_{outer}) of 0.3 for a power-law fluid. Given that the 9 5/8" production liner normally is cemented in a 12 1/4" hole the assumption is considered to be of sufficient accuracy.

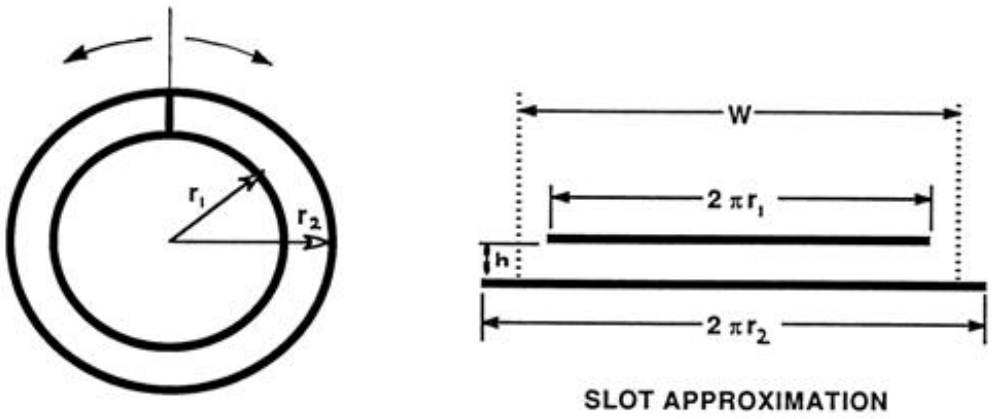

Figure 4.12: The annular space defined by r_1 and r_2 (a) is unfolded to an equivalent rectangular slot of width W (b). The slot approximation greatly simplifies the frictional pressure drop calculations [29].

An equivalent length, W, is defined as the average of the inner and outer circumferences. A simple balance of forces as shown in Fig. 4.13 yields [29],

$$\tau = \frac{dP}{dx} y + C_1. \tag{4.26}$$

Substituting Eq. (4.1) into Eq. (4.26),

$$\mu \frac{du}{dy} = \frac{dP}{dx} y + C_1. \tag{4.27}$$

Solving the differential equation and calculating the constants based on the boundary conditions for y=0 (u=0) and y=h (u=0) yields [29],

$$\left(\frac{dP}{dx}\right)_{fric} = \frac{48}{(D_o - D_i)^2} \mu U^2 \tag{4.28}$$

Direct comparison of Eq. (4.23) and Eq. (4.28) shows that for laminar, annular flow between two cylinders of diameters D_i and D_o the friction factor is given by,

$$f_F = \frac{24}{Re}. \tag{4.29}$$

The annular Reynold's number is given by Eq. (4.8) where $D_H = D_o - D_i$,

$$Re = \frac{\rho U (D_o - D_i)}{\mu}. \tag{4.30}$$

Hence, the annular friction pressure gradient for laminar flow of Newtonain fluids can be expressed as,

$$\left(\frac{dP}{dx}\right)_{fric} = \frac{192}{\pi} \frac{Q\mu}{(D_o - D_i)^3 (D_o + D_i)}. \tag{4.31}$$

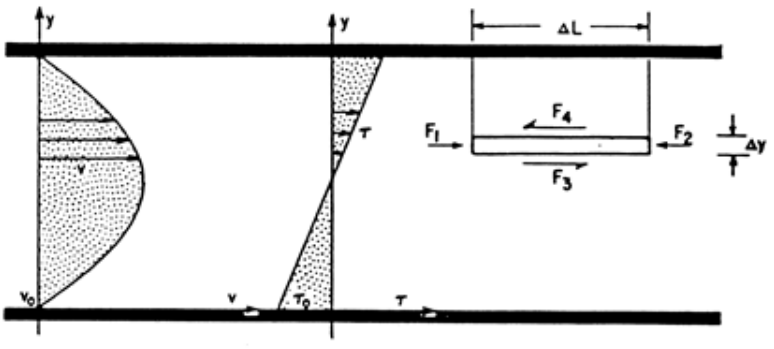

Figure 4.13: Balance of forces on a slot element. F_1 and F_2 represent pressure forces, while F_3 and F_4 are viscous forces. The direction of the viscous forces is intuitive, as the velocity below the slot element is higher than at the element itself. Hence, the element will be dragged in the flow direction from below and held back from above [29].

4.4.5 Frictional pressure gradient in concentric annuli power-law fluids

In the previous sections Newtonian fluids have been assumed as a constant viscosity simplifies and hence clarify some important concepts. In reality viscosity is a function of shear rate, temperature, pressure and time. The term viscosity is only of value if given for a specific shear rate and temperature for a non-Newtonian fluid [23]. Annular frictional pressure drop calculations for power-law fluids is introduced using the narrow slot approximation.

It can be shown that the Reynold's number in a concentric annuli for a Power-law fluid is expressed by [25],

$$Re_{pl} = \frac{\rho U^{2-n}(D_o - D_i)^n}{12^{n-1}\left(\frac{2n+1}{3n}\right)^n k} \tag{4.32}$$

The friction factor for laminar flow in a concentric annulus is given by Eq. (4.29), and the power-law frictional pressure drop can be calculated from Eq. (4.24) expressed by the Fanning friction factor,

$$\left(\frac{dP}{dx}\right)_{fric} = \frac{2}{D_o - D_i}\frac{24}{Re_{pl}}\rho U^2 = \frac{2^{2n+2}3^n\left(\frac{2n+1}{3n}\right)^n kU^n}{(D_o - D_i)^{n+1}} \tag{4.33}$$

To determine the turbulent and transitional frictional pressure gradient an expression for the friction factor must be determined and used as input in Eq. (4.24). Assuming a smooth pipe and $Re < 35000$, an empirical turbulent friction factor can be expressed as [25],

$$\frac{1}{\sqrt{f_F}} = \frac{4.0}{n^{0.75}} log\left[\frac{2}{3}Re_{pl}f_F^{1-\frac{n}{2}}\right] - \frac{0.4}{n^{1.2}} \tag{4.34}$$

Interpolation between the upper laminar border and lower turbulent border can be used to obtain the transitional flow friction factor.

Although of high accuracy, the Herschel-Bulkley model has not been used as frequently as the Power-law and Bingham plastic models. The reason is not only due to the complexity deriving the model's three parameters, but also due to the fact that analytical solutions for laminar and turbulent flow in annuli do not exist. Either graphical or trial and error methods have to be applied to solve the equations [30]. The equations are identical to Eq. (4.32), Eq. (4.33) and Eq. (4.34), but the parameters n and k needs to be modified due to the yield stress. The final equations are solved numerically. However, today most computer simulations apply the Herschel-Bulkley model due to its accuracy.

4.5 Effects of pipe eccentricity

In reality a casing string is never perfectly centered in a deviated well. The degree of centralization is referred to as stand-off. Stand-off values ranges from 0-100% where 100% represents a fully centralized casing string. When a casing string is not centralized a wide and a narrow section is created as illustrated in Fig. 4.14, affecting the fluid flow velocities and pressure gradients. Centralizers are installed on the casing strings to improve stand-off to meet the zonal isolation objectives (see Section 5.4.3). Annular velocities in the narrow and wide side can be quite significantly different in an eccentric annuli and may lead to cement channeling.

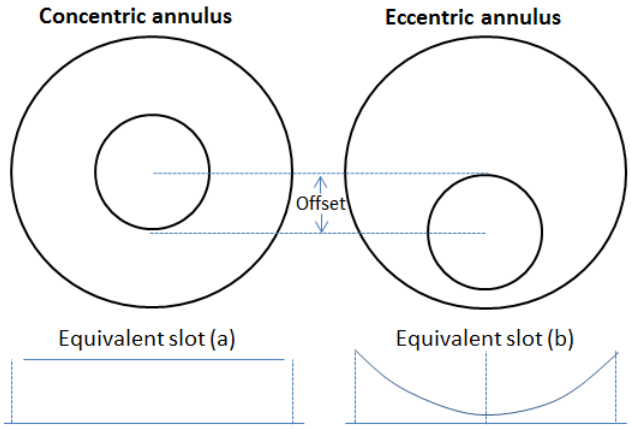

Figure 4.14: A concentric annulus (a) is desired during a cement job, but most casing strings, especially in deviated wells, are cemented in an eccentric environment (b). Eccentricity changes the flow geometry, and the slot approximation clearly shows a more complex situation [31].

Analytically representing the velocity distribution between the wide and narrow side is complex, even for laminar, Newtonian fluid flow. Intuitively, one expects a higher flow rate in the wide area as fluids follow the path of least resistance. Experiments and numerical simulations support the statement. Moran et al. [32] performed measurements on how the velocity of fluids of different viscosities varied between the wide and narrow side in an eccentric annulus. The experiments showed that high viscosity fluids tend to move at significantly higher velocities at the wide side as compared to the narrow side. However, lowering the viscosity decreased the difference between the wide and narrow side velocities as illustrated in Fig. 4.15.

The frictional pressure gradient is also affected by pipe eccentricity. Due to the relative larger flowing area on the wide side the annular friction decreases in an eccentric environment. Calculations are often done numerically based on a finite element method. Experiments have shown that frictional pressure losses on average were 18-40% lower in eccentric as compared to concentric annuli [33]. Furthermore, the data indicated that the decrease of friction was indepedent of fluid and flow regime. Laminar flow of both Newtonian and non-Newtonian fluids can be solved analytically. The results presented in Fig. 4.16 clearly show that pipe eccentricity decreases the annular frictional pressure drop [25].

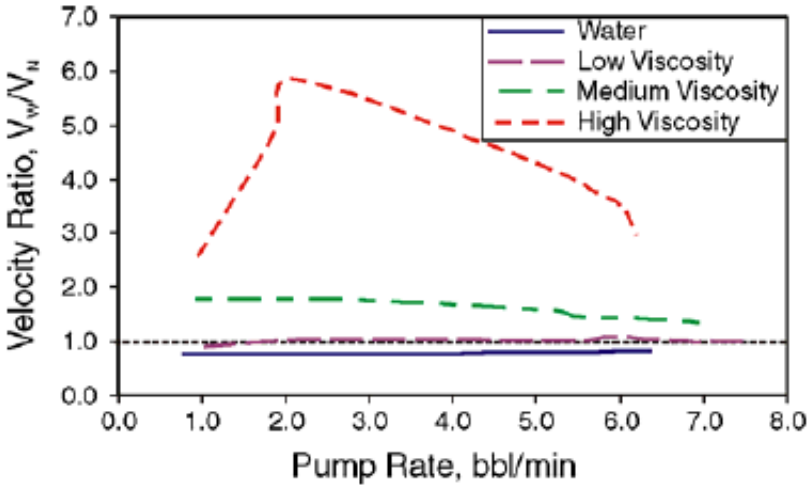

Figure 4.15: The velocity ratio (U_{wide}/U_{narrow}) plotted against flow rate for a number of different fluids to see how fluid viscosity affects the velocity distribution. 55 % stand-off was consistently used throughout the experiments. The data clearly show that high viscosity fluids are more likely to cause channelling as most of the flow travels at the wide side. Water travels faster at the narrow side as it does not have a yield point [32].

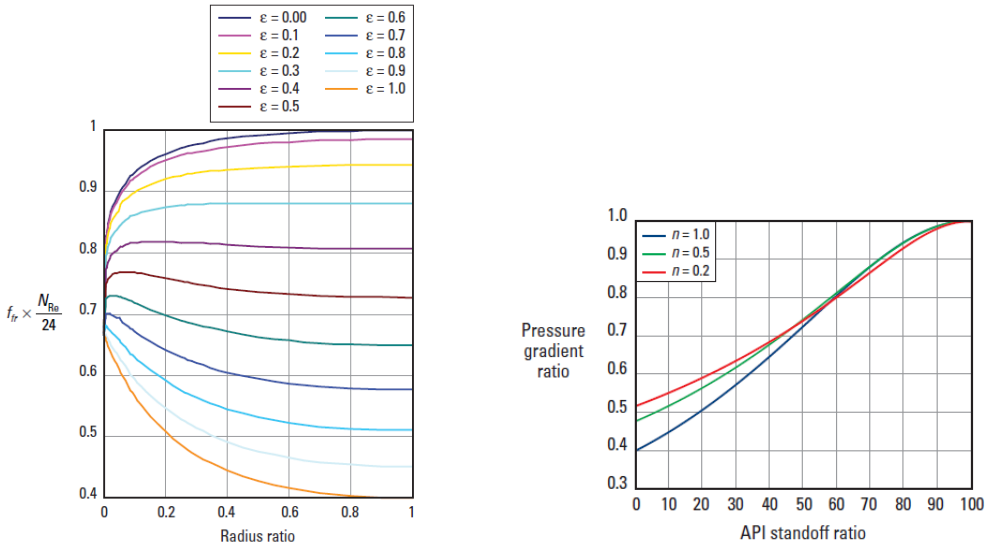

(a) Laminar flow of Newtonian fluid **(b)** Laminar flow of non-Newtonian fluid

Figure 4.16: Annular frictional pressure gradient ratio (eccentric/concentric) for laminar flow plotted against a) radius ratio and b) stand-off ratio for laminar flow of a) Newtonian fluids, and b) non-Newtonian fluids. Both a) and b) indicate that the frictional pressure drop decreases as eccentricity increases [25].

5 Well cementing

Well cementing is currently the most challenging aspect of drilling on the Valhall field. Great focus has been put upon zonal isolation and primary cementing during recent years. Valhall contains one of the most complex overburdens of BP's global portfolio. As a result, isolating the DPZs and meeting the zonal isolation objectives have proven difficult. Cementing the 9 5/8" production liner has been particularly challenging due to a very narrow operational window combined with a complex geology. Acoustic cement logs and observation of SCP in several annuli across the Valhall field have confirmed that the cement jobs have most likely not always been of satisfactory quality. Although recent improvements have been made in terms of zonal isolation there is still a lot of work to be done to design the optimal cement job. Several factors affect the outcome of a cement job, of which some is better understood than others. The most important factors are described in this chapter. It should be noted that understanding the factors separately is manageable, but to determine how a set of different factors interact and contribute to the overall outcome of the cement job is very challenging.

5.1 Portland cement

Portland cement is the most used material in the oil and gas industry to hydraulically seal off formations. Although not perfect, cement is the preferred material due to some of its beneficial properties. The cement is pumpable and develops strength within a reasonable time frame due to hydration. However, negative properties such as cement shrinkage, permeability and chemical degradation with time have led to discussions whether or not cement provide the sufficient long-term sealing capabilities, especially for P&A purposes. Very simply put, Portland hydraulic cement is made from pulverizing clinker which consists of calcium, silica, alumina and iron-compounds. The clinker is made by heating a mixture of different materials such as limestone and clays in a kiln. Hydraulic cement sets and develops compressive strength as a result of hydration. Water chemically reacts with the compounds in the cement. The cement hydration process is an exotermic reaction as illustrated in Fig. 5.1 [34].

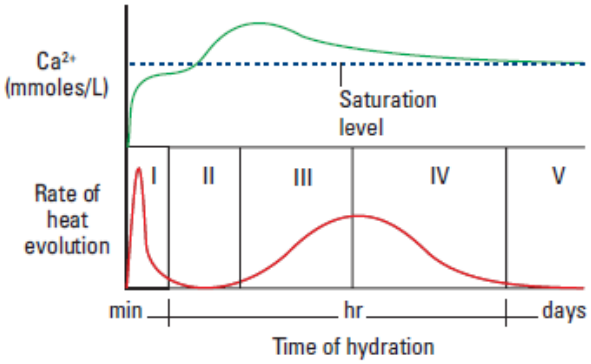

Figure 5.1: The rate of heat evolution and concentration of calcium ions, $[Ca^{2+}]$, are measures of the chemical interactions in the cement slurry. Based on the chemical activity the hydration process has been divided into five phases. Mechanisms within each phase are not uniformly described as different theories exist [34].

Well cements are classified in eight classes from A-H depending on setting depths and pressure/temperature capabilities, according to the API standard [2]. Class G cement is the base slurry for the Valhall field cement jobs. Combined with different additives the class G slurry can be used to cover a wide range of well depths and temperatures. Foam cements have been applied in wells with a narrow mud window globally, but after the Macondo blowout these cement types are not allowed by BP and will not be discussed in this thesis.

5.2 Additives

Temperature is the prime influence on cement setting times and strength development. Higher temperatures accelerate the hydration process. Well pressures also speed up the reactions, but the effect is not as pronounced. To optimize a cement job for a given application different additives are blended into the cement slurry to control setting times, strength development, densities, viscosities, etc. Additives modify the properties of the cement slurry, ideally providing enough time to successfully place the cement between the casing and the borehole wall, rapid strength development and zonal isolation for eternity. There are eight main groups of additives [35],

- Accelerators are added to decrease the setting time, and increase the rate of compressive strength development. Would typically be needed in low temperature wells. $CaCl_2$ is the most effective and economical accelerator.
- Retarders are added to increase the setting time, and decrease the rate of compressive strength development. Lignosulfonates are the most commonly used retarders. Retarders are added to allow the cement slurry to be pumped and displaced into the annulus before it starts setting and building strength.
- Extenders are used to lower the cement slurry density and increase the cement yield (volume/sack of cement). Microspheres of low density (e.g glass microspheres) can be added to the cement slurry to lower the effective density. In addition, clays allow for the addition of more water.
- Weighting agents are used to increase the cement slurry density. The most commonly used weight agent for both drilling fluids and cement slurries is barite.
- Dispersants are used to reduce the viscosity of the cement slurry. Different polymers are often used to obtain the desired viscosity.
- Fluid-loss control agents are used to control filtrate loss of the aqueous phase to permeable formations. Water-soluble polymers are used extensively today.
- Lost circulation control agents are used to control the loss of cement slurry to formations with a low horizontal stress. Different bridging agents and lost circulation material can be added.
- Special additives include anti-foam agents, elastic and flexible particles, fibers etc.

Combinations of additives and concentrations may lead to unwanted reactions and cement slurry properties. Thus, all cement slurries are mixed and tested by Halliburton prior to each job.

5.3 Operational sequence 9 5/8" liner

Equipment and technology are part of a dynamic environment. A liner string as opposed to a casing string is not hung off in the wellhead, but inside the previous casing string. Different methods and solutions have been applied to deliver the objectives of the 9 5/8" liner. The following section describes how the liner is run and cemented today.

A 12 1/4" hole is drilled and circulated clean using 14.6-14.8 ppg (lb/gal) OBM. The drilling assembly is pulled out of hole and preparations are made to run the 9 5/8" liner. A CRT (casing running tool) is connected to the top drive to efficiently and reliably perform connections of liner joints and run them in hole. One of the major advantages using a CRT tool is that circulation is possible through the DDM (derrick drilling machine) without any additional work. When the desired liner length has been run in hole a running tool followed by drill pipe is run to get the liner to the desired setting depth. The running tool is anchored inside the last liner joint and will not release as long as the liner is in tension.

The last liner joint consists of a liner hanger, packer and PBR (polished bore receptacle). Once the liner has been run on drill pipe to the planned setting depth, the cement head is installed on the drill floor and the liner hanger activation ball is dropped. The 2,25" steel ball lands in a ball seat located at the bottom of the running tool. Fluid is redirected to a flow path below a cylinder anchored with shear pins. The pressure is increased to approx. 2000 psi (depending on the number of shear pins) and held for two minutes. Once the pins are sheared the cylinder pushes a set of slips out and into the 13 5/8" casing wall. A 9 5/8" liner hanger slip segment is shown in Fig. 5.2b. The hanger is now set and the liner cannot move downwards. Increasing the pressure further to ± 3000 psi releases the running tool and turns the ball seat. Normal circulation can commence. The running tool is still engaged as compressive forces are applied.

(a) Cement head used in well 2/8-G-3.

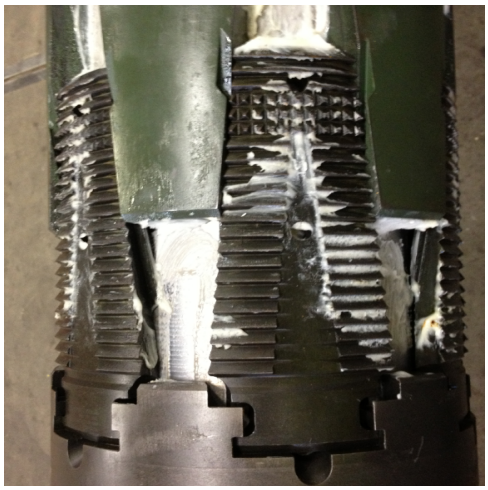

(b) Liner hanger slips.

Figure 5.2: The cement head (a) is installed on surface prior to the cement job. Spacer, cement and mud are subsequently pumped through the inlets located at the cement head. After running the liner the hanger is hydraulically set by pushing a set of slips into the 13 5/8" casing wall (b).

After successfully setting the liner hanger the cement operations can begin. Two pre-installed wiper darts are located inside the cement head. The 9 5/8" cement head is shown in Fig. 5.2a. Three fluid inlets are located at the cement head, one below, one above and one in between the darts. The darts serve two main functions. Firstly, to prevent fluid contamination inside the drill pipe. Secondly, the darts land and release a set of wiper plugs located inside the running tool as illustrated in Fig. 5.3. The wiper plugs mitigate the risk of contamination inside the liner. The bottom dart releases the bottom wiper plug, and the top dart releases the top wiper plug. Each wiper plug (including the landed dart) is pumped into a landing collar located typically 20-30 mMD above the liner shoe. The distance between the shoe and the landing collar is referred to as the shoetrack.

A spacer fluid is pumped through the cement head inlet located below the bottom wiper dart. The spacer fluid is a water-based preflush that serves to clean the inside of the pipe and the annulus to minimize mud contamination of the cement. When the desired volume of spacer has been pumped, the first wiper dart is released and cement slurry is pumped through the inlet located between the darts. Finally, the second dart is released and mud is pumped to displace the spacer and cement into the annulus. When the wiper plugs land in the landing collar an increase in standpipe pressure is seen. The bottom wiper plug is sheared at approximately 1000 psi, while the liner is pressure tested to 3000 psi after landing (bumping) the top plug.

(a) Wiper darts installed in cement head.

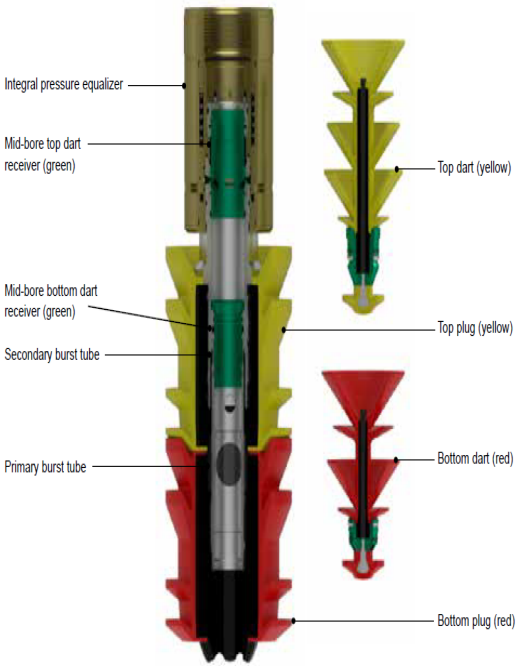

(b) Wiper plugs installed in liner hanger.

Figure 5.3: The wiper darts installed in the cement head prior to the 9 5/8" cement job on well 2/8-G-3 is shown in (a). The red dart is the bottom dart which is released after pumping spacer, and the yellow dart is the top dart which is released after pumping the cement slurry. When reaching the liner hanger area, the darts land and release a set of wiper plugs (b) [36].

A very important feature of the liner hanger system is that liner rotation can be achieved during the cement job. The liner hanger is mounted on a mandrel, which, in combination with a bearing, allows for liner rotation even after the liner hanger has been set. Torque is transferred to the liner from the running tool. Rotation is considered one of the most fundamental factors of a successful cement job.

The packer, located above the hanger, is set after bleeding off pressure from the liner test. A so-called dog sub is located inside the running tool. The already released running tool is pulled out until the dogs are above the PBR. Once out of the PBR the dogs come out, and minimum 60 klbs compression is put on the liner (pushing the 'dogs' against the PBR). Due to the compressive forces a set of pins are sheared and the packer element and a set of slips are set. The new set of slips prevent upward movement of the liner. The packer is pressure tested to 3000 psi by pumping through the kill line (into the annulus). Cement is yet to reach above DPZ 7 on the Valhall field. Hence, the gas tight packer is an important barrier to prevent SCP throughout the lifetime of the well.

When the remaining sections have been drilled a 9 5/8" tie-back casing is run and landed in the PBR. The PBR is a polished pipe which is designed to accept a seal stem. However, on the current Valhall design a seal stem is not applied [37].

5.4 Factors affecting a cement job

During a cement operation several factors affect the outcome of the job. Some are more obvious than others. Procedures and focal areas differ from field to field, and are often developed based on experience.

5.4.1 Hole cleaning

Prior to running a casing or liner string the drilled hole should ideally be totally free of cuttings. In deviated wells cutting beds at the lowside of the well is a well-known phenomenon. The cutting beds can be broken at sufficient flow rates and pipe rotation. Simulations prior to drilling operations provide a minimum flow rate needed to achieve sufficient hole cleaning. In addition, it has proven beneficial to circulate multiple BU (bottoms up) before pulling out of hole with the drilling assembly. The amount of cuttings seen over the shale shakers should decrease with time. In addition, the ECD tend to drop as cuttings are transported out of the hole. In recent years, only three cement jobs across DPZ 7 have been performed without losses on Valhall, 2/8-G-15, 2/8-N-9 T6 and 2/11-S-9. 2/8-G-15 and 2/8-N-9 T6 were circulated clean for more than 24 hours prior to the cement job. If failing to properly clean the hole the cuttings may compromise zonal isolation as channels of uncemented pipe, poor cement bonding and increased frictional pressure drop are more likely to occur.

Pack-off events during cementing are well documented. The pack-offs are normally caused by insufficient hole cleaning prior to the cement job. Wellbore instability situations in which cavings of variable sizes constantly enters the wellbore further complicates the situation. When a heavier and more viscous fluid (i.e. spacer and cement) is introduced to the annulus undisturbed, accumulated cutting beds on the

low-side of deviated hole sections tend to get picked up. As more and more cuttings are accumulated one may eventually block the entire fluid path in any wellbore restriction. The tight clearance between the liner hanger/PBR and the inside of the 13 5/8" casing is an obvious point of interest, but generally the hole may also pack-off in the open hole section. During a pack-off the pump pressure will increase and pressure up the fluid below the pack-off, and hence increase the ECD. At a certain pressure the pack-off is dissolved or a formation fracture is formed. Often the increased pressure leads to a formation fracture below the pack-off which may compromise the entire cement job. Due to the fact that no PWD (pressure while drilling) sub is installed during cement operations, one is highly dependent on observing the loss rate, torque (if liner is rotated) and pump pressure during the operation.

5.4.2 Mud system

Some important mud properties need to be defined to describe the challenges regarding mud systems associated with drilling and cementing.

- Plastic viscosity, PV, is defined as the Fann-reading at 600 rpm minus the 300 rpm reading, $PV = \theta_{600} - \theta_{300}$. The unit of measure is cP. PV is an indication of the solids content in the mud. Both barite particles, drilled solids (fine cuttings), lost circulation material etc. will contribute to increase the PV. Increasing the PV will generally also increase the ECD and surge/swab pressures [23].

- Yield point, YP, is defined as the Fann-reading at 300 rpm minus the PV, $YP = 2\theta_{300} - \theta_{600}$. The unit of measure is $lb_f/100ft^2$. YP is a measure of attractive forces between particles, and indicate the ability of the mud to carry cuttings. The YP is directly related to the frictional pressure drop.

- Gel-strengths measure the thixotropic properties of the mud, i.e. how the shear stress changes with time for a given shear rate. The unit of measure is $lb_f/100ft^2$. The gel-strengths indicate a fluid's ability to keep cuttings suspended when circulation is stopped. Gel-strengths are measured by leaving the mud static in the Fann viscometer for the required time period (10sec, 10 min etc.) and then reporting the maximum reading at 3 rpm shear rate.

From a drilling perspective, a viscous mud system which transports and keeps cuttings in suspension when circulation is stopped is ideal (i.e. high YP and gel-strengths). However, from a cementing perspective the opposite is true. High viscosities increase the ECD and could result in losses during the cement job. Failing to break gelled mud increases the risk of cement channeling. Prior to cementation some wells have been displaced to a low-rheology mud system to obtain and maintain good mobility, improve mud displacement by the cement and to reduce the ECD. From a cementing perspecitve the YP and gel-strengths should be maintained as low as possible without causing weight material to settle ('barite sag'). Proper hole cleaning prior to the displacement to a low rheology mud is a key success factor as cleaning the hole at a later stage will be much more challenging given the properties of the low rheology mud.

5.4.3 Centralization

Centralization has been given extremely high focus on Valhall, not only for 9 5/8" liner strings, but for all casing sizes. Effects of pipe eccentricity were discussed in Section 4.5. Proper pipe centralization minimize uncertainty regarding channels of gelled mud, displacement efficiency, effect of low rheology mud systems, rotation etc. The main tool to obtain the necessary stand-off is centralizers and their location along the casing or liner string. API defines standoff ratio as the smallest distance between the casing and the pipe wall, L_{min}, divided by the distance in a perfectly centered well as shown in Eq. (5.1) [38].

$$s = \frac{2L_{min}}{D_o - D_i}100\% \tag{5.1}$$

Centralizers come in a variety of different shapes and sizes. It is common to divide between three main groups of centralizers [39], [40]:

1. Rigid centralizers.
2. Bow spring centralizers.
3. Semi-rigid centralizers.

Rigid centralizers consist of solid blades which keep the casing string away from the borehole wall. Bow spring centralizers apply a compressable steel bow which is compressed according to the side forces acting on the casing string. The semi-rigid centralizers combine the concepts of both the rigid and bow spring centralizers. If the casing string is subjected to large side forces, such that the bow springs are heavily deflected, the smaller diameter rigid blades are exposed to maintain a minimum centralization [40].

Originally the bow type centralizers were mainly run in vertical or slightly deviated wells. The standoff ratios were considered very good as the size of the centralizers were larger than the hole size. They were not considered very efficient in deviated wells as the weight of the casing string would not be very well supported. The rigid design have always been recognised to provide standoff in deviated well sections as they are not compressible, but the casing string will never be perfectly centralized as the size is limited by wellbore restrictions (e.g. hole size). Today there are several alternatives on the market, and the bow springs have become very reliable in deviated wells. In addition to maximizing standoff ratios, the centralizers need to be flexible when tight spots are encountered, allow for pipe rotation and minimize torque and drag. The most commonly used centralizers today are the bow spring type [39], [41], [42].

The three most recent 9 5/8" liner centralizers applied on Valhall are presented in Fig. 5.4. Initially the rigid SpiraGlider centralizers were applied, but they have gradually been replaced by the Slider II and UROS bow spring centralizers.

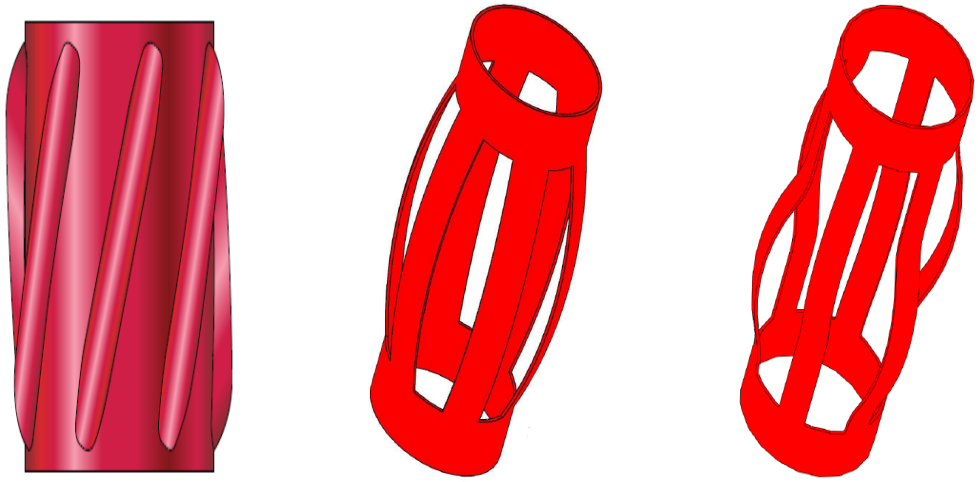

(a) SpiraGlider **(b)** Slider II **(c)** UROS

Figure 5.4: After conforming to the current Valhall IP casing design three different 9 5/8" liner centralizers have been applied. Standoff simulations have shown a gradual improvement from SpiraGlider to Slider II to UROS. Whereas the SpiraGlider and Slider II have an outer diameter of 11 3/4" and 12 1/4" respectively, the UROS bow springs are 13 1/2" uncompressed, which is a major advantage if the hole size is larger than 12 1/4".

Prior to each cement job extensive simulations are performed to optimize the centralizer program. A typical simulation is shown in Fig. 5.5. The number of centralizers per casing joint (one or two), casing/centralizer properties, well trajectory, well geometry, mud/cement densities and the separation between centralizers are of major interest. Important centralizer properties include the starting force, running force and restoring force. The starting force is defined as the maximum force required to push a centralizer into a hole diameter. Similarly, the running force is the maximum force required to run a centralizer through a hole section. Of most interest is the restoring force, which is a measure of the force exerted by the centralizer to the casing string to keep it away from the wellbore wall [39]. Sufficient and reliable restoring forces are required to obtain sufficient stand-off values. A minimum standoff of 80-90% is recommended by Halliburton for optimal displacement efficiency [10].

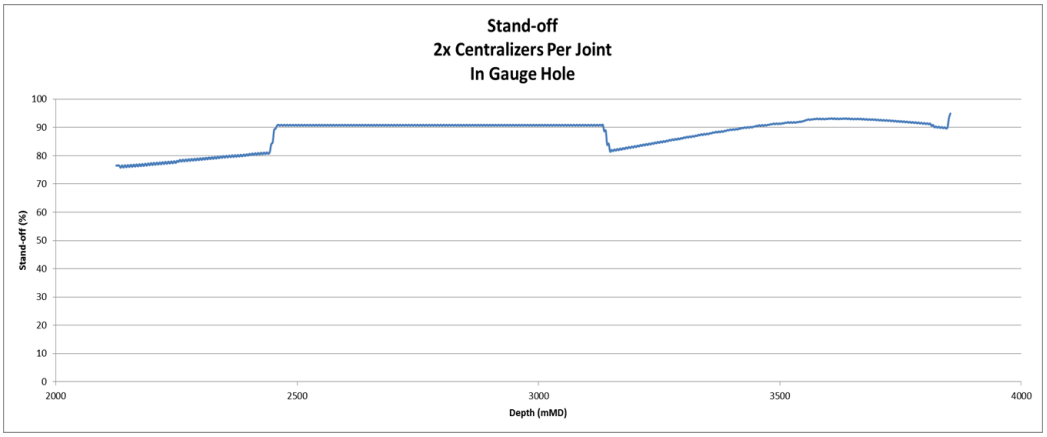

Figure 5.5: Typical Halliburton standoff simulation performed for well 2/8-G-3 (2014) applying Slider II centralizers. Depth is plotted against standoff, indicating that standoff values of 75-95% can be expected in the 12 1/4" hole section.

5.4.4 Circulation efficiency

Circulation efficicency is a term referring to how efficient a fluid displaces itself. The quantity is expressed by the percentage of the displaced annular volume to the total annular volume. When conditioning the mud and breaking gel-strenghs prior to a cement job it is important to know approximately how many annular volumes or bottoms up that should be circulated to minimize the risk of leaving channels of static, geled-up mud. The circulation efficiency of a fluid is directly related to the flow regime and its associated velocity profile. A perfectly flat velocity profile is optimal. In Section 4.3 typical velocity profiles for laminar and turbulent flow of Newtonian fluids were described. Laminar pipe flow of a Newtonian fluid is characterized by the fact that the centerline velocity is twice the average velocity. Hence, when circulating a full annular volume the majority of the flow will commence through the center part of the annulus, effectively leaving the mud closer to the wall static. To allow the entire annular volume to be circulated several annular volumes must be pumped to achieve an acceptable circulation efficiency. The circulation efficiency of different power-law fluids is presented in Fig. 5.6. Due to the flattened nature of the turbulent velocity profile, turbulence is preferred to optimize circulation efficiency. However, with a limited mud window turbulence cannot always be achieved without fracturing the formation. The velocity profile of power-law fluids flattens and circulation efficiency increases as the power-law index, n, decreases as shown in Fig. 5.6 [43].

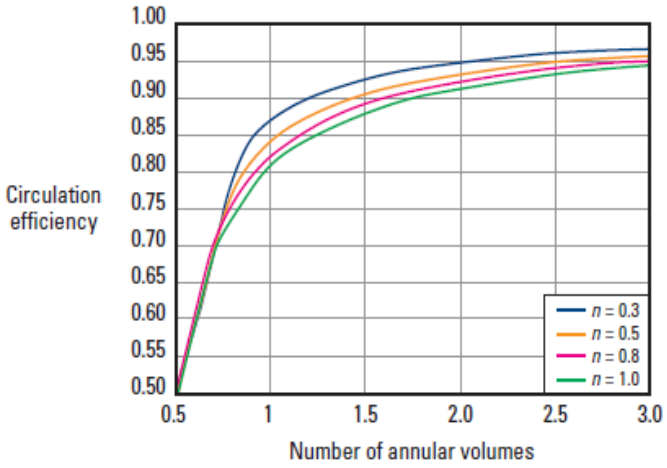

Figure 5.6: The circulation efficiency (laminar flow) in a concentric annuli for different power-law indexes. Newtonian fluids are characterized by n=1. As seen from the graph, the circulation efficiency increases as the power-law index decreases [43].

Eccentricity adds further variables to the situation. The complicated geometry creates a velocity profile where the flow of a viscous fluid generally prefer the wide side of the eccentric annuli. An unusual situation with turbulent flow on the wide side and laminar flow on the narrow side may be created. Intuitively one would expect the circulation efficiency to drop in an eccentric annuli. This is also the truth for most cases. An analytical solution with regards to pipe eccentricity is presented in Fig. 5.7 [43].

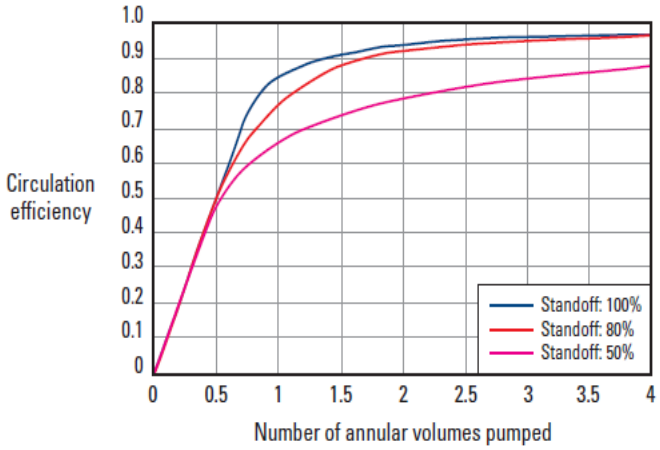

Figure 5.7: The circulation efficiency (laminar flow) in an eccentric annuli of different stand-off values for a power-law fluid (n=0.5). As seen from the graph, the circulation efficiency decreases with decreasing stand-off [43].

5.4.5 Displacement efficiency

Displacement efficiency, expressed in Eq. (5.2), refers to how efficient one fluid displaces another fluid ranging from 0-100% [44]. The topic represents the most challenging aspect of designing a cement job. All other topics described within this section can to some extent be related to cement displacement. The topic has been of major interest on Valhall, but a field proven solution is yet to be determined. Conceptually displacement efficiency is similar to circulation effiency, but the situation is complicated by effects at the interface of the displacing fluid and the fluid being displaced. During a cement job the spacer displaces the drilling fluid, and the cement again displaces the spacer. The rheologies and densities of the spacer and cement slurries can be designed to optimize displacement of the mud located in the annuli [45].

$$E(t) = \frac{\text{Volume of displacing fluid in annulus}}{\text{Annular volume}} \tag{5.2}$$

Displacement theories derived from different assumptions have been developed for decades. A general set of qualitative rules have been adopted based on field experience and experiments. Firstly, a sufficiently high flow rate should be achieved to avoid mud channeling on the narrow side of an eccentric annuli. The required annular velocity increases as standoff decreases. Secondly, a rheological hierarchy of the fluids pumped should exist where each fluid has a higher viscosity than its predecessor (i.e. $\mu_{mud} < \mu_{spacer} < \mu_{lead\,cement} < \mu_{tail\,cement}$). Another way to look at it is that each fluid should generate a higher frictional pressure drop than its predeccesor as shown in Fig. 5.8. Finally, a density hierarchy of the fluids pumped should also be designed for (i.e. $\rho_{mud} < \rho_{spacer} < \rho_{lead\,cement} < \rho_{tail\,cement}$). The density hierarchy in laminar flow is known to stabilize the interface between the fluids, and to flatten the profile of the interface [45], [46]. Viscous forces are dominant in highly deviated wells, whereas gravitational forces dominate in vertical and less deviated well sections. Although

intuitive, Bittleston et al. [45] state that "the level of fundamental understanding is low and predictions are generally conservative". Particularly predictions for highly deviated wells are pointed out as difficult as density differences may cause cement slumping at the low side. A combination of theory and experiments performed by Tehrani et al. [44] state that inclination reduces the displacement efficiency by decreasing the gravitational effects. A general rule of thumb to optimize fluid displacement is that the displacing fluid should be of 10% higher density and create a 20% higher frictional pressure drop than the fluid it is displacing [47]. Achieving a significant density hierarchy on Valhall 9 5/8" liner jobs with the limited available mud window is of course difficult, if not impossible.

In addition to stand-off, flow rates, densities, viscosities, well geometry etc. there is an interfacial aspect of the displacement process which could affect the outcome of the cement job. Predicting the profile of the interface between non-Newtonian fluids is challenging [46]. The interfacial tension between the fluids (mud/spacer and spacer/cement) will affect the displacement front. Ideally the displacement front is steady and stable without any fingering between fluid phases. In addition, the spacer is to be designed in such a way that it water wets the formation and casing to assure proper cement bonding. Surfactants are often added to the spacer to achieve proper water wetting and displacement efficiency characteristics [48].

A variety of different ratios including frictional pressure gradients, plastic viscosities, yield stresses, densities, fluid velocities and so-fort have been proposed based upon specific experimental setups [43]. The simplified models are very case dependent [43], [44]. Fully three dimensional displacement simulations are performed by Halliburton prior to each cement job to assure that the fluids and their properties are able to deliver the objectives of the job.

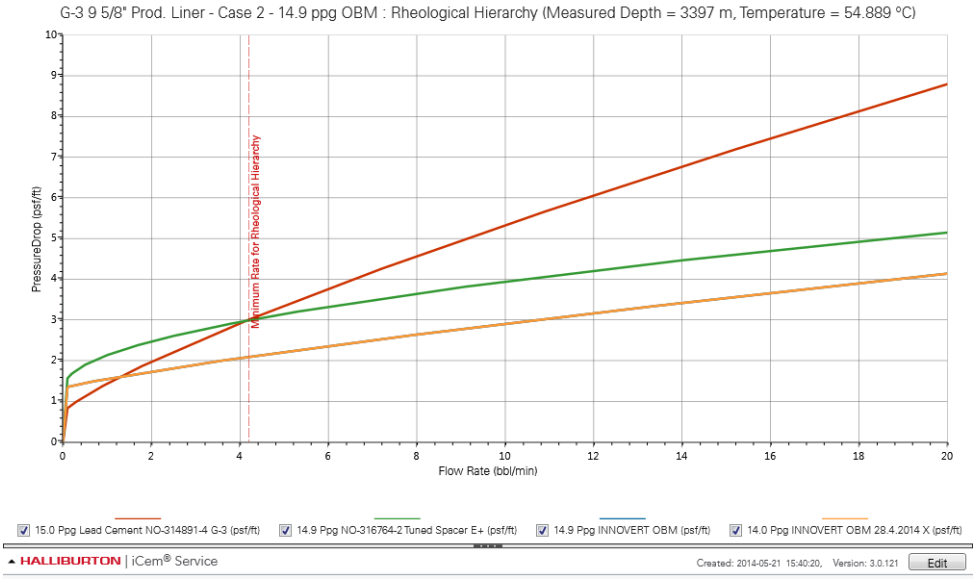

Figure 5.8: A typical rheology hierarchy where frictional pressure drop is plotted against flow rate. The yellow, green and red graphs indicate mud, spacer and lead cement respectively. The minimum flow rate is defined where rheological hierarchy is achieved. Simulations were performed by Halliburton for well 2/8-G-3.

Often when reading recommendations regarding mud displacement a minimum annular velocity is referred to. This velocity corresponds to the transition zone to turbulent flow, often given at a Reynold's number of 2000-3000. To give an indication of the flow regimes during a typical cement job at Valhall the rheological properties provided by Halliburton prior to drilling well 2/8-G-3 of the spacer, lead cement and tail cement are listed in Table 5.1. The Reynold's numbers have been calculated assuming power-law and Herschel-Bulkley fluid behaviour as described in Chapter 4. The correlation between the different rheology models and the Fann readings are shown in Fig. 5.9.

Table 5.1: Preliminary rheological properties of spacer, lead slurry and tail cement for 9 5/8" cement job on well 2/8-G-3 taken at 63 °C. The shear stress is given in ° from the Fann viscometer.

RPM	14.8 ppg spacer [°]	15.0 ppg lead [°]	15.8 ppg tail [°]
300	65	105	146
200	52	80	104
100	38	50	62
60	31	36	42
30	25	22	25
6	18	8	8
3	17	5	5

To analytically complete the calculations some assumptions have been made. The hole size is assumed constant at 12.25", the string is perfectly centered, the slot approximation is valid and the flow rate is equal to 336 gpm (gallon/minute). The results listed in Table 5.2 show that during the cement job a laminar flow regime should be expected both for the spacer, lead slurry and tail slurry. Hence, focus is to optimize laminar displacement.

Combining the laminar annular frictional pressure drop, Eq. (4.33), with the calculated Reynold's numbers it is easily observed that a rheological hierarchy is achieved for the fluids presented in Table 5.1.

Table 5.2: Reynold numbers calculated for spacer, lead slurry and tail slurry assuming power-law and Herschel-Bulkley fluid behaviour. The power-law index and consistency index have been calculated based upon the 300 and 200 rpm Fann readings, while the Herschel-Bulkley calculations are based upon a numerical solution of the flow equations. A displacement rate of 336 gpm and a hole size of 12 1/4" have been assumed in the calculations.

Fluid model	Re_{spacer}	Re_{lead}	Re_{tail}
Power-law	629	476	413
Herschel-Bulkley	552	500	442

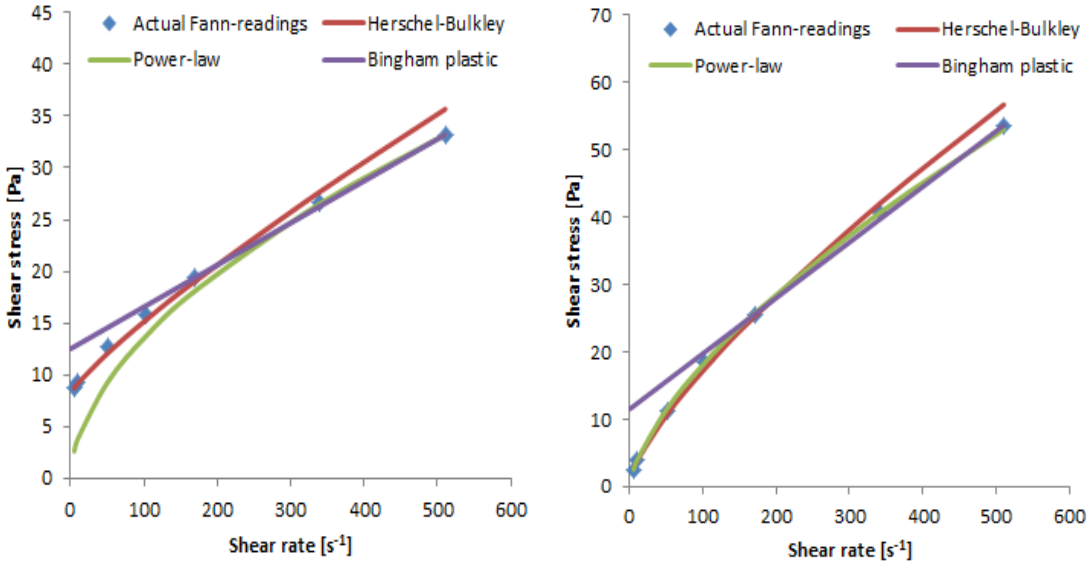

(a) 14.8 ppg spacer fluid. **(b)** 15.0 ppg lead slurry.

Figure 5.9: Shear stress plotted against shear rate for both the spacer fluid and the lead cement. The three most common rheological models have been applied. Herschel-Bulkley describes the spacer fluid most accurately, while the lead cement is best represented by the power-law model. All readings have been performed at 63 °C.

The maximum shear rate is at the pipe wall due to the nature of the velocity profiles. Assuming laminar flow, power-law fluid characteristics, concentric hole conditions and a typical 9 5/8" cement job displacement rate of 336 gpm an upper shear rate limit can be established. Combining Eq. (4.20) expressed by the hydraulic diameter and Eq. (4.33) an expression for the wall shear stress is obtained,

$$\tau_w = \frac{2^{2n}3^n\left(\frac{2n+1}{3n}\right)^n kU^n}{(D_o - D_i)^n}. \tag{5.3}$$

Applying the power-law defintion the maximum shear rate can be expressed by,

$$\dot{\gamma}_w = \left(\frac{\tau_w}{k}\right)^{1/n}. \tag{5.4}$$

Finally, inserting the rheologial Fann data given in Table 5.1 in the power-law model a maximum shear rate of 167, 154 and 147 s^{-1} is obtained for the spacer, lead and tail cement respectively. This corresponds to 98, 90 and 86 rpm on the Fann viscometer. Hence, one should be careful using the Bingham plastic model which is based upon the 600 and 300 rpm reading for the 9 5/8" cement job on Valhall. It should be noted that the calculations are meant as an indication. The choice of fluid model and their respective parameters will affect the results.

5.4.6 Liner rotation

Liner rotation is considered as one of the most critical factors of a successful liner cement job on Valhall. In some wells where the necessary torque is higher than the rating of downhole equipment (e.g. liner connections, running tool, liner hanger etc.) rotation is not possible. Qualitatively liner rotation is known to increase the displacement efficiency. The need of rotating the pipe increases as stand-off decreases. It is believed that pipe rotation increases the flow velocities at the narrow side of eccentric annuli, improving mud removal and cement bonding [49]. A tangential velocity component is introduced to the system as a direct result of rotation. Fluid is transferred from the wide to the narrow side as a result of the helical velocity profile as illustrated in Fig. 5.10 [50]. Although efficient, pipe rotation must be applied together with optimal fluid properties and stand-off to assure proper zonal isolation.

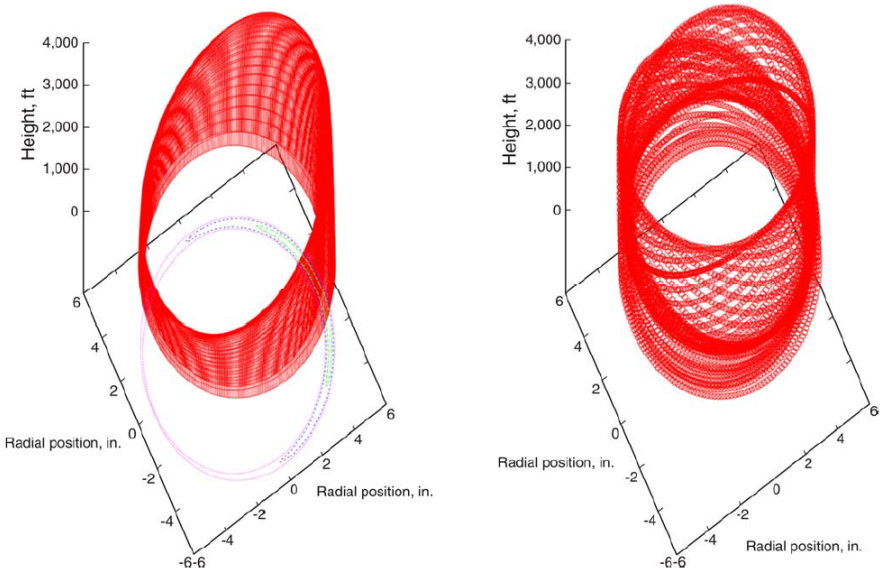

Figure 5.10: Simulated effect of pipe rotation on cement displacement on 9 5/8" liner job in Italy. The helical velocity profile greatly contributes to an improved displacement across the narrow side. Stand-off ranged from 60-75%. After performing the cement job the well was acoustically logged, confirming the value of pipe rotation [50].

Determining the effect of pipe rotation on annular frictional pressure drop is of significant interest. The general conception is that annular frictional pressure drop increases due to the relative longer flowpath of the drilling fluid. However, the Halliburton simulations do not include the effect of pipe rotation which could prove a non-negligible source of error. Depicting the effect of pipe rotation is difficult, but the work of Hemphill et al. [51] highlights some important variables affecting the ECD increase.

- Drilling fluid rheological properties are not important for accurate modeling.
- The ECD increase is higher the narrower the annuli.
- The ECD increase is nearly linear with respect to drill pipe rotational speed.

A simplified correlation was developed for the increase in pressure, ΔP [psi], with D_i/D_o ratios ranging from 0.43 to 0.85 for different rotational speeds, N, as expressed in Eq. (5.5). The length of the section is symbolized by L [51].

$$\Delta P_{rotation} = -1.0792 \left(\frac{D_i}{D_o}\right) + 0.00017982 \left(\frac{D_i}{D_o}\right)^2 LN \tag{5.5}$$

Assuming 1500 mMD of 9 5/8" liner inside 12 1/4" hole and 2000m 5 7/8" DP inside 13 5/8" casing with a rotational speed of 30 rpm yield an increase in the bottomhole pressure of approximately 25 psi according to Eq. (5.5). Intuitively it seems very strange that the rheological properties of the annular fluids do not affect the change in ECD. Equation (5.5) can be useful as an indication, but more sophisticated simulations are needed to fully describe the rotational ECD effect.

To simulate the effect of pipe rotation the Virtual Hydraulics software provided by MI Swaco has been applied. Although generally achnowledged for its accuracy, the system has one major disadvantage. Only one fluid system can be treated at a time. A situation with mud, spacer and cement in the flow conduit cannot be reproduced [52]. Simulations were performed with a high rheology mud (Carbosea OBM), a low rheology mud (Warp OBM) and with the water-based cement slurry to discover how viscosity and rotational speed affect the ECD. Simulations were performed at 300 gpm for 0, 20, 40, 60, 80 and 100 rpm for all three fluids. The results are presented in Fig. 5.11. As opposed to the results of Hemphill et al. [51] rheology clearly affect the ECD contribution from rotation, especially at high rotational speeds.

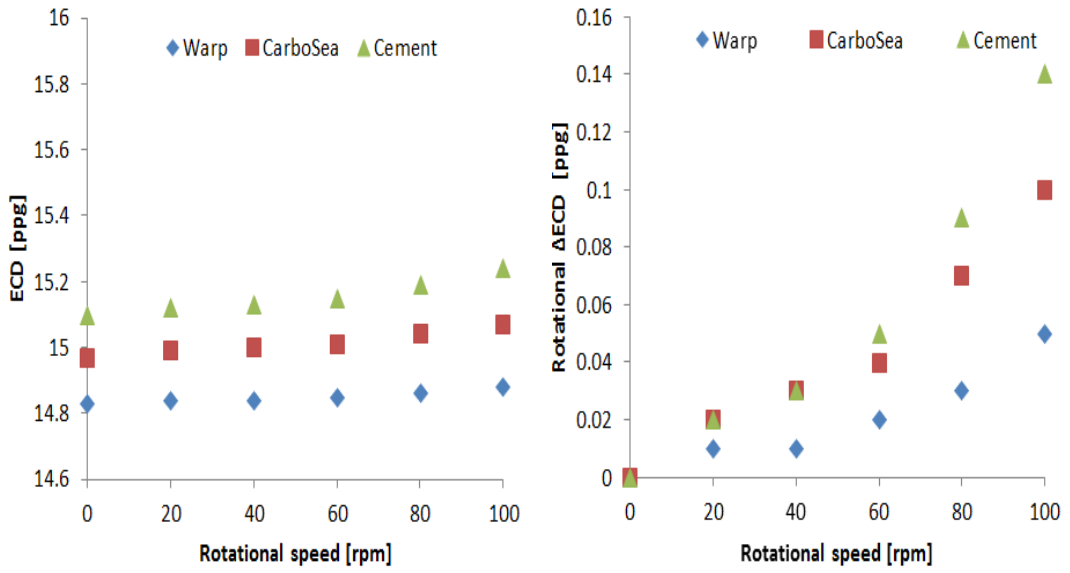

(a) ECD data **(b)** Rotational ECD contribution.

Figure 5.11: Comparison of simulations showing ECD (a) and how different fluid system affect rotational ECD contribution (b). The flow rate is held constant at 300 gpm. The low rheology Warp OBM clearly shows the most desirable ECD trend. The 2/8-G-3 wellpath was applied in the simulations.

Pipe reciprocation is also considered beneficial in some fields as the fluid velocity relative to the pipe is increased. On Valhall 9 5/8" liner cement jobs, given the available mud window, reciprocation is not considered a realistic option as surge pressures could breakdown the formation. In addition, with the current liner hanger system it is considered good practice to set the hanger prior to the cement operations in case something goes wrong in the activation process.

5.4.7 Spacer design and fluid compatibility

Spacers are an important measure to prepare the well for the cement job. Both spacer properties and volumes are carefully planned to remove mud from the annulus and to water wet the formation and casing wall. Even a thin layer of oil from the drilling fluid can prevent the cement from properly bonding to the casing [53]. As a consequence most spacers are water based, including those used on Valhall. To assure that the spacer/lead cement and spacer/mud is compatible lab experiments are conducted prior to each job. The compatibility test is performed by measuring the rheological properties of the cement/mud by gradually increasing the contamination (i.e. fraction of spacer). A highly viscous and clumpy interface is not desirable as frictional pressure drop and probability of channeling will increase.

Halliburton [53] describes four main parameters which affect spacer performance,

- Spacer rheology at relevant wellbore temperatures.
- Spacer compatibility with mud and cement.
- Volume of spacer necessary to provide desired separation between mud and cement.
- Contact time and pump rate to efficiently remove mud and aid displacement.

In the 18 5/8" and 13 5/8" cement jobs in well 2/8-G-3 the volume of spacer pumped was drastically increased (more than doubled) to enhance the exposure time. The results have been fairly positive in terms of cleaning the well and contributing to proper cement bonding. However, it is too early to conclude on the effect of increasing the spacer volume. Generally, as the spacer is of higher density than the drilling fluid (according to the density hierarchy) an extensive spacer volume would also increase the ECD which again could limit other important parameters such as pump rates. Each job needs to be carefully evaluated to find an optimal solution.

Mud contamination of the cement slurry can change its properties significantly. The main consequences of cement contamination are a dramatic increase in setting times and deterioration of mechanical properties [54]. As a result the intervals of contaminated cement will most likely not show up on the cement log. In addition, microannuli and bonding capabilities could jeopardize zonal isolation. Hence, spacer volumes should always be large enough to ensure that the mud and cement will be separated throughout the entire pumping schedule.

5.5 Cement failure mechanisms

Even if a successful primary cement job is obtained the sealing capabilities of the cement may be altered during the lifetime of a wellbore. Temperature and pressure fluctuations during production provide a major challenge. It is common to divide between three different cement failure mechanisms. The mechanisms are illustrated in Fig. 5.12.

Firstly, cement debonding occurs when the bonding of the cement to the formation or casing steel fails. Standard Portland cement shrinks by 2-4% by volume if no external water feed is available during hydration. As a result a microannulus may be created which compromises zonal isolation. Pressure testing of the casing string may also contribute to the creating of microannuli along the wellpath as a result of the expanding casing string. Furthermore, casing movement due to for example subsidence may effectively cause the cement to debond. Secondly, cement cracking mainly occurs as a result of pressure and temperature fluctuations. As the parameters change the casing and cement is subject to cyclical loads, which may induce stresses which subsequently cracks the cement sheath. This is a tensile failure. Cement is known for its high compressive strength, but its tensile strength is relatively low. Finally, shear failure typically results in complete cement failure of the cement sheath. Subsidence, temperature increase, pressure testing and vibrations from downhole equipment (e.g. pumps and drillstring) have been identified as root causes [1].

One should always keep in mind that if sustained casing pressure or pressure build-up in permeable formations are experienced at some point in the lifetime of a well it is not necessarily due to a poor primary cement job. The stresses working on the formation, cement and casing is highly complex and needs to be taken into account.

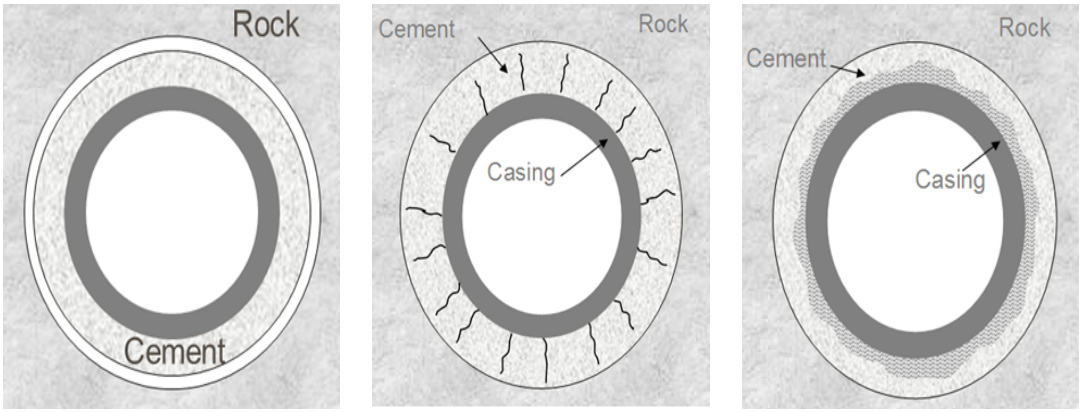

(a) Debonding **(b)** Cracking **(c)** Shear failure

Figure 5.12: Debonding (a), cracking (b) and shear deterioration (c) are the three main cement failure mechanisms. The debonding shown in (a) represents a bonding failure between the cement/formation, but a failure at the cement/steel interface may also occur [55].

5.6 Remedial cementing

Remedial cementing involve operations carried out to cure different well problems or to improve the zonal isolation status. A variety of different methods exist to improve the well status. To keep this thesis within its limits only the two main remedial cement job methods applied to improve the zonal isolation of a wellbore at Valhall is briefly introduced.

Squeeze cementing is often applied if the desired FIT or LOT below the casing shoe cannot be obtained or if a clear indication of poor cement bonding around the shoe is observed from the cement log. The operation is performed by placing a certain volume of cement in the bottom of the hole, pulling out of the plug, shutting the well in and increasing the pressure to squeeze the cement into the formation/annulus. As the cement will follow the path of least resistance it is very uncertain where the cement actually will go, although operational pressures may be used as an indication.

Port collars are installed in the casing strings at Valhall for remedial purposes. The port collars are located at strategic positions in the casing strings to allow for proper zonal isolation if the log from the primary cement job indicate that the governing requirements for the cement job have not been met. A special tool is run to operate the port collars. At closed position the port collars provide a gas tight seal, but if opened direct flow paths to the annulus is present. As a result cement may be squeezed through the port collars. In some cases two port collars at different positions are opened at the same time, which allows for displacing cement through the deeper port collar and taking returns through the one above. The results from the port collar jobs are logged according to BP procedures to assure proper zonal isolation. After a port collar cement job has been performed the port collars are permanently closed.

5.7 SBT log: Cement evaluation

Acoustic logs have been applied since the 1960s to evaluate the cement status behind a casing string [56]. Although formation pressure testing (i.e. FIT or LOT) give an indication of the cement quality around the casing/liner shoe it is insufficient to determine the general cement status. As cement hydration is an exothermic process temperature logs can be run to measure the TOC (top of cement). Similarly if a radioactive tracer is added to the cement slurry it can be logged and TOC determined. The major disadvantage with the TOC logs is that the condition of the cement below TOC is not described. A major channel or heavy contamination may be present although TOC is seemingly at a sufficient height to assure zonal isolation. To reduce the uncertainty operators tend to prefer to acoustically log the cement sheath. Classical CBLs (cement bond logs) can be run, but often more sophisticated methods such as the SBT (segmented bond tool) or ultra-sonic (USIT) logs are applied. After 2012 all 18 5/8", 13 5/8" and 9 5/8" cement jobs on Valhall have been logged using the SBT log.

Acoustic logging apply the theory of sound propagation. Of main interest is the compressional and shear waves, of which the compressional waves have the higher propagation velocity. Shear waves cannot propagate through fluids. A classic CBL setup includes a transmitter which continously emits burts of acoustic energy and a receiver which measures the reflected wave pressure variations [56], [57]. A sound wave propagates spherically from the receiver. When acoustic energy reaches an interface between materials of different acoustic impedance (i.e. casing/cement, casing/mud and cement/formation) some of the energy is reflected and some is refracted as shown in Fig. 5.13 and Fig. 5.14a. Greater differences in acoustic impedance cause larger fractions of reflected energy. The acoustic impedance, Z, is defined as the product of a material's density, ρ, and sound propagation velocity, V, as shown in Eq. (5.6).

$$Z = \rho V \tag{5.6}$$

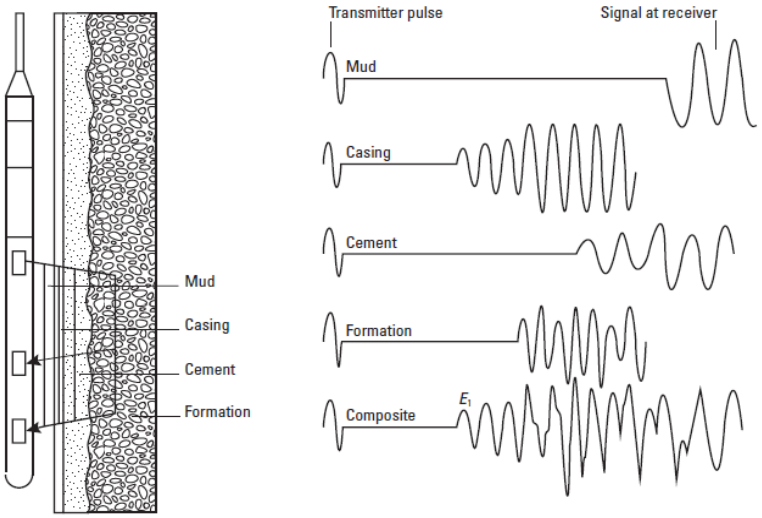

Figure 5.13: Typical sequence of wave arrivals. The VDL is a graphical representation of the composite display [56].

Good cement bond to both the casing and formation creates a favorable accoustic coupling between the casing, cement and formation. As set cement has an acoustic impedance more similar to the casing wall than drilling fluids a CBL will show a lower wave amplitude (energy) in properly cemented intervals as compared to intervals of free pipe as shown in Fig. 5.14b. Amplitude is defined as the acoustic energy of the first wave arrival. Generally, the first arrival is the casing wave arrival, but there are certain 'fast formations' in which sound propagates faster than in steel. Fig. 5.13 shows a typical wave arrival sequence. The CBL log gives an indication of the casing/cement bond if (and only if) the casing wave arrives before the formation wave. To measure the cement/formation bonding a VDL (variable density log) is run. The VDL expresses the entire wave train and similar qualitative analysis as described above is used to identify the cement/formation bonding. If the cement to formation bonding is good, the energy will go through the cement and into the formation. As formations are never perfectly homogenous arrival times will vary, and wavy patterns seen at the VDL are good examples of this. The wavy patterns provide a qualitative indication of good cement/formation bonding. Similarly, straight traces indicate that no cement is present in the annulus [56], [58]. A VDL presentation is given in Fig. 5.15.

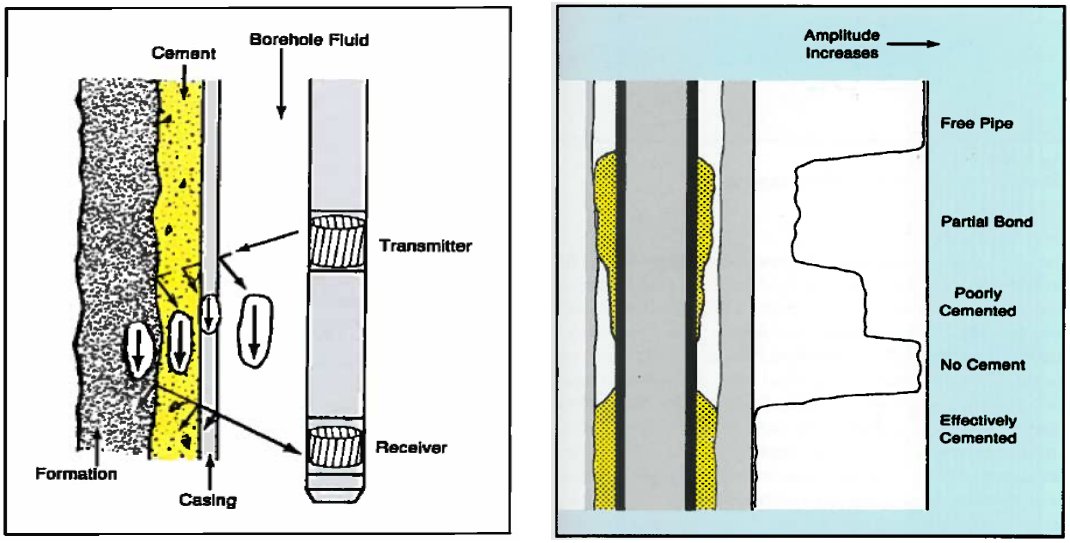

(a) Acoustic interfaces in a wellbore **(b)** Qualitative log interpretation

Figure 5.14: Simplified description of the downhole sequence during a CBL log (a), and the qualitative log interpretation (b). Low amplitudes are generally accepted as intervals of good cement.

The SBT log is an advanced acoustic log which is based upon the same principles as the CBL. It measures the cement quality, both vertically and laterally, around the circumference of the casing. Six pads, each consisting of one transmitter and one receiver, measure 60° angular segments of the cemented annulus. Illustratively, the setup can be thought of as running six independent CBLs at the same time. The purpose of the SBT log is to reduce some of the interpretation uncertainty found in the classic CBLs. Traditional bond log measurements average the cement condition around the borehole which make it very difficult to map out channels and circumferential bond variations in general. Due to the setup of the pads Baker Hughes reports

that the SBT is insensitive to fast formations, temperature and pressure fluctuations, moderate tool eccentering and borehole fluids. The six receivers measure the attenuation as opposed to amplitude. Attenuation is defined as the loss of energy. High attenuation readings indicate a well bonded segment of the casing string [57].

Some of the SBT limitations include:

- The pads need to be in contact with the casing wall to provide correct information. Debris or cement on the inside of the casing wall from the cement job may influence the log response.
- Logging casing strings larger than 20" or with a wall thickness > 1-1.125in can also be difficult as a lot of the signal is dampened by the steel and not by the annular cement bond.
- Detecting microannuli is often challenging, although in theory it is observable from the log response. From an operational perspective, the best way to determine whether or not a microannulus is present is to apply 1000 psi pressure to the casing and re-log the cement job. The pressure will expand the casing wall and (hopefully) mitigate the microannulus effect on the log response.
- On Valhall discussions have been ongoing regarding the Halliburton WellLife tail cement. Apparantly, the cement system is difficult to spot on the SBT log. Whether this is due to poor cement bonding to the casing and formation or a log related issue is yet to be determined.

Different graphical representations of the SBT log exist, but the most intuitive is the variable attenuation display. The attenuation display is made by subsequently adding the readings from all six segments. Light areas (low attenuation) indicate poor cement quality, while dark areas (high attenuation) indicate good cement quality as illustrated in Fig. 5.15.

Cement bond logs are often subject to skepticism of their validity. Especially the effect of microannuli, cement setting time prior to logging, eccentered tools, tool calibration, mud channels etc. cause uncertainties difficult to quantify [59]. Furthermore, the logs have been criticized of being too dependent upon subjective interpretations. Although the SBT and ultrasonic tools are accepted as more reliable than the original CBL-VDL setup discussions have been ongoing on Valhall whether or not one can fully trust the log outcome. Today, however, acoustic logging of the cement behind casing status is the only method to fully justify that the zonal isolation objectives have been met.

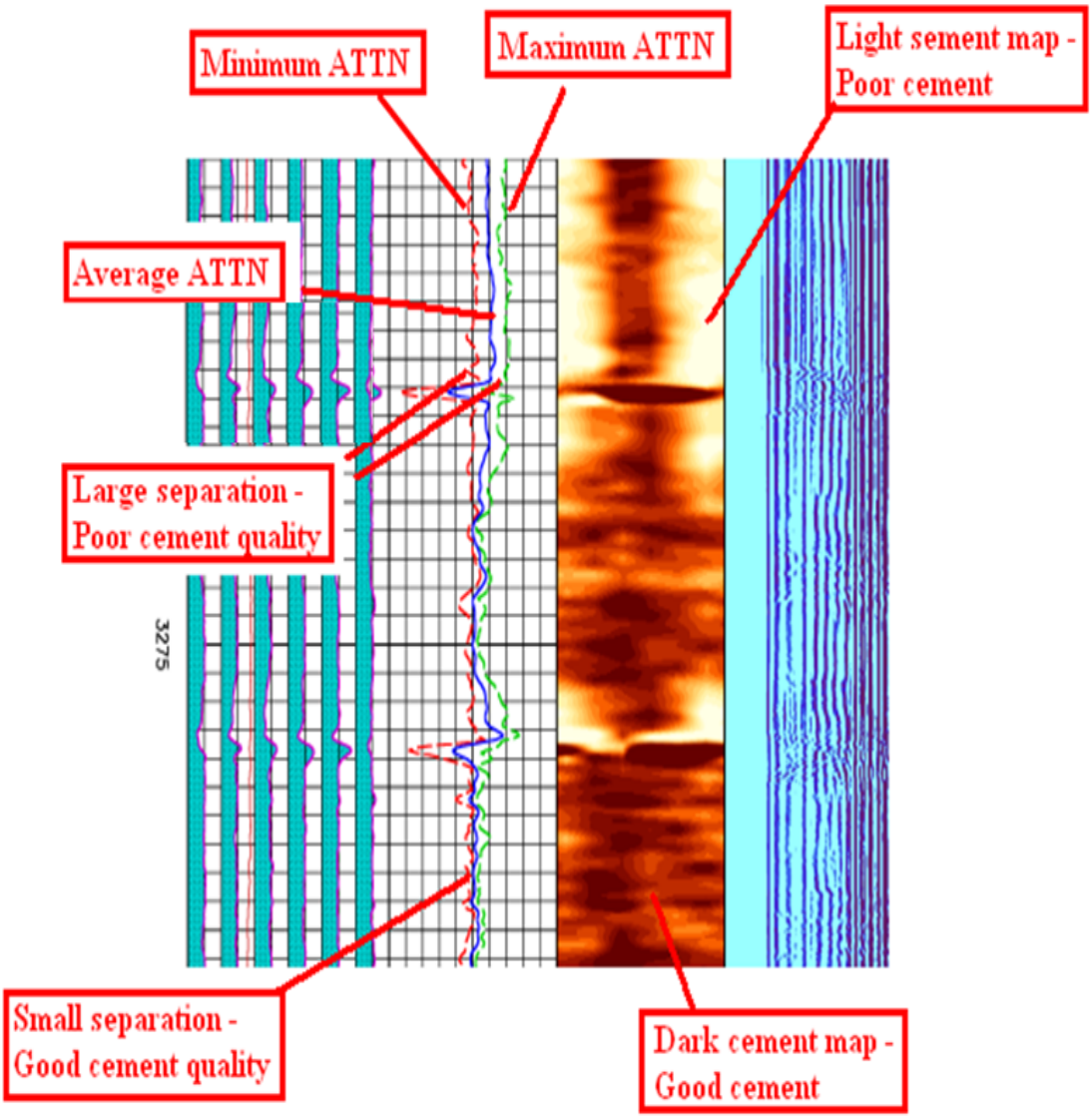

Figure 5.15: Some of the typical tracks used for interpretation of a SBT log. From the left: Track 1 measures each of the six attenuation readings from the respective pads. Track 2 shows the minimum, average and maximum attenuation. Intervals of circumferentially bonded cement correspond to high attenuation readings with low separation between minimum and maximum attenuation. Track 3 presents the attenuation display, which is basically a graphical plot of track 1 making it easier to identify channels and ares of good/poor circumferentially bonded pipe. Track 4 is the VDL where all wave arrivals are plotted as a function of time.

6 Case histories

Six wells have been drilled after the new casing design was implemented, two on Valhall IP, three on the North Flank and one on the South Flank. All 9 5/8" cement jobs have been logged. The different 9 5/8" case histories are presented chronologially with special focus on lessons learned and the steps taken to gradually improve the cement operations. From earlier experiences a thief zone was expected within DPZ 7 at approximately 1600 mTVD. All depths in this chapter are given relative to the drill floor (RKB) for the different rigs. The relevant well information have been found in EOWRs (end of well reports) and DDRs (daily drilling reports) for the respective wells [60], [61], [62], [63], [64].

6.1 Well 2/8-N-1 B

2/8-N-1 was drilled from Maersk Reacher on the North flank in 2012-2013. It was the first recent well in which the 13 5/8" casing string was set above DPZ 7. As a result the 9 5/8" liner was cemented in an environment where both DPZ 7 and DPZ 8 were exposed. It should be mentioned that the original plan was to set the 13 5/8" casing string deep as usual (below DPZ 7), but due to heavy losses and well stability issues the casing could not be run. A sidetrack was initiated and the plan revised.

6.1.1 Pre-job planning and simulations

The 9 5/8" cement job was planned with a TOC at 1950 mMD/1417 mTVD. Actual ECD and stand-off simulations are presented in Fig. 6.1 and Fig. 6.2. Weatherford provided rigid SpiraGlider HD centralizers and standoff simulations, while ECD simulations were performed by Halliburton. To minimize the risk of hole stability issues a mud weight of 14.8-15.0 ppg was recommended. Top of DPZ 7 and DPZ 8 were expected at 1609 mTVD and 2275 mTVD respectively.

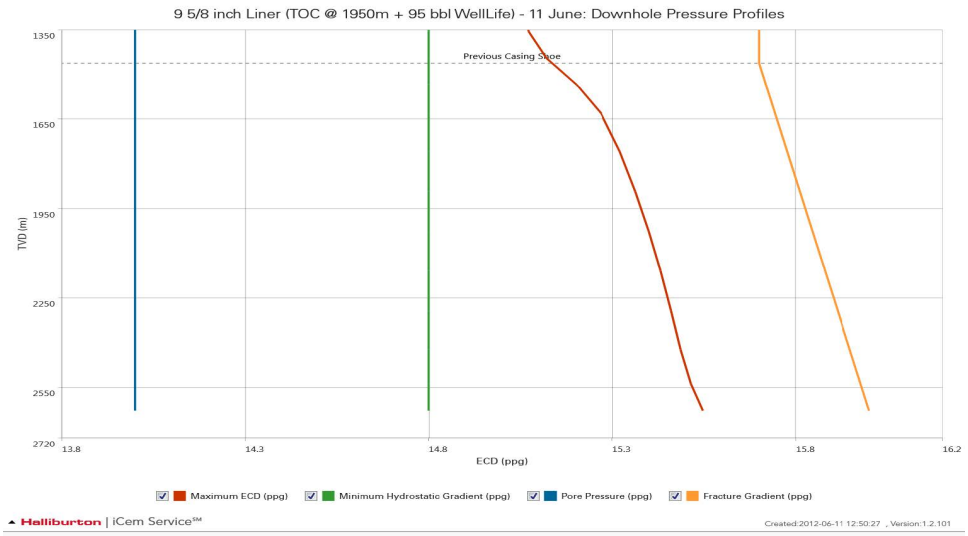

Figure 6.1: Halliburton ECD simulations (displacement rate of 420 gpm) prior to 2/8-N-1 cement job. The maximum ECD (red) should stay below the fracture gradient (yellow), but above the collapse gradient (green). Wellbore cementing pressures are seemingly well within the limits.

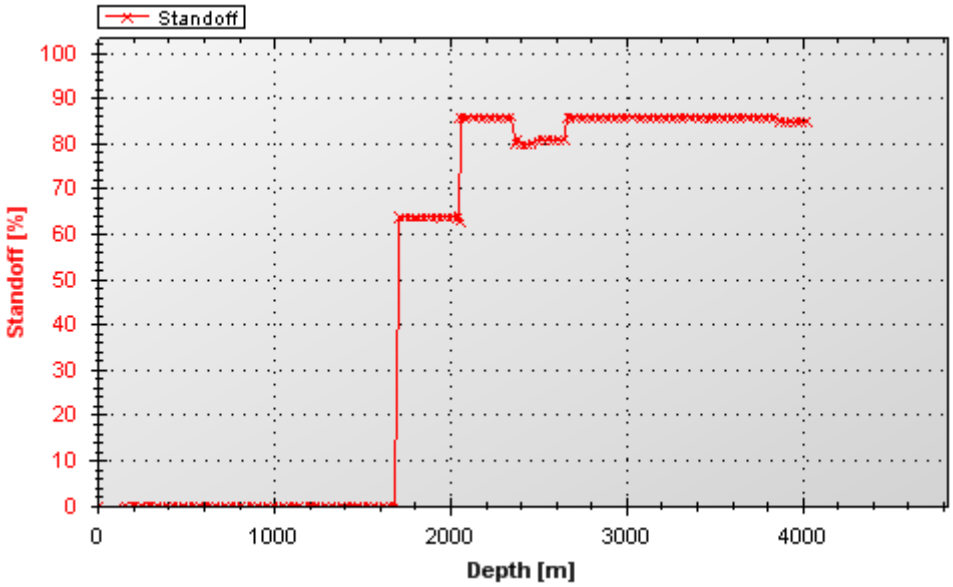

Figure 6.2: Weatherford standoff simulations ranging from 64-86%. The calculations were performed under the scenario of cement in the annulus and mud inside the liner. The assumption provide an optimistic simulation due to increased buoyance. Hence, the simulations should only be used as an upper estimate.

6.1.2 Job execution

Ran in hole with a 12 1/4" drilling BHA (bottom hole assembly) and drilled out the 13 5/8" shoetrack and 3m of new formation. Performed a FIT to 15.7 ppg EMW. Drilled 12 1/4" hole section from 2055 mMD/1463 mTVD to section TD (total depth) at 4019 mMD/2626 mTVD using 14.7-14.8 ppg CarboSea OBM. Initially some issues were experienced with the mud system which had to be conditioned as high YP values caused very high ECD readings. 0.5-1.0 ppb (lb/bbl) LC lube (synthetic graphite) and $CaCO_3$ were maintained throughout the section for lost circulation purposes. The casing setting point was selected within the Sele formation (Rogaland Gp). Circulated 8xBU while pulling out of hole to 3736 mMD. Both the amount of cuttings over the shakers and the ECD trend indicated that the hole had been circulated clean.

DPZ 7 and DPZ 8 were encountered from 2368-2530 mMD/1607-1704 mTVD and 3499-3530 mMD/2346-2366 mTVD. The actual wellbore inclination is illustrated in Fig. 6.3.

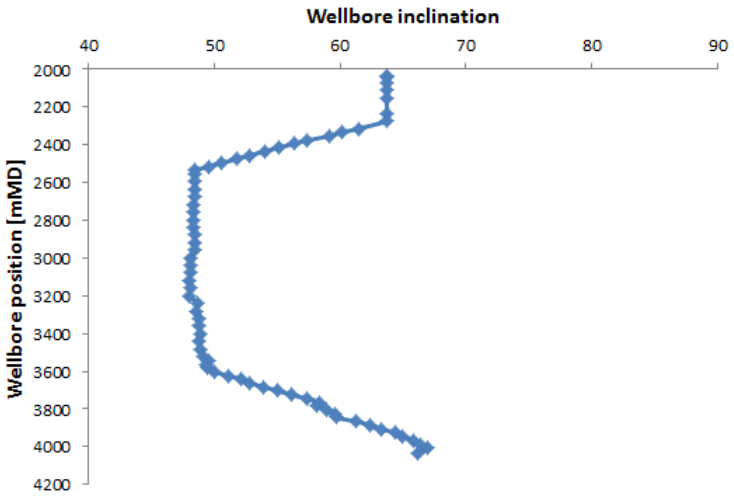

Figure 6.3: 12 1/4" section wellpath 2/8-N-1. The actual survey data is plotted against wellbore position (mMD). Inclination was kept between 48-67°.

Ran the 9 5/8" liner at 4min/stand running speed in open hole. Tried to establish circulation 4m into open hole, but 10-20% losses were experienced. The liner could not be run past a restriction encountered at 4005 mMD. Hence, the decision was taken to set liner slightly shallower than planned at 4004 mMD. Lost all returns when trying to establish circulation at TD. Installed cement head, activated hanger and prepared for cement operations. Mud gel-strengths (10sec/10min) of 15/27 lbf/100ft^2, PV of 55 cP and YP of 27 lbf/100ft^2 were recorded prior to the cement operation. The following fluids were pumped:

- 88 bbl 14.9 ppg spacer (no returns at 330 gpm).
- 350 bbl 15.0 ppg lead cement slurry (no returns at 252 gpm).
- 95 bbl 15.8 ppg WellLife tail cement slurry (no returns at 250-420 gpm).
- Displaced cement with 10 bbl spacer and 616 bbl 14.8 ppg OBM at 420 gpm. Slowed down displacement rate to 210 gpm for the last 60 bbl.

The top plug did not bump (i.e. land as expected in landing collar). Returns were not observed during the displacement process. Liner rotation could not be established when displacing the cement due to torque limitations. To evaluate the outcome of the cement job a SBT log was run 92 hours after displacing the cement.

6.1.3 SBT log

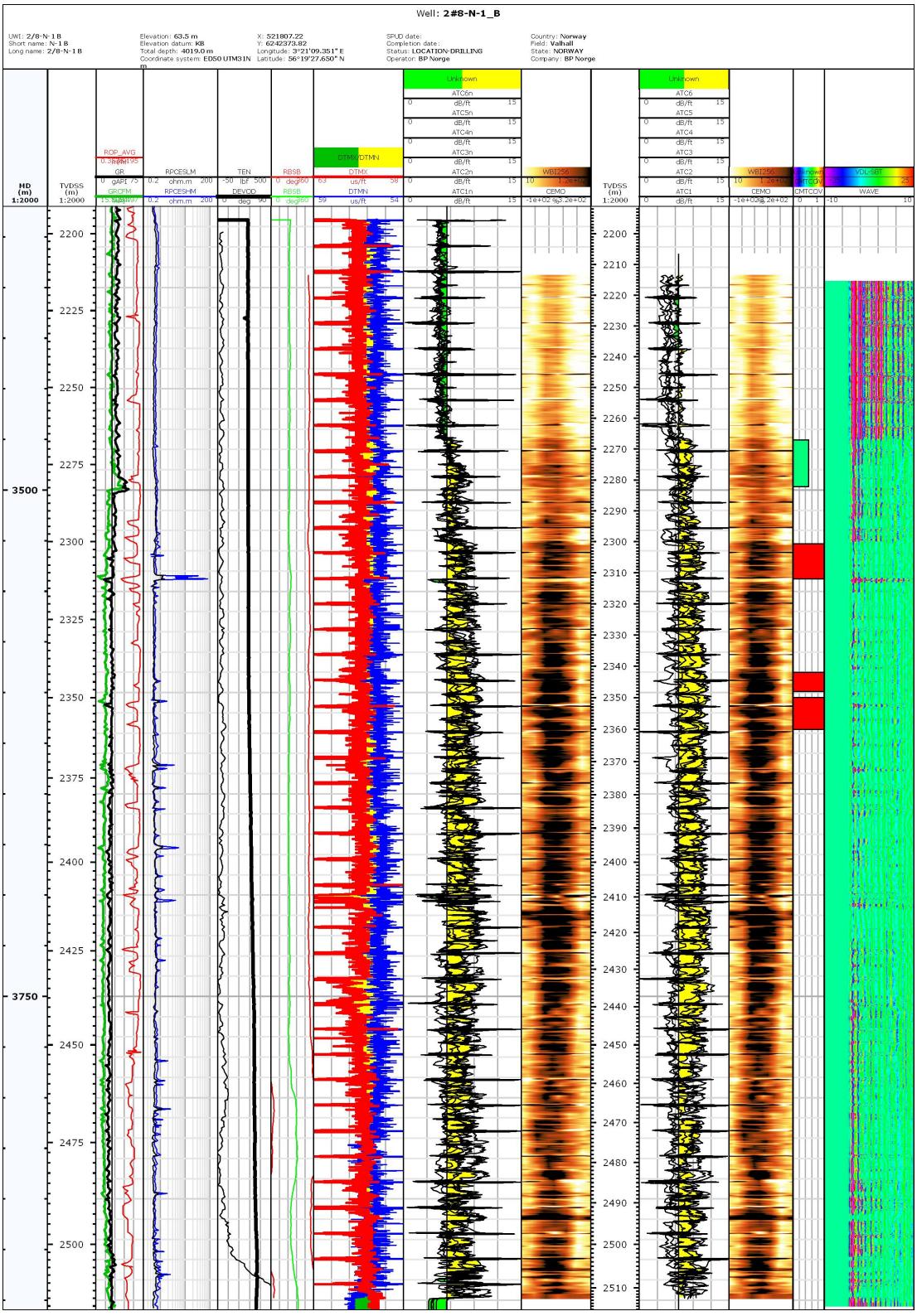

Figure 6.4: Interpreted SBT log results 2/8-N-1. Two logging runs were performed, one without applied pressure and one with 1000 psi applied pressure. No differences appeared, indicating that there is no reason to suspect a microannulus affecting the results. Red bonds indicate circumferentially bonded cement.

6.1.4 Results

The interpreted SBT log presented in Fig. 6.4 confirmed TOC at 3475 mMD/2330 mTVD which is basically at the top of DPZ 8. Severe cement channeling for the majority of the cemented interval was observed. No circumferentially bonded cement was identified above the base of DPZ 8. Three intervals of greater than 5 mTVD circumferentially bonded cement were identified as listed below.

- 2364.2-2375.5 mTVD.
- 2405.5-2411.5 mTVD.
- 2413.5-2423.5 mTVD.

A cumulative cement sheath of 27.3 mTVD provide zonal isolation between DPZ 8 and DPZ 9 (Tor reservoir). No cement was identified between DPZ 8 and DPZ 7. The log results indicate that a loss zone was present somewhere around DPZ 8.

Circulation could not be established without inducing severe losses prior to the cement job. Hence, the mud gel-strengths could not be sufficiently broken. In addition to the fact that liner rotation could not be obtained, this is thought to be one of the main reasons for the channelized cement. Possible ballooning was reported when running in hole with the liner. Initial mud losses occured when running in hole (surge), which gradually bled back during static periods. Probably a fracture was induced during drilling or running of liner, which weakened the formation strength. The ballooning effect stopped after reaching approximately 3400 mMD/2281 mTVD which may be an indication of the actual loss zone.

6.2 Well 2/8-G-23

2/8-G-23 was drilled as an injector on Valhall IP in 2013. It was the first well drilled from the crestal part of the field with the new casing design. Focus was pointed towards achieving 30 mTVD of circumferential cement below and above DPZ 8 to meet the zonal isolation requirements.

6.2.1 Pre-job planning and simulations

The outcome of the 9 5/8" liner cement job in well 2/8-N-1 was taken into consideration to further improve the job quality, both from an operational and a planning point of view. The deep loss zone observed below DPZ 8 in 2/8-N-1 was thought to be a special case, hence the main focus continued to be upon the more documented loss zone within DPZ 7. Lost circulation during displacement is generally not considered a major issue if the loss zone is well above DPZ 8. However, it is impossible to fully quantify the loss zone just from the job parameters. ECD trends, mud weights and LCM additives during drilling were highlighted to avoid weakening the formation prior to running and cementing the 9 5/8" liner. The Halliburton ECD simulations performed prior to the cement job is presented in Fig. 6.5. Liner rotation was identified as a key success factor to obtain circumferentially bonded cement. TOC was expected at approximately 2000 mMD/1600 mTVD.

The practice of running the rigid SpiraGlider HD centralizers was continued in well 2/8-G-23. Simulated standoff ratios ranged from 70-80% in open hole as shown in Fig. 6.6.

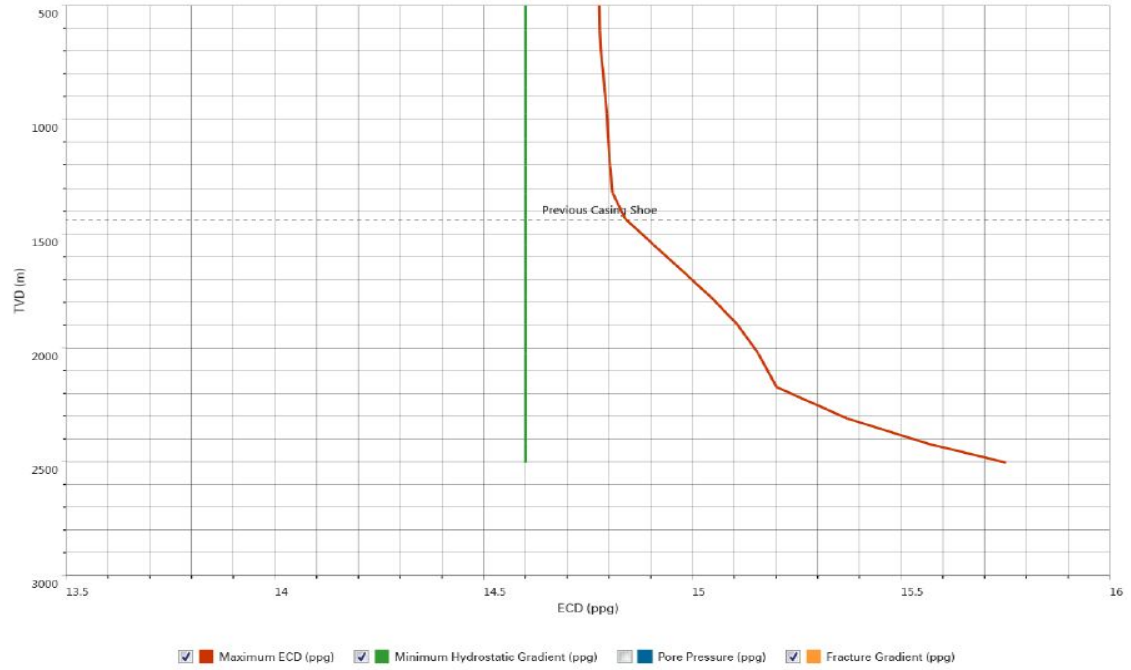

Figure 6.5: Halliburton ECD simulations (displacement rate of 336 gpm) prior to 2/8-G-23 cement job. Simulations are based upon in-gauge hole conditions. The maximum ECD (red) should stay below the fracture gradient, but above the collapse gradient (green). The fracture gradient has not been included in the graph, but the well pressures were reportedly within the limits.

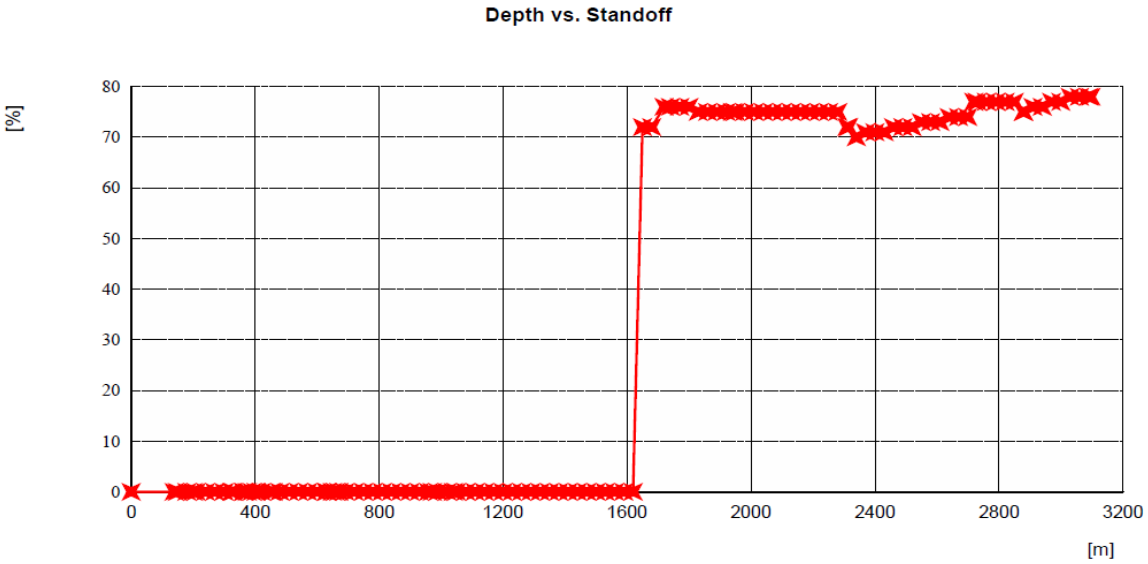

Figure 6.6: Weatherford standoff simulations plotted against depth. The calculations were performed under the scenario of mud both inside and outside of the liner. One SpiraGlider centralizer was installed per liner joint.

6.2.2 Job execution

Due to insufficient cement status around the 13 5/8" shoe a cement squeeze job had to be performed to obtain the desired FIT prior to drilling the 12 1/4" section. Successfully performed a FIT to 15.4 ppg EMW after the squeeze job. The 12 1/4" hole section was drilled from 1752-3121 mMD/1457-2504 mTVD using 14.6 ppg CarboSea OBM. Logs confirmed DPZ 7 from 1825-2045 mMD/1514-1676 mTVD and DPZ 8 from 2682-2729 mMD/2196-2239 mTVD. As seen from Fig. 6.7 wellbore inclination within DPZ 8 was significantly reduced as compared to 2/8-N-1 which is highly beneficial from a wellbore stability point of view. A stringer was penetrated at 2375 mMD and returns were partially lost. Several stringers were penetrated just above and within DPZ 8. Drilling commenced to section TD located 7 mTVD into the Sele formation wihtout any further issues. Connection gas was observed from approximately 2650 mMD, but the hole was seemingly in good condition. Maximum ECD at TD was recorded to 15.15 ppg. Circulated 5xBU while continuing to add LC-lube and $CaCO_3$ to bridge off fractures. The CarboSea mud was conditioned to optimize its rheology prior to the cement operations. No indication of poor hole conditions was seen when pulling out of hole.

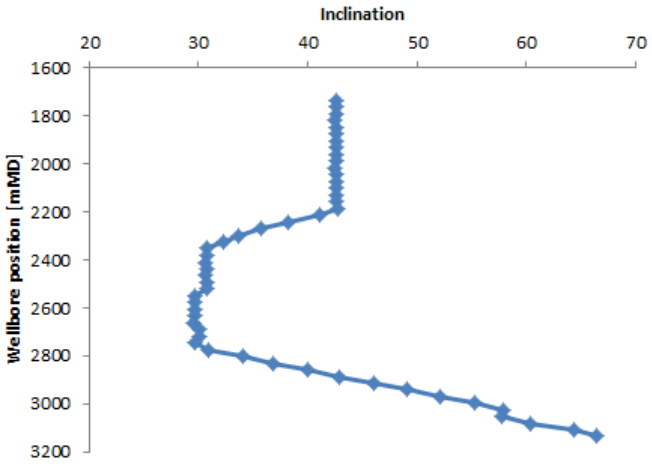

Figure 6.7: 12 1/4" section wellpath 2/8-G-23. The actual survey data is plotted against wellbore position (mMD). Inclination was kept between 29-66°.

Gas levels of 72% were recorded when running in hole with the liner. Ran in hole in stages while continously circulating out gas until acceptable levels were achieved. Minor losses were observed when running in hole with liner, but the hole condition was overall very good. Positioned liner at 3120 mMD/2503.5 mTVD and managed to initiate liner rotation. Attempted to break circulation at 101 gpm which subsequently induced losses. Returns were only observed when liner was rotated. Decision was taken to proceed to cement job as planned. Ideally, a longer circulation period should have been achieved to mobilize the gelled mud. Installed cement head, activated hanger and prepared for cement operations. Mud gel-strengths (10sec/10min) of 18/27 lbf/100ft^2, PV of 38 cP and YP of 24 lbf/100ft^2 were recorded prior to the cement operation.

The following fluids were pumped:

- 120 bbl 14.7 ppg spacer (no returns at 170 gpm).
- 138 bbl 14.7 ppg GasStop lead cement slurry (no returns at 170 gpm).
- 80 bbl 15.2 ppg WellLife tail cement slurry (minor returns, approx. 10 bbl, at 220 gpm).
- 26 bbl 15.8 ppg conventional tail cement slurry (no returns at 176 gpm).
- Displaced cement with 14 bbl spacer and 436 bbl 14.6 ppg OBM at 345 gpm. Slowed down displacement rate to 169 gpm prior to landing top plug. Plug bumped according to plan (1 bbl early).

The top plug landed after 450 bbl which was 1.1 bbl (7 strokes) earlier than the estimated top plug bump volume. 35 rpm liner rotation was maintained throughout the displacement process. Total losses were experienced during the entire displacement, effectively indicating that a loss zone was present somewhere along the wellpath. A SBT log was run 77 hours after bumping the plug to evaluate the cement job.

6.2.3 SBT log

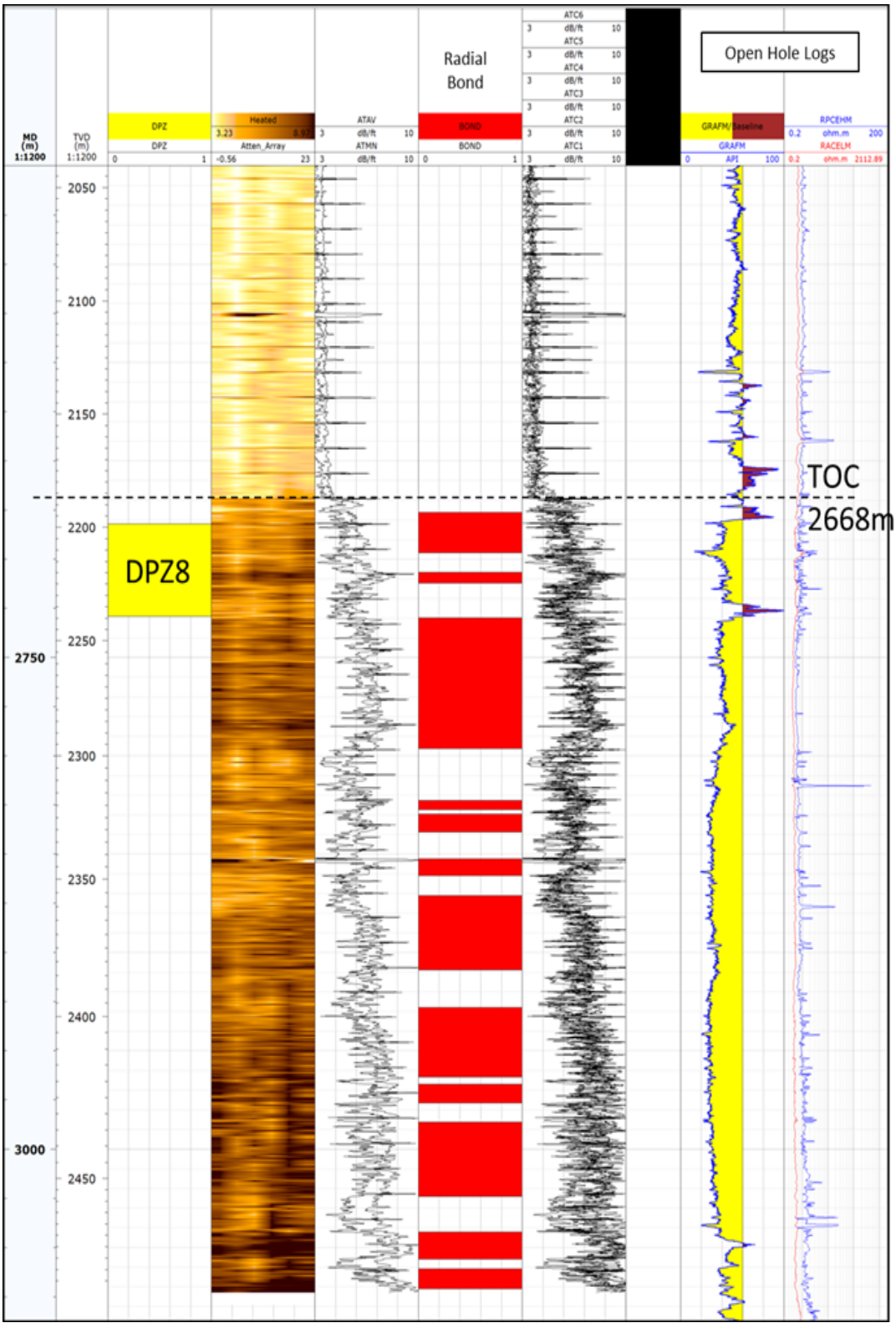

Figure 6.8: Interpreted SBT log results G-23. A clean cut TOC is seen at 2668 mMD. Circumferentially bonded cement intervals of sufficient height are marked by red bonds. The log showed very good cement quality below TOC. Due to the lack of circumferentially bonded cement above DPZ 8 a remedial job was later performed through a port collar.

6.2.4 Results

The interpreted SBT log is presented in Fig. 6.8. Actual TOC was found at 2668 mMD/2184 mTVD as compared to the planned TOC at approximately 2000 mMD/ 1600 mTVD. The TOC coincides almost perfectly with the top of DPZ 8. Most likely the loss zone was located within one of the many stringers drilled above and within DPZ 8. Reducing the inclination across DPZ 8 has probably contributed to increasing the available mud window in terms of increasing the fracture initiation pressure. Although proper circulation prior to the cement job could not be achieved, it is thought that the liner rotation significantly improved the displacement efficiency. Even at lower displacement rates the SBT log did not indicate lowside channeling as seen in well 2/8-N-1. As per GP 10-60 requirements a minimum of 30 mTVD circumferentially bonded cement above and below DPZ 8 is needed. Only 9 mTVD of circumferential cement was achieved above DPZ 8. As a result a remedial port collar squeeze job was sucessfully performed at a later stage (after running 7 5/8" drilling liner) to improve the zonal isolation status.

Significant improvements were seen as compared to the 9 5/8" liner cement job on 2/8-N-1. More than 250 mTVD of circumferentially bonded cement were observed from the shoe to the TOC.

6.3 Well 2/8-N-9 T4

2/8-N-9 was the third and final well of the 2012/2013 North Flank drilling campaign. It was drilled as a horizontal producer in the Tor formation in 2013. Prior to drilling the 12 1/4" section three technical sidetracks had been performed in shallower hole sections due to hole problems.

6.3.1 Pre job planning and simulations

To meet the requirements of GP 10-60 the lessons learned from well 2/8-N-1 and 2/8-G-23 were carefully analysed. It was decided to displace the wellbore to a low rheology mud system, Synteq OBM, prior to running the liner to improve displacement effiency and to reduce the risk of losses below and within DPZ 8 as seen in the previously drilled wells. To reduce the ECD while cementing a low density preflush was planned for. The cement job was planned with a TOC at 2850 mMD/1800 mTVD (below DPZ 7).

Two 12.25" Centek Slider II bow type centralizers were installed per liner joint. Stand-off simulations indicated 85-90% in open hole as illustrated in Fig. 6.10. This represented a clear improvement from the previously applied rigid Spiraglider centralizers.

Different fluid and displacement scenarios were simulated to land on the ECD profile seen in Fig. 6.9. Decreasing the displacement rate from 420 gpm to 336 gpm as compared to well 2/8-N-1 B in combination with 150 bbl 14.4 ppg preflush contributed to an acceptable pressure regime.

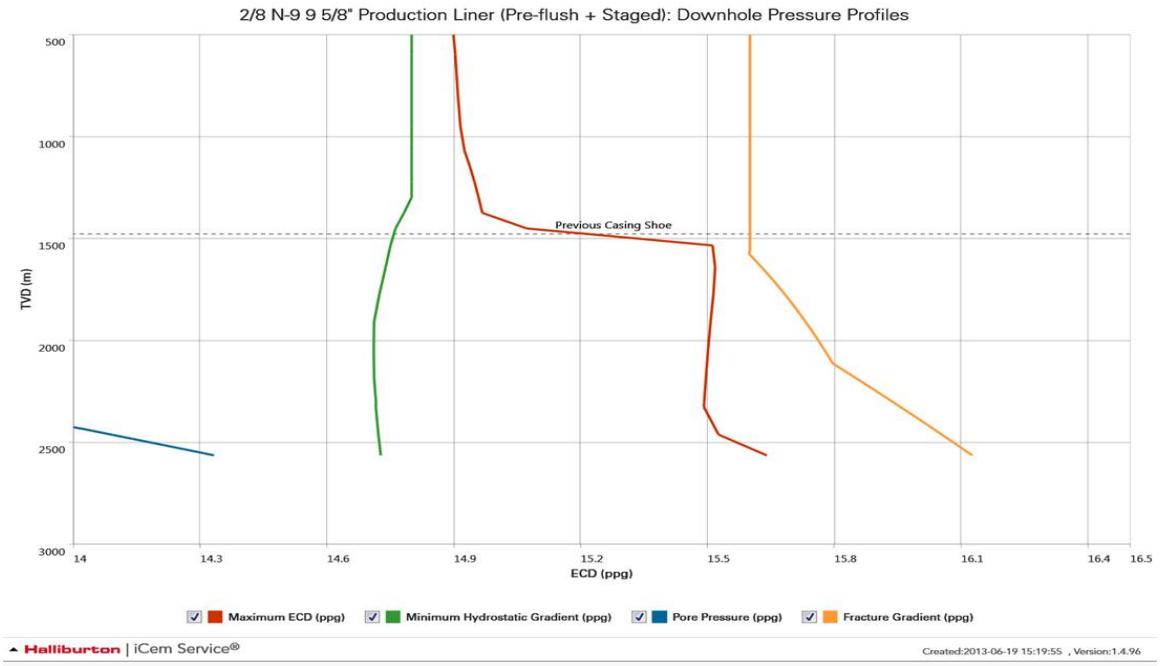

Figure 6.9: Halliburton ECD simulations (displacement rate of 336 gpm) prior to 2/8-N-9 T4 cement job with 14.8 ppg Synteq OBM. Simulations are based upon in-gauge hole conditions. The maximum ECD (red) should stay below the fracture gradient (yellow), but above the collapse gradient (green). The well pressures were seemingly well within the limits. However, predicting stringer depths and the corresponding fracture gradient have proven difficult.

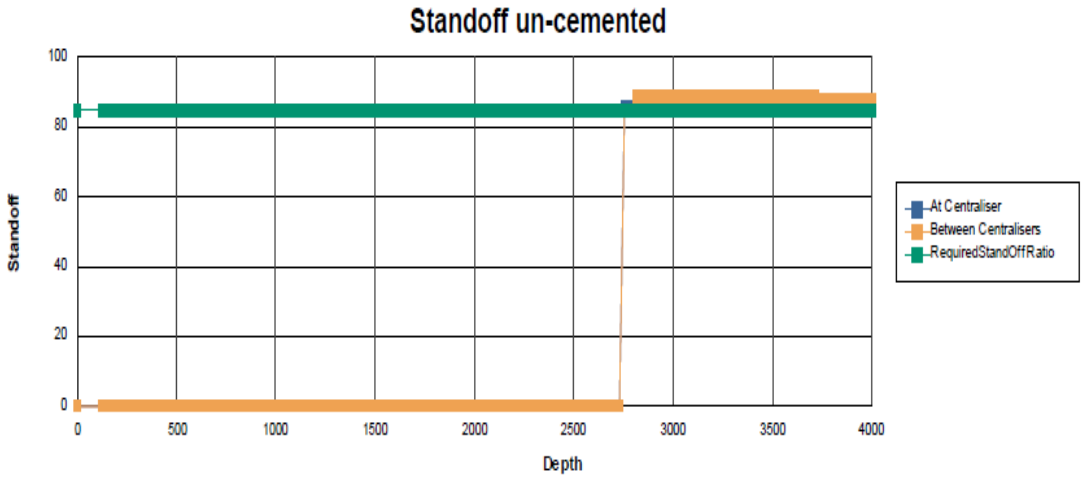

Figure 6.10: Centek standoff simulations plotted against depth. The calculations were performed under the scenario of mud both inside and outside of the liner. Two Slider II bow-type centralizers were installed per liner joint. The 'at centralizer' (blue) and 'between centralizers' (yellow) coincides, which is the reason why the 'at centralizer' simulations apparantly are missing. A required standoff ratio of 85% was pre-defined to optimize displacement efficiency.

6.3.2 Job execution

Observed some pack-off tendencies when drilling out of the 13 5/8" shoe. Performed a FIT to 15.6 ppg. Drilled 12 1/4" section from 2283 mMD/1481 mTVD to section TD at 4020 mMD/2565 mTVD using 14.8 ppg CarboSea OBM. The actual wellbore inclination is shown in Fig. 6.11. Logs confirmed DPZ 7 and DPZ 8 at 2548-2763 mMD/1609-1743 mTVD and 3601-3627 mMD/2324-2342 mTVD respectively. Pack-off tendencies were seen when passing a fault zone at 2463 mMD/1563 mTVD. Initially added 1 ppb of LC-lube and $CaCO_3$ at an 80/20 blend ratio. From 3550 mMD the concentration was increased to 3 ppb at a 50/50 blend ratio to artifically increase the fracture gradient in stringers in the region near DPZ 8. Drilling commenced without any major issues. A check trip was performed to the 13 5/8" shoe prior to displacing the well to Synteq OBM. Hole conditions appeared good. Displacement to Synteq went according to plan with the exception of increased drag and torque values indicating an increased friction factor as compared to the CarboSea OBM.

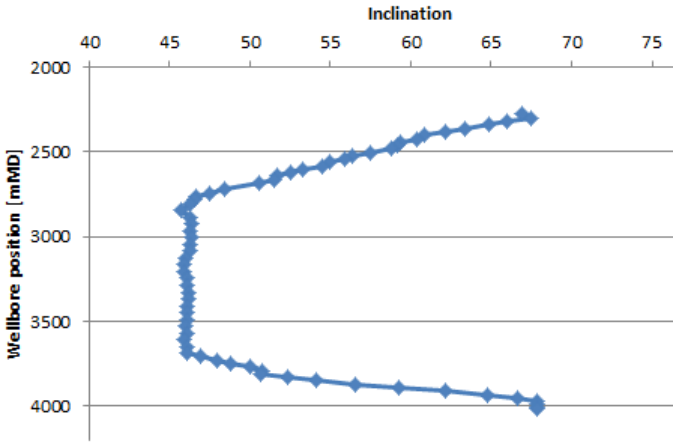

Figure 6.11: 12 1/4" section wellpath 2/8-N-9 T4. The actual survey data is plotted against wellbore position (mMD). Inclination was kept between 46-68°.

Ran 9 5/8" liner at 10min/stand to setting depth at 4015 mMD/2563 mTVD. Neither significant losses nor major problems was reported when running in hole. Sat hanger, installed cement head and prepared for cement operations. Liner rotation could not be established due to torque limitations. Stalled out at 28 kftlbs. Decision was made to go through with the cement operation as per plan. Mud gel-strengths (10sec/10min) of 11/18 lbf/100ft^2, PV of 30 cP and YP of 15 lbf/100ft^2 were recorded prior to the cement operation. The following fluids were pumped:

- 150 bbl 14.4 ppg Synteq OBM preflush (observed partial returns at 330 gpm).
- 120 bbl 14.9 ppg spacer (no returns at 335 gpm)
- 125 bbl 15.0 ppg lead cement slurry (no returns at 335 gpm)
- 90 bbl 15.8 ppg WellLife tail cement slurry (partial, increasing to full returns at 210 gpm)
- 40 bbl 15.8 ppg conventional tail cement slurry (full returns at 210 gpm)

- Displaced cement with 11 bbl spacer and 576 bbl 14.8 ppg Synteq OBM at 165 gpm. The displacement rate was reduced from the planned 336 gpm to 165 gpm based on an evaluation of the lost circulation events. Lost a total of 378 bbl during the displacement. No returns seen after 462 bbl pumped (bottom plug landed after 336 bbl).

The top plug landed after 587 bbl which was 0.5 bbl (4 strokes) earlier than the estimated top plug bump volume. Even at half the planned displacement rate severe downhole losses were experienced. A total of approximately 20 bbl mud returned after the lead cement entered the annulus. If assuming a deep loss zone the returns is equivalent to a TOC at 3908 mMD in an in-gauge hole with no cement channeling. A SBT log was run 48 hours after bumping the plug to quantify the outcome of the cement job.

6.3.3 SBT log

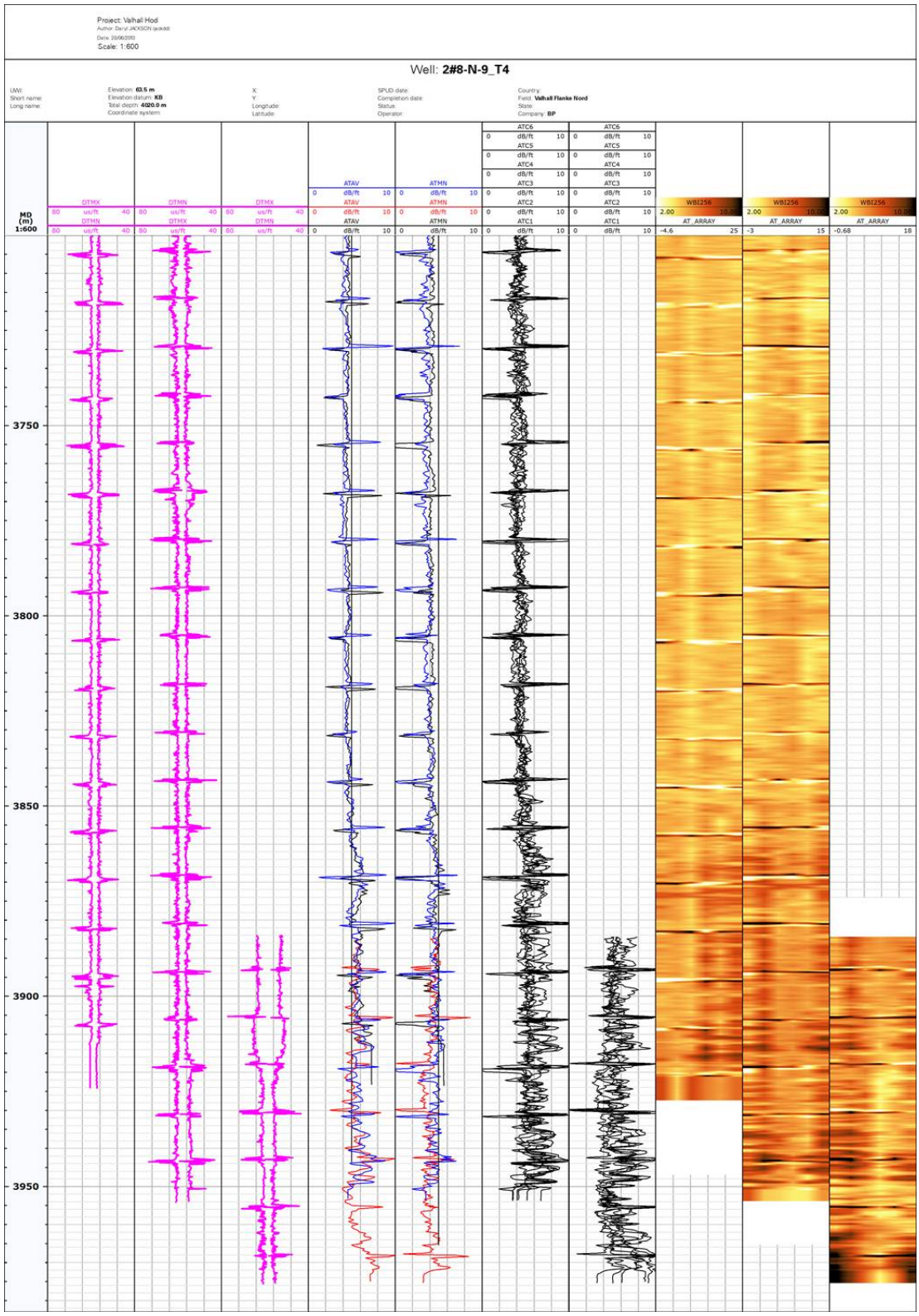

Figure 6.12: Interpreted SBT log results N-9 T4. TOC is seen at 3850 mMD/2490 mTVD, but the cement below TOC is channelized and generally of poor quality. The requirements of GP 10-60 were not met below nor above DPZ 8.

6.3.4 Results

The interpreted SBT log is presented in Fig. 6.12. TOC was found at 3850mMD/ 2490mTVD, but the cement below this was channelized and above there was a very long section of circumferential free pipe. The requirements given in GP-10-60 were not fulfilled. The data quality appeared good so there is no reason to doubt the correctness of the data. Furthermore, a SBT re-log was performed with 1000 psi pressure, but no changes appeared as compared to the previous log (thus there is no reason to suspect a micro annulus).

When pumping the low density pre-flush losses were experienced although the calculated ECD was not higher than when drilling the same formation without losses (15.3-15.4 ppg). As a result one theory is that the formation was broken down between drilling and pumping the pre-flush. Two possible events were addressed. Firstly, when circulating the liner with 450 gpm Synteq mud simulations showed that the ECD at the 13 5/8" shoe was 15.9-16.0 ppg (above fracture gradient). Secondly, when setting the liner hanger with 3700 psi surface pressure some of the pressure is transmitted to the formation. Both events were supported by losses.

A fault was drilled at 3862 mMD which overlaps fairly well with the logged TOC. It should however be noted that the cement below 3850 mMD was channelized. No rotation and a very low displacement rate of 165 gpm are probably the main contributors of the poor annular cement quality seen below 3850 mMD.

Clearly the zonal isolation requirements were not met. Port collars were installed in the string for remedial cementing purposes, but given their location it was not deemed possible to provide barriers both above and below DPZ 8. Decision was taken to cut and pull the 9 5/8" liner, P&A 2/8-N-9 T4 12 1/4" section and redrill the entire section. The process initiated approximately one month of additional work. At a rig-rate of close to 5 million NOK per day the cost of a poor primary cement job is enormous.

6.4 Well 2/8-N-9 T6

After completing the P&A operations in well 2/8-N-9 T4 and finalizing the plan on how to improve the primary cement job on the next sidetrack, operations could continue. An initial attempt to kick-off (2/8-N-9 T5) was unsuccessfull. Finally, 2/8-N-9 T6 was initiated and drilling could commence.

6.4.1 Pre job planning and simulations

Based upon a thorough evaluation of the failed 9 5/8" liner cement job on 2/8-N-9 T4 an improved plan was prepared. The following changes were addressed and implemented in the plan to reduce the risk of losses and poor displacement efficiency:

- Reduce pump rate when circulating through liner prior to cementation. As the fluid flow area is reduced compared to when there is drill pipe in hole, the velocity will increase, and hence the change in ECD can be significant.

- Reduce the ROP (rate of penetration). The inclination in the section is mainly between 45-60° and cutting beds at the lowside is a concern for proper hole cleaning. Reducing the ROP will provide more time circulating and breaking the beds.
- Increase concentration of LCM when drilling through DPZ 7 and DPZ 8. Efforts should be made to keep the concentration of LC-lube at a minimum of 5 ppb throughout the section.
- Increase torque rating of liner running tool and liner connections to be able to rotate the string during cementing. A BP connection specialist confirmed that the applied threads (Vam Top) could be made up to 40 kftlbs as compared to the 23.150 kftlbs on T4. This reduces the risk of stalling out when trying establish liner rotation.
- Set shallower 12 1/4" TD to reduce probability of deep losses. A shorter wellbore also reduces the ECD and torque.
- Geomechanical studies showed that a reduction in mud weight can be evaluated during drilling.
- Increase volume of pre-flush to further decrease the ECD by decreasing the effective weight of the hydrostatic column of mud/preflush/spacer/cement.
- Reduce number of centralizers from 2 to 1 per joint as there were some concerns regarding pack-offs.
- Cancel WellLife cement as it is difficult to spot on the SBT log.
- Add Omnilube V2 lubricator to the Synteq mud to reduce the friction factor. Ideally, this will allow for liner rotation.
- Spend more time cleaning the hole prior to displacing to Synteq OBM.

The planned TOC was at 2982 mMD/1907 mTVD. As the new wellpath, T6, was very similar to the previous one, T4, new standoff simulations were not performed. It was decided to replace some of the 12.25" Centek Slider II centralizers used on T4 with 13.5" Centek UROS bow-type centralizers. Replacing the Slider II with UROS in the original T4 simulation (2 centralizers per joint) showed perfect simulated centralization (100 %). Even running 1 UROS centralizer per joint showed 94-100 % stand-off. Due to limited availability only the first 9 joints above the shoetrack were dressed with 2xUROS centralizers per joint. The remaining centralized joints included the Slider II centralizers. Fig. 6.14 shows the post-job stand-off simulation performed under the assumption of a hole size of 13 1/2".

Several of the planned changes were implemented to reduce the ECD. The simulation in Fig. 6.13 was performed with actual well data. Of main interest is the fact that Carbosea OBM was in the hole, and the actual hole size was estimated to 14.0". As compared to 2/8-N-9 T4 (Fig. 6.9) the ECD at TD was reduced from 15.62 ppg to 15.38 ppg. It should, however, be mentioned that the hole size probably was

overestimated, and hence the T6 ECD simulations shown in Fig. 6.13 only provide a lower limit.

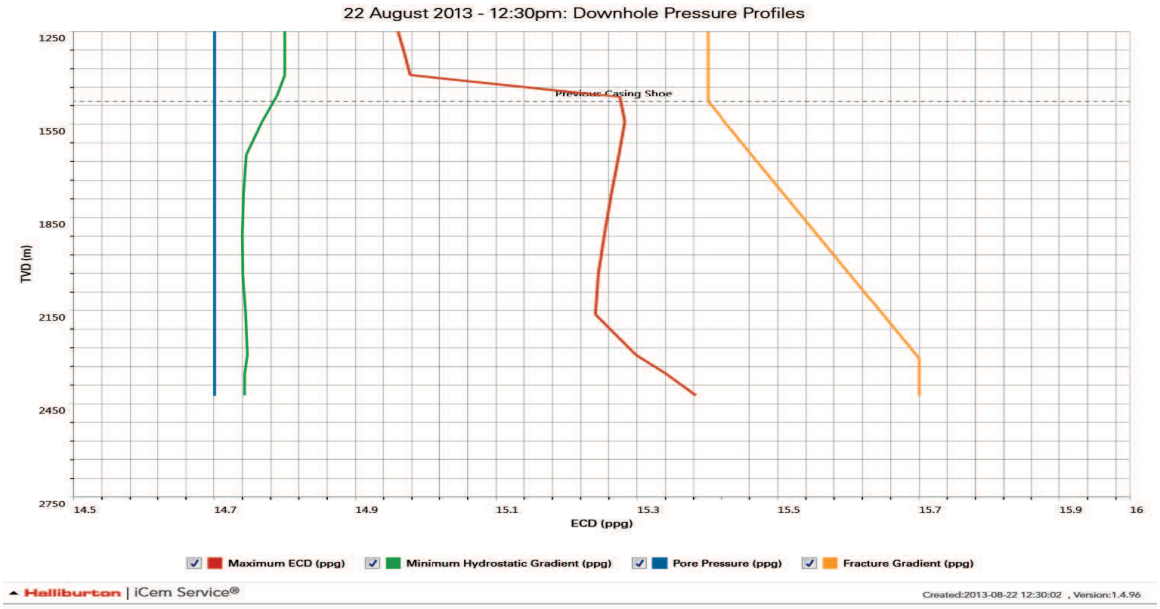

Figure 6.13: Halliburton ECD simulations (displacement rate of 336 gpm) prior to 2/8-N-9 T6 cement job with 14.8 ppg CarboSea OBM. Simulations are based upon caliper data indicating a hole size of 14". The maximum ECD (red) should stay below the fracture gradient (yellow), but above the collapse gradient (green). The well pressures were seemingly well within the limits. However, predicting stringer depths and the corresponding fracture gradient have proven difficult.

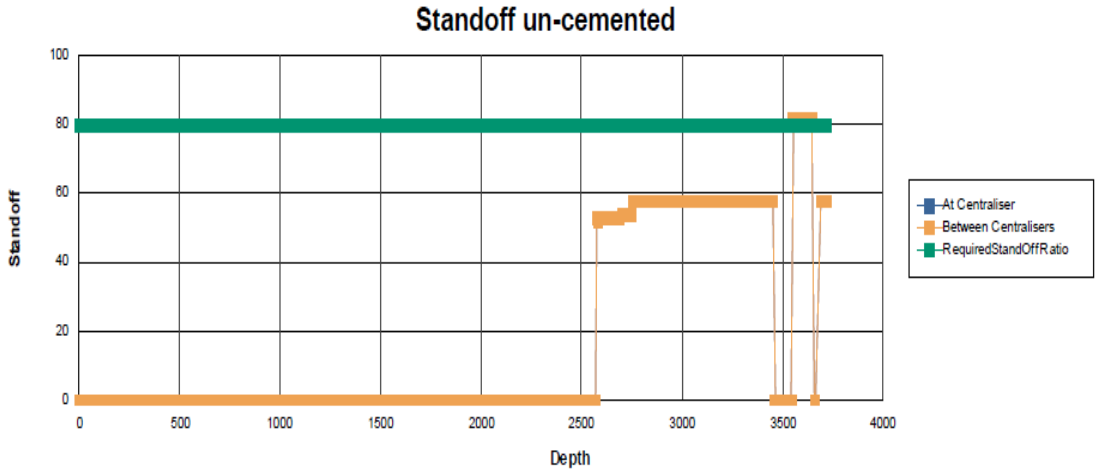

Figure 6.14: Centek standoff simulations plotted against depth. The simulations were performed after the 2/8-N-9 T6 cement job for data gathering purposes. The calculations were performed under the scenario of a hole size of 13 1/2" and mud both inside and outside of the liner. UROS centralizers were applied on the bottom 9 liner joints, wheras the remaining centralized joints were dressed with Slider II centralizers. Due to an error with the simulation software the liner joints which are not centralized are automatically calculated as 0% stand-off. Stand-off values of 52-80% were simulated. A standoff of 80% was required to optimize displacement efficiency.

6.4.2 Job execution

Re-drilled 12 1/4" section from kick-off point at 2310 mMD/1492 mTVD to section TD at 3718 mMD/2422 mTVD using 14.8 ppg CarboSea OBM. TD was set in the middle Eocene, 143 mTVD shallower as compared to T4. The average ROP was reduced from 39 m/hr in T4 to 21 m/hr in T6. Hole packed off at 2452 mMD/1561 mTVD in a stringer area. Lost 15 bbl to the formation. Observed ECD spikes of 15.5 ppg when working the trouble area. To facilitate proper hole cleaning 30 bbl high viscosity/high density sweeps were circulated around every 300m drilled. The first sweep at 2734 mMD led to an increased amount of cuttings over the shakers, but the effect of the later sweeps were not as pronounced. Pack-off tendencies were observed at 2740 mMD. Logs confirmed DPZ 7 and DPZ 8 at 2538-2738 mMD/1609-1738 mTVD and 3569-3595 mMD/2318-2336 mTVD respectively. Initiated 6xBU at TD to clean the hole while slowly pulling out to 3499mMD. 200m of caliper data was obtained to optimize cement volumes. The hole was observed to be in good condition. Performed wipertrip to 13 5/8" casing shoe and ran back in hole to displace the well to Synteq OBM.

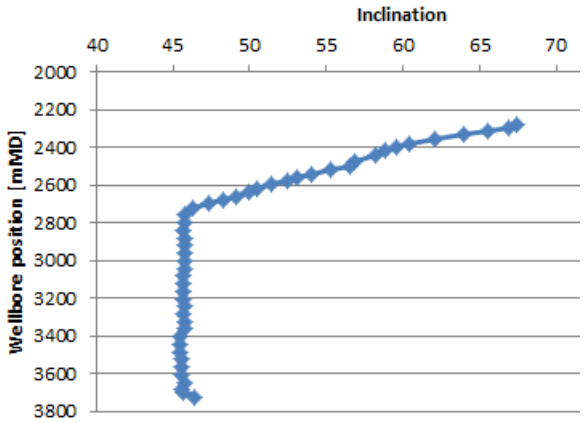

Figure 6.15: 12 1/4" section wellpath 2/8-N-9 T6. The actual survey data is plotted against wellbore position (mMD). Inclination was kept between 45-68°.

Circulated several BU when back at TD. Significant amounts of cuttings were observed over shakers during the first 3xBU. Displaced hole to 14.8 ppg Synteq OBM, but the torque increased as observed in well T4, even though lubricants were added to the mud system. Pulled out to 13 5/8" shoe and observed 80 klbs increase in drag as compared to previous trip. More than 20 ppb of different LCM were introduced to the Synteq OBM which may have contributed to strengthen the formation. Decision was made to run back to TD and displace back to "thin" 14.8 ppg CarboSea OBM to maximize probability of obtaining liner rotation during cement job. Pumped a total of 14xBU at 1000-1200 gpm flowrate after displacing to CarboSea while pulling out to 3345 mMD/2161 mTVD. Large amounts of cuttings were observed over the shakers. Lubricated out of hole (i.e. pumped at low flow rates with no rotation) and prepared for liner running. Lubricating out of hole is thought to be beneficial as it reduces the risk of failed material entering the wellbore.

Ran in hole with 9 5/8" liner. Significant barite sag was observed of the thin (i.e. low rheology) CarboSea OBM. Mud weights out of hole were reported in the region

between 13.9-15.4 ppg. No losses observed, but some restrictions were encountered in region between 3155-3534 mMD/2029-2294 mTVD. Several pack-off tendencies observed when breaking circulation and establishing rotation near section TD. Worked area between 3627-3718 mMD. Hole conditions improved, and stable 14.8 ppg mud weights were recorded at surface. Staged up flow to 300 gpm. Installed cement head, activated liner hanger and prepared for cement operation.

Major uncertainties regarding the actual hole size made the volume schedule difficult to decide. Three caliper logs were performed in area between 3675-3475 mMD with different mud systems. The caliper logs got increasingly confusing as time went on, indicating an increasingly large hole size. Caliper data and volume of cuttings were used to calculate the actual average hole size. Three different hole diameter calculations were performed:

1. 13.4" from caliper data and pumped volume data when displacing to Synteq.
2. 14.1" from caliper relogs and mud loss plot prior to pulling out of hole after displacing back to CarboSea.
3. 13.5" from caliper memory data.

The cement job was designed assuming a 14" hole size. Established 20 rpm liner rotation with 24 kftlbs torque. Mud gel-strengths (10sec/10min) of 13/17 lbf/100ft^2, PV of 41 cP and YP of 13 lbf/100ft^2 were recorded prior to the cement operation. The flow rate was increased in stages to 330 gpm with no losses. The following fluids were pumped:

- 176 bbl 14.4 ppg pre-flush at 330 gpm (no losses).
- 120 bbl 14.9 ppg spacer at 330 gpm (no losses).
- 133 bbl 15.0 ppg lead cement at 210 gpm (no losses).
- 120 bbl 15.8 ppg tail slurry at 170 gpm (no losses).
- Displaced cement with 11 bbl 14.9 ppg spacer and 509 bbl 14.8 ppg CarboSea OBM at 330 gpm. No losses observed during displacement.

The top plug landed after 521 bbl which was 0.7 bbl (6 strokes) later than the estimated top plug bump volume. Maintained 30 rpm rotation during entire displacement process. The job went perfectly according to plan with no losses for the first time on Valhall with both DPZ 8 and DPZ 7 exposed. To confirm that the cement had bonded properly to both the formation and casing a SBT log was run 63 hours after bumping the plug to evaluate the results.

6.4.3 SBT log

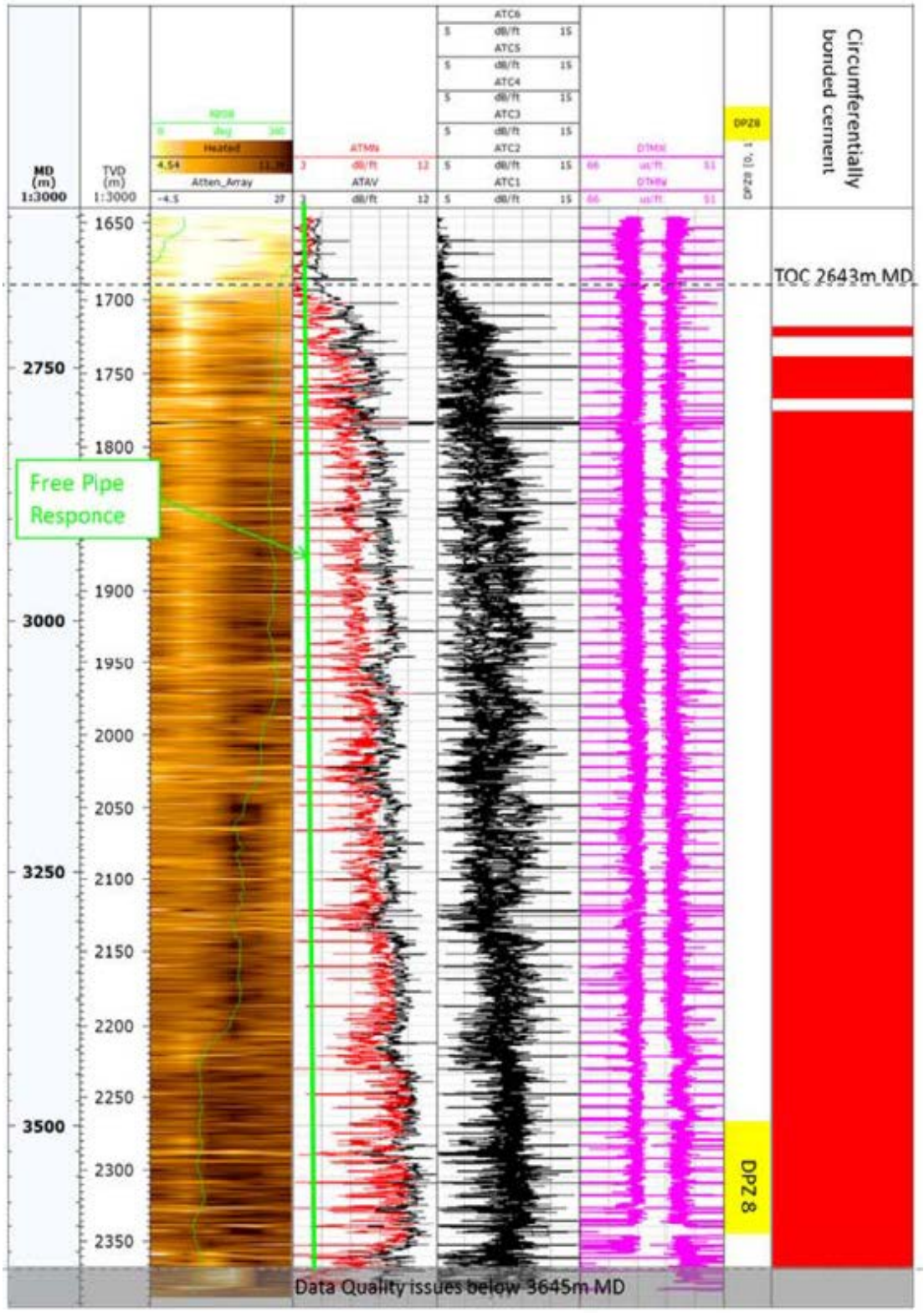

Figure 6.16: Interpreted SBT log results 2/8-N-9 T6. TOC was identified at 2643 mMD/1674 mTVD. The log showed perfect cement bonding for the entire interval and the GP 10-60 requirements were met.

6.4.4 Results

Excellent zonal isolation was achieved in well 2/8-N-9 T6. 543 mTVD of circumferentially bonded cement were identified above DPZ 8 as illustrated in Fig. 6.16. Similarly, 26 mTVD of good circumferentially bonded cement were identified below DPZ 8 (between DPZ 8 and DPZ 9). The well was found to be in compliance with GP 10-60. Several changes were implemented to improve the cement job as compared to the 2/8-N-9 T4 failure. Obtaining liner rotation, applying a thinner fluid, increasing the concentration of LCM, setting the liner shallower and the fact that a lot of time was spent cleaning the hole are thought to be the main contributors to the best 9 5/8" cement job on Valhall to date.

Given the updated hole size estimate of 14" the job was designed with a TOC at 2900 mMD/1850 mTVD. With the logged data it is clear that the average hole size had been overestimated. From the cement volumes pumped the actual average hole size can be calculated as,

$$D_{avg} = \sqrt{\frac{4}{\pi}\left[\frac{\text{Volume of annular cement}}{\text{Length of annular cement}} + \text{Closed end liner displacement}\right]}. \quad (6.1)$$

The closed end liner displacement is given in the 9 5/8" liner specification sheet as 0.295 bbl/m. Subtracting the shoetrack volume (9 bbl) from the total cement volume pumped and assuming circumferentially bonded cement all the way to TOC a hole size estimate is obtained,

$$D_{avg} = \frac{1\text{in}}{0.0254\text{m}}\sqrt{\frac{4}{\pi}\left[\frac{244\text{ bbl}}{(3716-2643)\text{m}} + 0.295\frac{\text{bbl}}{\text{m}}\right]0.15899\frac{\text{m}^3}{\text{bbl}}} = 12.8''.$$

The hole size calculation provide a low-end estimate due to two main reasons. Firstly, the circumferentially bonded interval of cement did not extend all the way to TOC as seen in Fig. 6.16. Secondly, although the SBT log seemingly show a perfectly cemented interval the log is not accurate enough to state that 100% of the annular volume was surrounded by cement for the entire interval. Nevertheless, the hole size was probably in the region of 13". This have affected both the actual ECD and standoff values as compared to the simulated cases.

Too many changes were made at the same time to be able to separate and quantify their individual effect. At the same time it should be stressed that everything was not perfect on this job either. The weight material sag in the thin CarboSea OBM could potentially have caused major wellbore stability issues. To further improve the cementing operations it was recommended to cancel the displacement to Synteq mud and not to condition the CarboSea OBM prior to running liner. Instead, different mud systems optimized for cementing should be evaluated.

6.5 Well 2/8-G-1

2/8-G-1 was drilled as a horizontal producer on Valhall IP in 2013/2014. With the experiences from both the failed and successful liner cement jobs on 2/8-N-9 extensive planning were conducted to avoid losses and to get circumferentially bonded cement at a sufficient height above and below DPZ 8.

6.5.1 Pre job planning and simulations

Based on the experiences from well 2/8-N-9 T6 the 9 5/8" liner setting depth was moved back to the middle Eocene formation to reduce the risk of penetrating loss zones near TD. LC-lube and $CaCO_3$ additions of 5 ppb at a 80:20 ratio were decided upon to effectively strengthen the formation and reduce fluid loss in permeable zones. Key points of a successful cement job were identified as liner rotation, sufficient displacement rates and ECD optimization. Prior to cementing the liner the well was planned to be displaced to a thin Warp OBM to aid displacement. Simulations showed significant ECD reduction when running and cementing the 9 5/8" liner in Warp. In addition, the Warp OBM does not build high gel-strength as the CarboSea when left static, hence the risk of channeling due to gelled mud was significantly reduced. A 6.8 ppg base oil pre-flush was planned to reduce the hydrostatic ECD contribution while cementing. It should be noted that the displacement to Warp OBM had to be aborted during the operational phase of G-1 (see Section 6.5.2).

The planned TOC was at 2223 mMD/1600 mTVD.

Discussions whether or not to open the hole to 13-13.5" to further decrease the ECD was initiated based on the learnings from N-9 T6. The underreaming proposal was turned down in this particular well due to small simulated ECD differences and due to the risk of decreasing the displacement efficiency by reducing the annular velocities.

The centralizer program originally included the rigid Spiraglider centralizers as used in well 2/8-N-1 B and 2/8-G-23, but due to the simulated Centek UROS stand-off values in well 2/8-N-9 T6 the program was revised. Two UROS centralizers were installed per joint in the bottom 100m of the liner, while the remaining liner interval was centralized by one UROS per liner joint. The stand-off simulations (Fig. 6.18) showed excellent results, and a significant improvement as compared to the previous Valhall IP well (2/8-G-23). A hole size of 12.6" was assumed in the simulations (15% open hole excess).

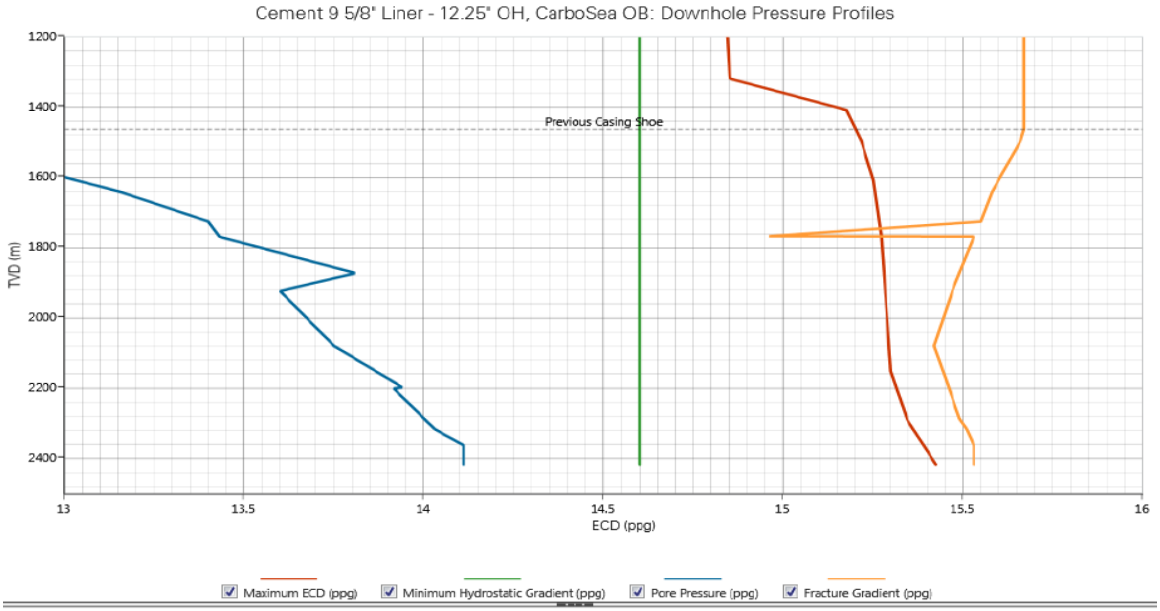

Figure 6.17: Halliburton ECD simulations prior to 2/8-G-1 cement job with 14.6 ppg CarboSea OBM. The initial displacement rate of 336 gpm is gradually reduced to 80 gpm to maintain the ECD below the fracture gradient. Simulations are based upon in-gauge hole conditions. The maximum ECD (red) should stay below the fracture gradient (yellow), but above the collapse gradient (green). The well pressures were seemingly well within the limits. However, predicting stringer depths and the corresponding fracture gradient have proven difficult. The previously identified weak zone at the base of DPZ 7 was included in the fracture gradient (although losses at this depth are considered acceptable).

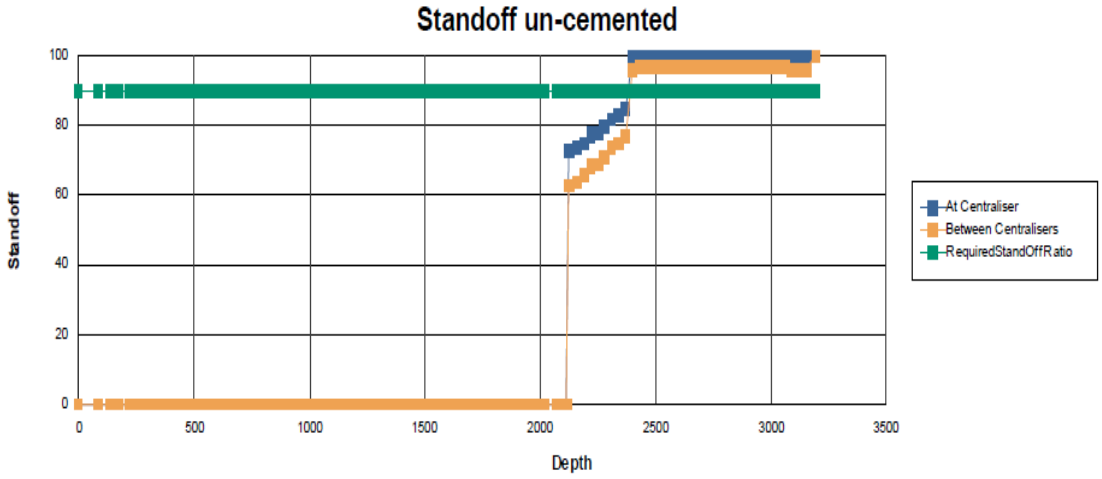

Figure 6.18: Centek standoff simulations plotted against depth. A hole size of 12.6" was assumed to make the simulations as realistic as possible. The calculations were performed under the scenario of mud both inside and outside of the liner. Simulations indicate 66-100% standoff in the cemented interval. A required standoff ratio of 90% was pre-defined to optimize displacement efficiency.

6.5.2 Job execution

Drilled out 13 5/8" shoetrack, performed FIT to 15.6 ppg and re-logged 13 5/8" casing cement. Drilled 12 1/4" hole from 2016-3192 mMD/1467-2421 mTVD with 14.6 ppg CarboSea OBM. DPZ 7 was identified from 2082-2295 mMD/1504-1656 mTVD and DPZ 8 from 2904-2952 mMD/2183-2225 mTVD. Losses were experienced at approximately 2318 mMD/1528 mTVD when drilling through a stringer, and circulation was partially lost at 2430 mMD/1770 mTVD. Spotted two LCM pills to mitigate the losses. Variable loss rates while drilling and flow-backs during connections were observed for the remaining part of the section (wellbore ballooning). It is believed that the ballooning effect was due to the fractured stringer at 2430 mMD. Pack-off tendencies seen in stringer at 2904 mMD/2184 mTVD. Lost a total of 715 bbl during drilling.

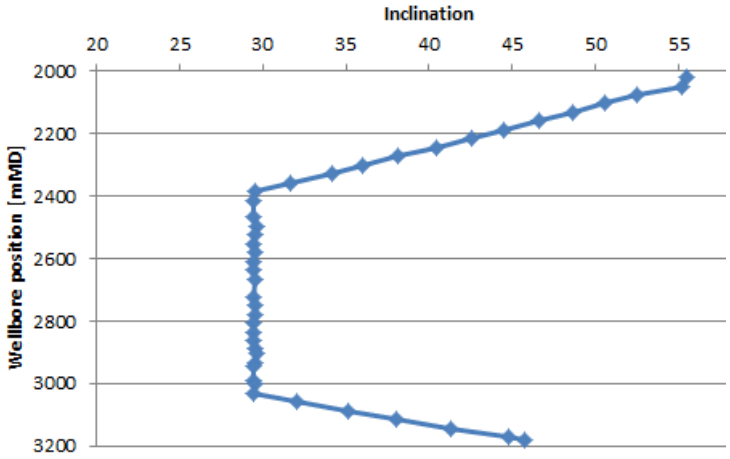

Figure 6.19: 12 1/4" section wellpath 2/8-G-1. The actual survey data is plotted against wellbore position (mMD). Inclination was kept between 29-57°.

Circulated 7xBU with 1000 gpm at section TD (120-140 rpm). No abnormal amounts of cuttings reported over the shakers. Performed check trip to 13 5/8" shoe to assure that the hole was sufficiently clean prior to displacement to Warp OBM. Overpulls were observed at 2966/2238, 2824/2114 and 2631/1946 mMD/mTVD. Observed events of lost circulation when tripping back in hole. Full returns were reported on the last stand. Tried to establish sufficient circulation rate to perform mud displacement without losses. The RAP (rig action plan) stated that the displacement rate should be in the region of ± 900 gpm. However, loss rates of 10-20% were observed with only 100-150 gpm flowrate. Due to the risk of creating a wellbore of two wellbore fluids (Warp below the thief zone and CarboSea above) the Warp displacement was cancelled. A sonic caliper log of the bottom 200m indicated that the hole was in-gauge.

At this point the loss zone was still believed to be within the fractured zone at 2430 mMD/1771 mTVD. As this zone was sufficiently high above DPZ 8 to meet the zonal isolation requirements it was decided to go on with the cement operation as planned. Pulled out of hole and prepared for running the liner. At surface the 12 1/4" bit was found balled up, probably from the 13 5/8" check trip. Water from a 13 5/8" squeeze job may have caused the surrounding shale to swell and stick to the bit/BHA.

Ran 9 5/8" liner to setting depth at 3183 mMD. Lost a total of 325 bbl while running in hole with the liner. Installed cement head, activated hanger and prepared for cement operations. Mud gel-strengths (10sec/10min) of 14/18 lbf/100ft^2, PV of 37 cP and YP of 21 lbf/100ft^2 were recorded prior to the cement operation. The following fluids were pumped:

- 30 bbl 6.8 ppg base oil pre-flush (no returns at 98 gpm). Assuming an in-gauge 12 1/4" hole the pre-flush will reduce the hydrostatic pressure at TD with a maximum of 190 psi or 0.45 ppg EMW (see Section 7.3.1).
- 120 bbl 14.8 ppg spacer (no returns at 245 gpm).
- 131 bbl 15.0 ppg lead cement slurry (no returns at 170-210 gpm).
- 65 bbl of 15.8 ppg tail cement slurry (no returns at 170 gpm).
- Displaced cement with 14 bbl spacer and 425 bbl 14.6 ppg CarboSea OBM at 336 gpm. A total of 7 bbl returns observed during displacement. No returns were observed after cement entered the annulus.

The top plug landed after 439 bbl which was 1.4 bbl (10 strokes) earlier than the estimated top plug bump volume. Established and maintained 30 rpm rotation throughout the displacement process. A SBT log was run 51 hours after bumping the plug to evaluate the cement status. The actual final circulation pressure of 390 psi compared to the simulation pressure of 434 psi indicated a significantly deeper than expected loss zone.

6.5.3 SBT log

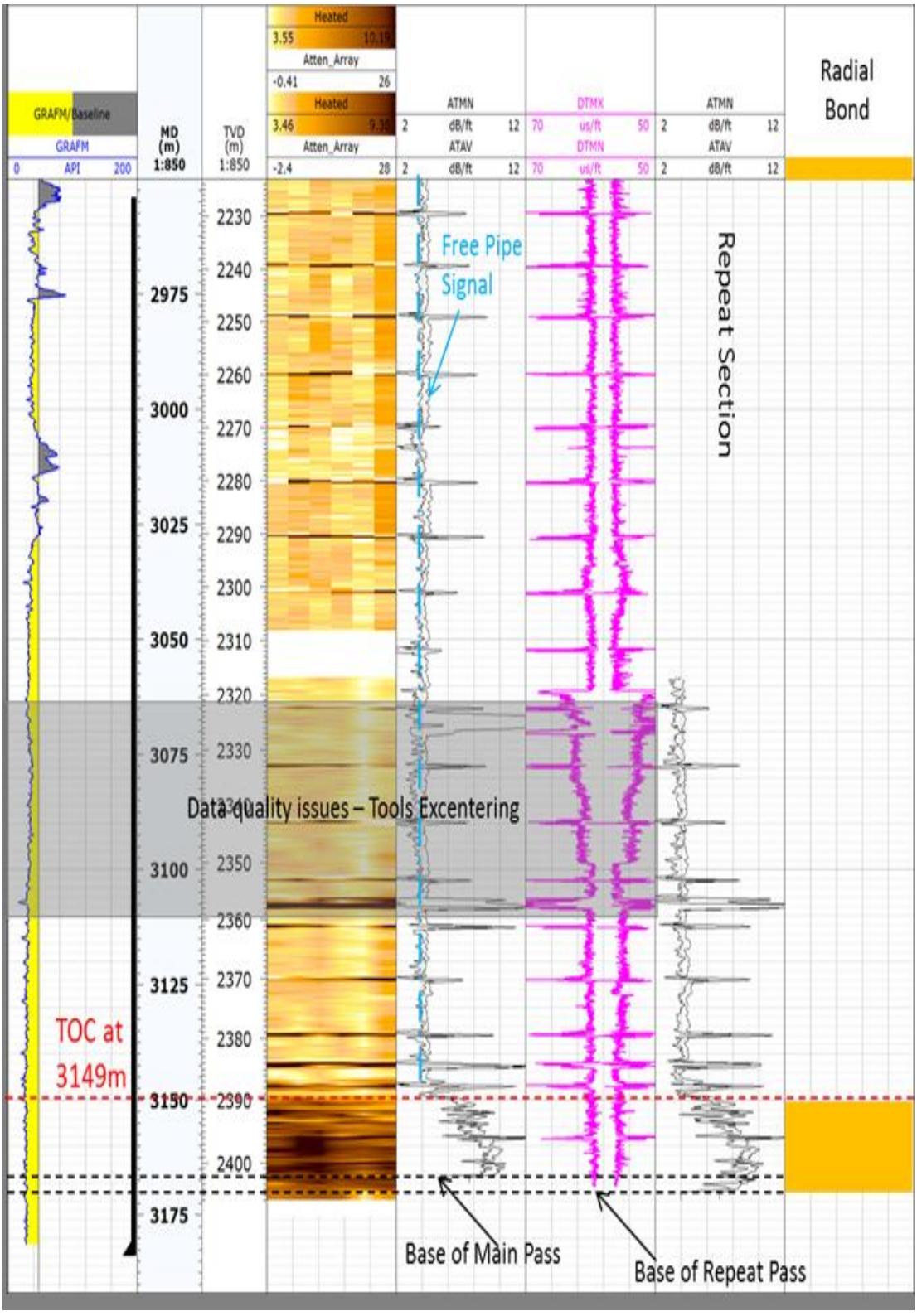

Figure 6.20: Interpreted SBT log results G-1. TOC was identified at 3149 mMD/2389 mTVD. The log showed no cement behind casing for the majority part of the section. GP 10-60 requirements were not met through the primary cement job, but a succcessful remedial cement job through port collars were performed at a later stage.

6.5.4 Results

The SBT log presented in Fig. 6.20 showed TOC at 3149 mMD/2389 mTVD. A total of 21 mMD/15 mTVD of circumferentially bonded cement were identified. Both the main pass and the re-log confirmed free pipe of the majority of the section. The requirements of GP 10-60 were not met below nor above DPZ 8.

A contingency action of cementing through port collars were planned for in case of a similiar outcome as in well 2/8-N-9 T4. The remedial cement job included cementing through one port collar and taking returns through one above. A total of 80 bbl 15.0 ppg cement slurry were successfully spotted between DPZ 8 and DPZ 7 with 94% returns. SBT logs after the remedial job indicated delayed cement setting times either due to mud contamination or due to lower than anticipated wellbore temperatures. The remedial cement job was approved based on volume control (returns during cementing).

Although zonal isolation requirements were met after the remedial job, 2/8-G-1 was a step backwards after the successful 2/8-N-9 T6 cement job. However, G-1 cannot be directly compared to N-9 T6 due to the fact that losses were induced during the drilling phase of G-1. The clear cut TOC from the SBT log indicates that there was a thief zone at approximately 3149 mMD/2389 mTVD. Throughout the entire section it was believed that losses to a fractured stringer at approximately 2430 mMD occurred. In hindsight it is believed that a deep fracture was induced during the wiper trip prior to pulling out of hole with the drilling assembly. The balled-up bit is thought to have contributed to an abnormally high surge pressure, effectively breaking down the formation (at the thief zone). The event was supported through losses. Hence, when starting the cement job at least one additional loss zone near section TD were present in addition to the shallow stringer. Typically at Valhall the virgin fracture gradient of 15.5 ppg is reduced to 15.0-15.1 ppg once a fracture has been initiated. From the DOE (drilling optimization engineer) stringer plot, the closest stringer was located at 3140 mMD/2383 mTVD which fits fairly well the logged TOC.

On the positive side, rotation of the liner was established without any major issues. The cemented interval below the loss zone showed very good circumferential bonding. Rotation in combination with excellent centralization and sufficient displacement rates are important parameters. Cancelling the displacement to Warp OBM given the deep loss zone was probably a good decision given the outcome of the cement job. Sandblasted liner joints were installed in three intervals to allow the cement to better bond to the rough surface. No conclusion can be drawn on the effect of these joints from this job.

Towards the next cement job (2/8-G-3) focus was pointed towards achieving the Warp OBM displacement. The low rheology mud is highly beneficial for cementing due to its low ECD and high mobility characteristics. Excellent results were achieved in the 18 5/8" and 13 5/8" cement jobs in well 2/8-G-3 after displacing to Warp OBM. Although displacement to a new mud system after drilling is a suboptimal solution, it is still considered to increase the probability of a good cement job.

6.6 Well 2/8-G-3

2/8-G-3 was planned as a horizontal producer in 2014. It was the third well drilled from Valhall IP after implementing the new casing design. As neither of the primary cement jobs in the first two wells (2/8-G-23 and 2/8-G-1) were in compliance with GP 10-60 the key objectives were still to avoid losses and get circumferentially bonded cement above DPZ 8.

6.6.1 Pre-job planning and simulations

Avoiding the lost circulation events observed during the previous cement jobs were identified as a key success factor. The initiatives evaluated and implemented to do so are listed below:

- IKM riser drainage centrigual pump was installed to reduce the fluid level inside the riser during the cement job. Approximately 20 mTVD can be drawn down inside the riser, reducing the hydrostatic EMW of 0.12 ppg at section TD.
- Close monitoring of the PWD (pressure while drilling) data. Any excessive pressure spikes or lost circulation events could potentially turn out to be the loss zone during cementing. The PWD data allow corrective actions to be taken in case of too high or low wellbore pressures.
- If a fracture is induced and lost circulation experienced, it was specified to treat and heal the losses before drilling ahead (based on the learnings from G-1).
- Displace wellbore to Warp OBM prior to performing the cement job. The hole should ideally be perfectly clean of cuttings before the displacement.
- Maintain concentration of LCM in drilling fluid.
- Evaluate to pump a pre-flush ahead of the spacer. The base oil pre-flush applied in well 2/8-G-1 is thought to be too light to effectively displace the mud in the hole.
- Control and limit liner running speed to limit surge pressures.

As compared to 2/8-N-9 T6 and 2/8-G-1 where the liner setting depth was picked in the middle Eocene, it was decided to go back to the deep setting depth in the Sele formation. Justification for the choice of liner setting depth is specified in Section 7.4. The major disadvantage of setting the liner in Sele formation is increased ECD while cementing the 9 5/8" liner. The option of underreaming the hole section was, given the same arguments as for 2/8-G-1, turned down.

Given the excellent UROS centralizer standoff simulations performed for 2/8-G-1 and 2/8-N-9 T6 it was no point in evaluating to apply different centralizers. However, to optimize liner standoff the centralizer concentration was slightly modified as compared to 2/8-G-1. A combination of one and two centralizers per liner joint indicates almost perfect centralization in an in-gauge 12 1/4" hole as shown in Fig. 6.21.

In terms of ECD simulations a number of different scenarios were simulated. It should be noted that both the mainbore and the subsequent sidetrack were abandoned due to hole stability issues. The stand-off simulation presented in Fig. 6.21 was performed prior to drilling the first sidetrack (T2). Furthermore, the maximum allowable ECD during cementing was updated due to the fact that losses were observed at approximately 15.3 ppg during drilling. Hence, to minimize the risk of deep losses it was concluded that the cementing ECD should, if possible, be maintained below 15.3 ppg at DPZ 8. To do so the TOC was planned deeper and the displacement rates were modified (towards the end of the displacement) to meet the requirements.

A major challenge associated with drilling wellbore 2/8-G-3 was crossing a stress ridge, an area with increased shear stresses, caused by reservoir compaction/subsidence. The risk of wellbore collapse was present, but thought to be manageable.

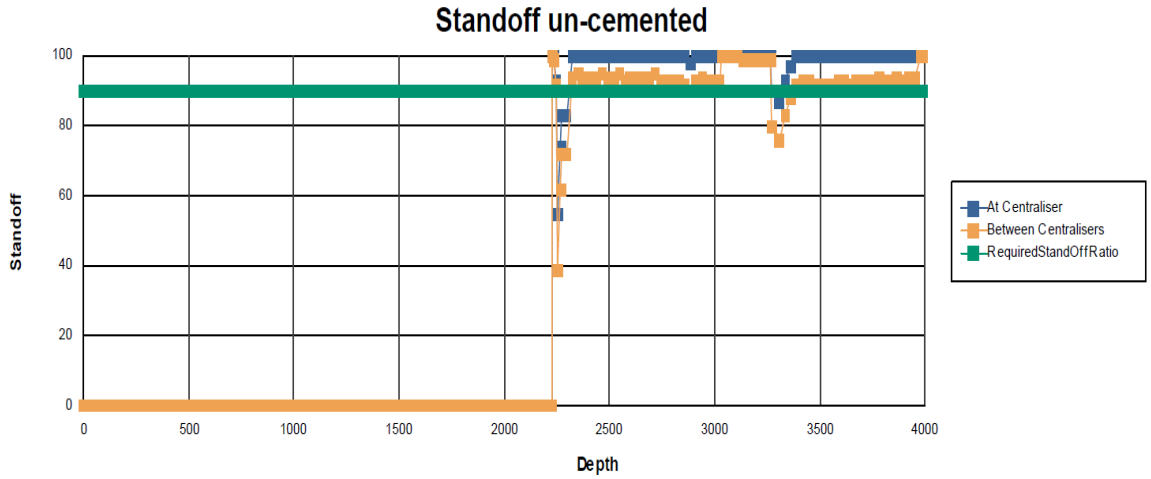

Figure 6.21: Centek standoff simulations ranging from 76-100%. The calculations were performed under the assumption of mud both inside and outside of the liner. The distinct drop in standoff at approx. 3300 mMD is a result of high local doglegs of maximum 4.54deg/30m.

6.6.2 Job execution

Initially drilled out shoetrack, 3m of new formation and performed an abnormally low XLOT. Squeezed cement around the 13 5/8" shoe to improve zonal isolation status below DPZ 6 (behind 13 5/8" casing). After relogging the 13 5/8" cement job, a new FIT was successfully performed to 15.5 ppg EMW. Drilled 12 1/4" hole section from 2229 mMD/1479 mTVD to section TD at 3882 mMD/2582 mTVD using 14.6 ppg CarboSea OBM. Except from a minor lost circulation event within DPZ 7 no issues were observed until approximately 3400 mMD where pack-off tendencies were observed. Drilling commenced to section TD without any major problems. Circulated 8xBU while racking back one stand of drill pipe every BU. Initiated a wipertrip to the 13 5/8" shoe to confirm that the hole was clean and stable. Severe hole problems observed from approximately 2912 mMD/1902 mTVD. Started to circulate 2.5xBU and immediately observed a signficiant amount of cuttings over the shakers. Huge cavings were occasionally observed throughout the hole cleaning process. Continued

to backream out of the hole to the 13 5/8" casing shoe. Some overpulls observed. Hole problems experienced when running back in hole at ±3000 mMD/1957 mTVD. Significant amount of cuttings were still observed over the shakers (probably from backreaming activities). Tight spots were occasionally observed when working the way back to section TD. Decided to perform a new checktrip due to uncertainty whether or not the liner could be run through the tight spots. Backreaming were again initiated, and cuttings continued to flow over the shakers. Finally managed to run past the trouble zone without any major issues. Ran back to bottom and started circulating prior to displacing the wellbore to Warp OBM. A total of 7 days were spent trying to gain control over the hole conditions after reaching section TD. At TD the drillstring twisted off and 832 mMD of the string were left in hole. It was decided to set P&A plugs and redrill the section.

Spent 16 days setting the P&A and kick-off plugs. To avoid the wellbore instability issues seen in the mainbore it was decided to move the wellpath further away from the stress ridge and increase the MW to 14.7 ppg. Sucessfully kicked off from the 13 5/8" shoe and drilled 2/8-G-3 T2 from 2236 mMD/1483 mTVD to section TD at 4003 mMD/2585 mTVD. DPZ 7 and DPZ 8 were penetrated from 2332-2608 mMD/1537-1691 mTVD and 3446-3477 mMD/2266-2289 mTVD respectively. Lost a total of 35 bbl to a minor stringer at 3017 mMD/1941 mTVD. A few large cavings were observed each stand. Increased concentration of LC-lube and $CaCO_3$ to 5 ppb prior to entering top of DPZ 8. Lost a total of 30 bbl in DPZ 8 and observed pack-off tendencies from 3447-3449 mMD identified by approximately 100 psi pressure spikes. It is believed that an ECD in the region of 15.3 ppg initiated the losses. Losses declined and eventually stopped throughout DPZ 8. An increase in the amount of cavings from 1 to 10 per stand were seen at approximately 3550-3650 mMD. The overall load of cavings was still small. Drilling to section TD commenced without any further problems. Based on the experiences from 2/8-G-3 (mainbore) it was decided to cancel the wipertrip, and circulate the hole clean from TD to minimize the time spent prior to displacing to Warp. Initially circulated 6xBU. The shakers cleaned up after approximately 2xBU, supporting the general belief that the overall hole condition was good. However, the Warp OBM was found to be of variable densities in the pits offshore. As a result a total of 19xBU were circulated before the Warp displacement could commence. Displaced the wellbore to 14.8 ppg Warp OBM without any major issues. Recorded a total of 30 bbl losses during the displacement, of which 23 bbl flowed back when circulation was stopped. PWD data indicated the the hole had not been subjected to any critical loads during the drilling phase of the section. Caliper data from when pulling out of hole after performing the Warp displacement indicated the 12 1/4" hole was in-gauge. The PWD sub indicated that swab pressures had been below the collapse curve from 2800-3000 mMD when pulling out of hole with the drilling assembly. When running in hole with the liner an obstruction was encountered at approximately 2800 mMD. Pack-off tendencies were observed, and the liner came close to getting stuck in the collapsed hole. It was decided to pull out of hole, set new P&A plugs and redrill the section again.

Wellbore 2/8-G-3 T3 was delayed to prepare a new plan and was not cemented before completing this thesis.

6.7 Well 2/11-S-9

Wellbore 2/11-S-9 was drilled on the South Flank parallell to drilling 2/8-G-3 on Valhall IP. It was the first well on the South Flank drilled according to the new casing design.

6.7.1 Pre-job planning and simulations

To avoid wellbore instability issues and lost circulation events several different options were addressed to maximize the probability of a successfull 9 5/8" liner cement job. The initiatives implemented are listed below. Liner rotation, strict pressure control during drilling and the LCM strategy was continued as for 2/8-G-3. TOC was planned at 2580 mMD/1998 mTVD (330 mTVD below the base of DPZ 7) when accounting for 15% open hole excess.

- To avoid applying two mud systems, CarboSea for drilling and Warp for cementing, it was decided to test the Halliburton Innovert OBM which is applicable both for drilling and cementing. The main advantage with the Innovert mud system is that flow is initiated very easily (at low pressures), although the gel-strengths are high enough to keep particles and cuttings in suspension when static. Hence, the risk of cement channeling is reduced as compared to the CarboSea OBM. In terms of ECD, the Innovert system is beneficial as compared to the CarboSea, but not as efficient as Warp.

- Based on simulations and the lessons learned from 2/8-N-9 T6 it was decided to underream the hole section to 13" to reduce the ECD while drilling/cementing and to reduce the surge pressure when running liner. It was debated whether or not the decreased annular velocities would jeopardize the cement displacement efficiency, but simulations showed compliant circumferential cement at a sufficient height above DPZ 8.

- The planned TOC was moved approximately 300 mTVD deeper than the base of DPZ 7 to reduce the cementing ECD. By planning for a deeper TOC one may achieve i) less hydrostatic pressure from the high density cement, ii) less frictional pressure drop from the high rheology cement, and iii) less frictional pressure drop across the liner hanger and PBR as the spacer is not displaced into the tight clearance.

- An IKM centrifugal pump was installed to draw down the riser liquid level as for well 2/8-G-3.

The 9 5/8" liner setting depth was picked in the middle Eocene as for 2/8-N-9 T6 and 2/8-G-1. Justification for the choice of liner setting depth is specified in Section 7.4. The main advantages of a shallow setting depth are reduced ECD and torque in addition to the decreased risk of penetrating weak zones near the top of the reservoir.

The Halliburton ECD simulation shown in Fig. 6.22 indicates that the maximum ECD at TD, 15.3 ppg EMW, is well within the predicted fracture gradient. It should be noted that the hydrostatic reduction from the IKM pump is not included in the Halliburton cement simulations. A combination of one and two UROS centralizers per liner joint were applied to optimize standoff in the underreamed hole section. As

shown in Fig. 6.23 the simulated standoff values ranged from 92-100% in the cemented interval. The planned displacement rate of 8 bpm is equivalent to an annular velocity of 0.55 m/s or 108 ft/min. Rheological hierarchy is achieved at ±3 bpm.

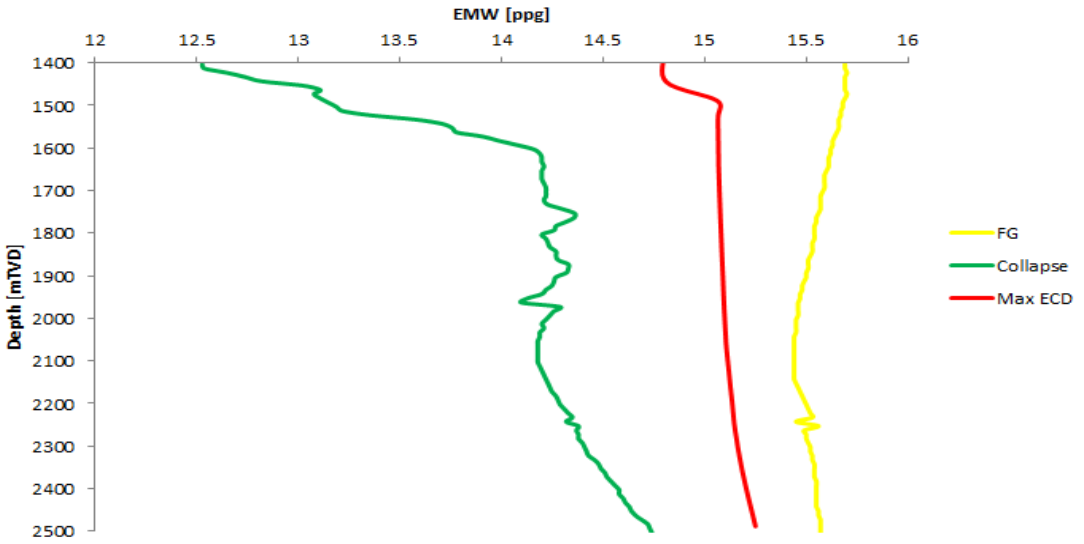

Figure 6.22: Halliburton ECD simulations prior to 2/11-S-9 cement job with 14.7 ppg Innovert OBM in the hole. A displacement rate of 336 gpm is maintained throughout the displacement until the last 20 barrels where the displacement rate is reduced to 2 bpm. Simulations are based upon in-gauge hole conditions (13"). The maximum ECD (red) should stay below the fracture gradient (yellow), but above the collapse gradient (green). The well pressures were seemingly well within the limits. A conservative approach of applying the minimum horizontal stress as the FG has been applied.

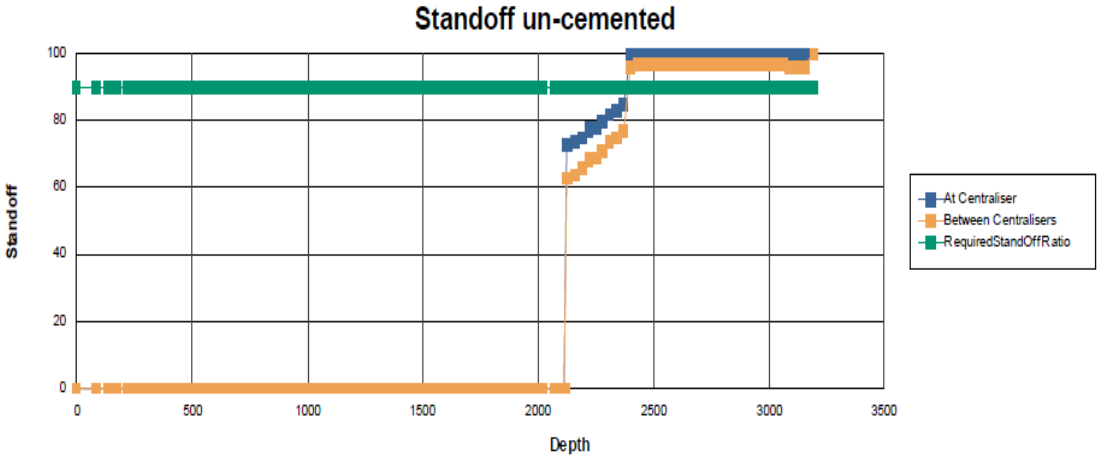

Figure 6.23: Centek standoff simulations plotted against depth for the UROS centralizers. A hole size of 13" was applied in the simulations. The calculations were performed under the scenario of mud both inside and outside of the liner. Simulations indicate 92-100% standoff in the cemented interval. A required standoff ratio of 80% was pre-defined to optimize displacement efficiency.

6.7.2 Job execution

Drilled shoetrack, 3m of new formation and performed a FIT to 15.6 ppg EMW. Activated underreamer and drilled 12 1/4" x 13" hole section from 1933 mMD/1481 mTVD to TD at 3104 mMD/2488 mTVD. Based on the experiences from the two collapsed wellbores in 2/8-G-3 it was decided to drill the section with a MW of 14.7 ppg with the option of raising it further based on the actual hole conditions. Drilling commenced without any issues. Adjusted ROP and flow rate to maintain ECD below 15.25 ppg EMW throughout the section. No cavings or pack-off events were identified, and the hole condition was generally very good. Increased concentration of LCM prior to entering top of DPZ 8. DPZ 7 and DPZ 8 were encountered from 2051-2207 mMD/1554-1670 mTVD and 2785-2825 mMD/2202-2241 mTVD, respectively. At TD the well was circulated clean at a flow rate of 1200 gpm. To mitigate the risk of swab pressures falling below the formation collapse pressure it was decided to pump out of hole from TD to 471 mMD. PWD data showed that the drilling and pulling out of hole had commenced within the fracture and collapse pressure limits. Fig. 6.24 shows the actual wellbore inclination plotted against the wellbore measured depth. It can be observed that the wellbore inclination was maintained below 40° for the majority part of the section which is highly beneficial from a wellbore stability point of view. A caliper log was not performed, but given the excellent hole conditions there is no reason to suspect an over/under-gauge hole size.

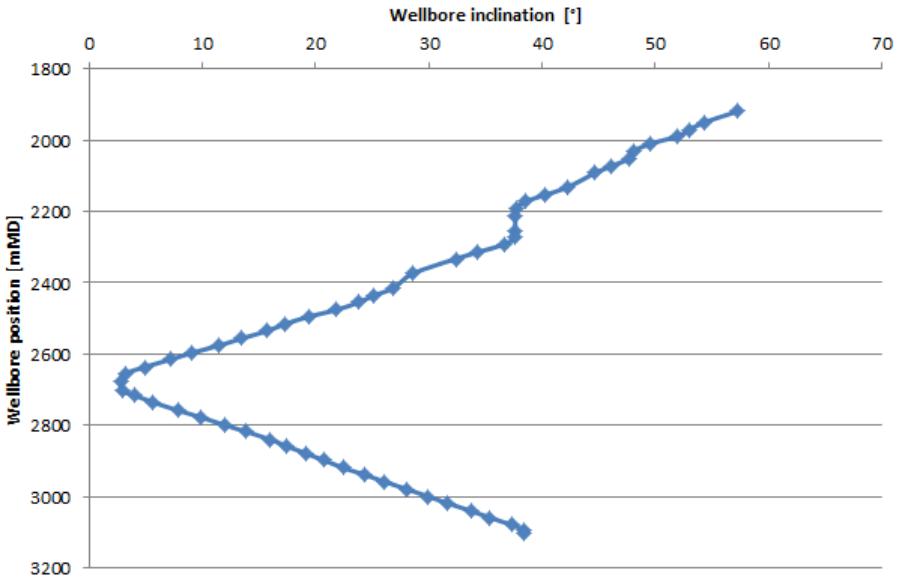

Figure 6.24: 12 1/4" section wellpath 2/11-S-9. The actual survey data is plotted against wellbore depth (mMD). Inclination was maintained between 3-56°.

Ran 9 5/8" liner to TD without any major problems at a running speed of 10min/stand. Broke circulation at 180 psi/30 gpm at 3073 mMD. In comparison, circulation was broken at 270 psi/30 gpm at 3667 mMD in well 2/8-N-9 T6 with CarboSea OBM. Although the wellpath and geometry is not identical, the data supports the beneficial effect of the fragile gel-strengths of the Innovert mud system. Activated the IKM pump and reduced the annular height inside the riser with 15 mTVD. Staged up flow

and circulated at 336 gpm without any losses. Observed some barite sag tendencies as mud weights of 15.1 ppg were recorded in the return flow. Conditioned mud prior to the cement operations to assure even mud weight in the wellbore. Installed cement head, activated liner hanger and prepared for the cement operation. Mud gel-strengths (10sec/10min) of 11/26 lbf/100ft^2, PV of 31 cP and YP of 16 lbf/100ft^2 were recorded prior to the cement operation. The following fluids were pumped:

- 120 bbl 14.9 ppg spacer (334 gpm, no losses).
- 62 bbl 15.0 ppg lead cement slurry treated with WellLife LCM (168 gpm, no losses).
- 92 bbl 15.8 ppg tail cement slurry treated with WellLife LCM (210 gpm, no losses).
- Displaced cement with 11 bbl 14.9 ppg spacer and 420 bbl 14.7 ppg Innovert OBM (336 gpm). No losses observed during the cement displacement process.

Experienced some issues when shearing out the bottom plug. The expected primary shear pressure of the bottom plug is 900-1100 psi. During the operation a surface pressure of 5130 psi was observed before the plug eventually sheared. Although highly uncertain, it has been proposed that the WellLife LCM could have blocked off the rupture disc within the bottom plug. Nevertheless, the displacement went perfectly according to plan with no losses. 20 rpm rotation was maintained throughout the entire displacement process. The top plug landed after 431 bbl which was 1.7 bbl (14 strokes) later than the estimated top plug bump volume. A SBT log was run 60 hrs after bumping the top plug job to evaluate the cement status.

The IKM pump efficiently lowered the riser liquid level with 15 mTVD. This corresponds to a hydrostatic reduction of 38 psi or 0.09 ppg EMW at section TD / 0.15 ppg EMW at the 13 5/8" shoe. On Maersk Reacher the riser drain outlet is located approximately 32 mTVD below the rig floor, hence further riser liquid draw down could have been achieved if necessary.

6.7.3 SBT log

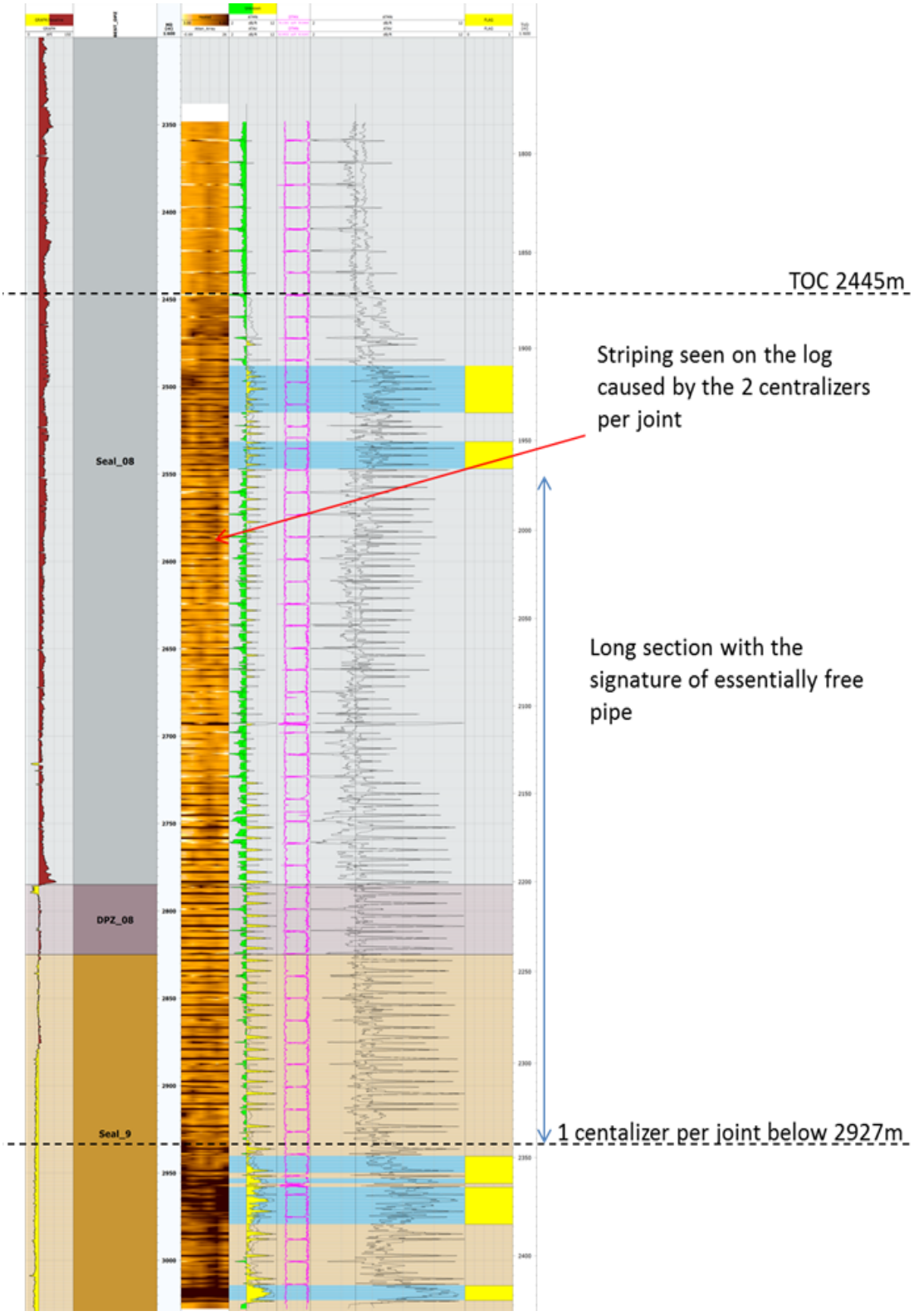

Figure 6.25: Interpreted SBT log results 2/11-S-9. TOC was identified at 2445 mMD/1870 mTVD. The log showed a total of 91.1 mMD/83.6 mTVD circumferentially bonded cement. Intervals of good circumferential cement is marked in yellow in the right column. GP 10-60 requirements were met.

6.7.4 Results

The SBT log results is illustrated in Fig. 6.25. A total of 91.1 mMD/83.6 mTVD of circumferentially bonded cement were identified. As the shoetrack was not drilled out prior to logging one could potentially have 46 mMD of additional circumferential cement. The intervals of logged compliant cement quality are listed below:

- 2488-2514.9 mMD/1909.4-1934.9 mTVD
- 2531.4-2547 mMD/1950.7-1965.8 mTVD
- 2939-2956 mMD/2348.1-2363.4 mTVD
- 2958.1-2979.4 mMD/2365.3-2384.3 mTVD
- 3014.4-3024.7 mMD/2414.7-2423.4 mTVD

DPZ 8 is isolated from DPZ 9 by 43.1 mTVD of circumferentially bonded cement, and DPZ 7 is isolated from DPZ 8 by 40.5 mTVD of circumferentially bonded cement. As a result the zonal isolation requirements of GP-10-60 are fulfilled. Compliant intervals of cement were identified near the base and top of the cemented part of the well. In between, from 2547 mMD/1966 mTVD to 2939 mMD/2348 mTVD, a long section of free pipe is evident from the SBT log. The planned TOC at 2580 mMD was calculated under the assumption of 15% OH excess (effective hole diameter of 13.43"). Applying in-gauge hole conditions and the fact that the 13" underreamer was located 51m behind the drill bit yield a theoretical TOC at approximately 2500 mMD. Compared with the logged TOC at 2445 mMD the data strongly indicate that there has not been any signficant cement channeling in the Innovert mud system. In addition, the hole size appears to be in-gauge.

An interesting observation is that the downhole centralizer locations seemingly constitute circumferentially bonded cement in the interval of free pipe. The phenomenon is indicated by the striping effect seen on the attenuation display on the SBT log. No centralizers were installed above the logged TOC, hence it is not possible to fully determine whether the log response is due to circumferential cement or due to the centralizer material. However, the log response is unusual and could indicate that the centralizers are imbedded in solid cement and that the liner itself is affected by a microannulus. Due to the fact that the zonal isolation requirements were fulfilled, no 1000 psi pressure pass was performed to test the theory.

On the positive side 2/11-S-9 was only the second well to deliver a fully GP-10-60 compliant primary cement job across Valhall. The job was performed without losses at the planned displacement rate of 336 gpm. Although not perfect, the SBT log confirmed that circumferentially bonded cement can be achieved at lower annular velocities when underreaming the hole section. Furthermore, as no significant channeling was observed there is reason to believe that the Innovert mud system and the UROS centralizers can provide the required setup of a successful 9 5/8" liner cement job across the Valhall field. For future cement jobs it should be evaluated to increase the rotational speed from 20 to 30 rpm during cement displacement to further decrease the probability of channeling.

7 Results & Discussion

Different initiatives have been implemented to improve the quality of the 9 5/8" liner cement jobs. Steps have gradually been taken in the right direction, but the liner cement job has proven difficult to achieve on a consistent basis. 2/8-N-9 T6 is by far the best cement job to date. To identify the key parameters and success factors some of the variables from the case histories are further analysed and discussed in this Chapter.

7.1 Lost circulation events

A lot of focus has been pointed towards the previously identified loss zone at the base of DPZ 7, but the case histories clearly show that there is more to the story. Four out of six 9 5/8" liner cement jobs have suffered from deep losses below, within or near the top of DPZ 8 as illustrated in Fig. 7.1. Only 2/8-N-9 T6 and 2/11-S-9 were cemented with full returns.

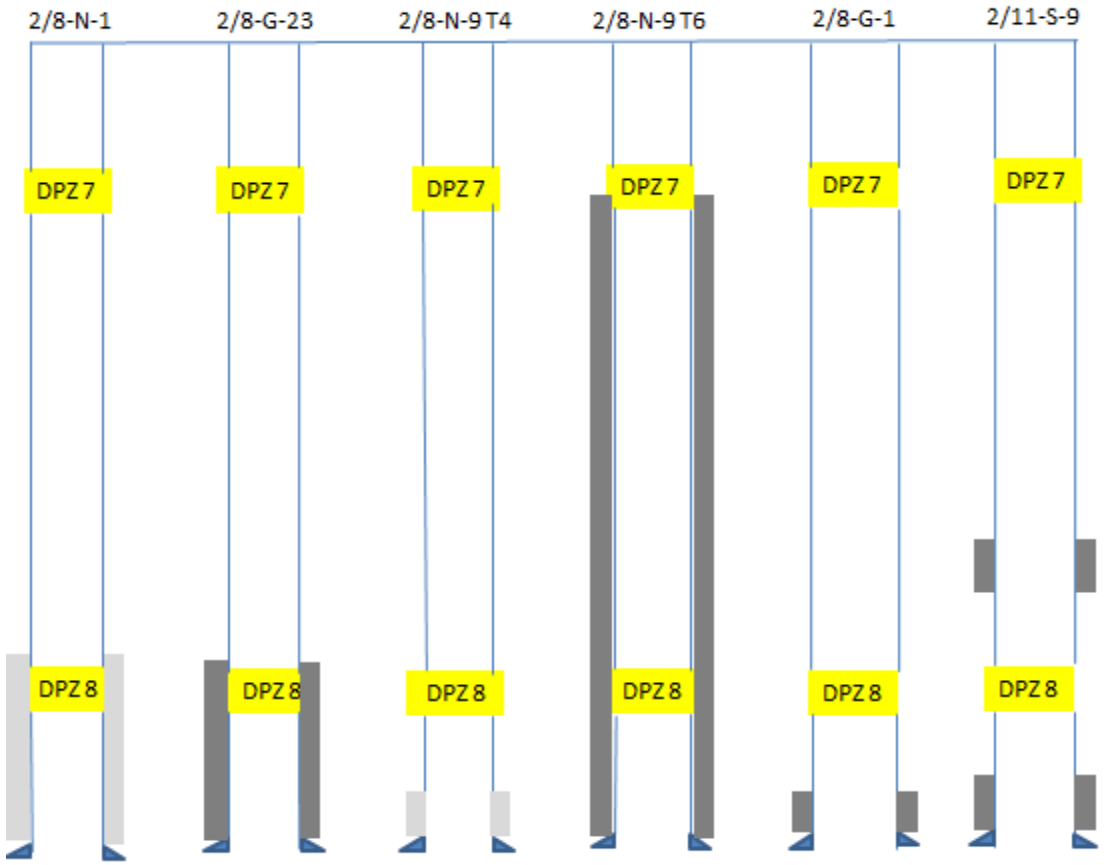

Figure 7.1: Illustrative overview of the 9 5/8" cement jobs across Valhall with both DPZ 7 and DPZ 8 exposed. All wells except 2/11-S-9 planned for a TOC just below or within DPZ 7. Lost circulation events were experienced in all wells except for 2/8-N-9 T6 and 2/11-S-9. Light grey indicate poor cement quality, and dark grey indicate good circumferentially bonded cement. The color index is meant to indicate the general cement status behind the liner. For accurate information see Chapter 6.

.

During a cement job the general guidelines on Valhall have been to continue pumping if the loss zone is believed to be above the required TOC. Normally the losses are assumed within DPZ 7 which is acceptable from a zonal isolation point of view. The case histories have provided data indicating that identifying any other loss zones during drilling and liner running is extremely difficult. Assuming a loss zone within DPZ 7 is definitively a too optimistic approach. Measures should be taken to minimize the probability of losses within the many stringers in the region near DPZ 8. In addition, unpredicted faults and natural fractures may complicate the situation even further. The LCM strategy is under constant development to artifically strengthen the formation. From a theoretical standpoint, one should not continue drilling until identified loss zones have been treated and eventually healed.

Virgin fracture pressure typically decreases by 0.4-0.5 ppg EMW once a fracture is initiated on Valhall [65]. As a result the fracture reinitiating pressure can, if not treated properly, be found at approximately 15.0-15.1 ppg at the base of the 12 1/4" section. All measures taken to reduce the ECD (low density pre-flushes, low rheology mud systems, IKM pump, limited flow rates, underreaming hole section etc.) may be useless if a fracture is accidently initiated without proper treatment (i.e. LCM). The big question is how to respond if lost circulation events are encountered at a depth lower than the acceptable TOC. Given the outcome of the 2/8-N-9 T4 cement job it would be preferable, both from an operational and economical perspective, to pull the liner and re-drill the section when circulation could not be established. Although 2/8-G-23 was cemented with no returns which evidently showed cement above and within DPZ 8 (not enough to be in compliance with GP 10-60), too much is left to chance.

Analysing well 2/8-N-1 B, 2/8-G-23, 2/8-N-9 T4 and 2/8-G-1 there is one common denominator in terms of lost circulation events. The lost circulation events are highly uncertain, and prior to cementing it is difficult to address their extent and location. Losses are often experienced when running in hole with the liner. Good practice is considered to monitor losses while running in hole with the liner. If the loss rate is reduced when running past DPZ 7 it is generally a good indication that the loss zone is within the zone. Similarly, if the loss rate decreases when running past DPZ 8 one should assume that the losses are deep and evaluate the probability of getting cement above the zone.

- 2/8-N-1 B: When liner was run into open hole too high flow rates caused an estimated ECD in excess of 15.9 ppg. This event is thought to have fractured the formation. The extent or location of the fracture(s) was not known. Losses were observed (11 bbl) when runing in hole without circulation from 3248-3654 mMD. Could not break circulation at low flow rates without inducing losses prior to setting liner hanger.
- 2/8-G-23: Gains and losses observed while running in hole with liner (no issues while drilling). Losses while running in hole and gains while static indicated hole ballooning. The trend improved at approximately 2600 mMD (indication of loss zone).
- 2/8-N-9 T4: Main reason for losses in this case is thought to be a fault near section TD.

- 2/8-G-1: Surged formation when performing wiper trip. The most viable theory is that the balled-up bit caused an abnormally high surge pressure which effectively broke down the formation below DPZ 8.

7.2 Displacement efficiency

A variety of different parameters affect the displacement efficiency. The cement jobs are only approved if a density and rheology hierarchy exist in the simulated displacement model. As seen in the case histories the density hierarchy is very limited due to the available mud window. Adhering to the 10% density rule is not possible given the available mud window. Typically the Halliburton simulations show that a displacement rate of 4 bpm (168 gpm) is sufficient to obtain the desired rheology hierarchy. The requirement has been fulfilled in all wells described in the case histories. Similarly, spacer design and contact time with the formation are important to prepare the wellbore for the cement job, but as the spacer volume has been maintained at approximately 120 bbl the data set is insufficient to analyse the effect of spacer contact time. Liner rotation, displacement rates and centralization are further analysed against the logged annular cement bond. The mud system is also a key parameter describing the displacement efficiency, but this topic is treated separately in Section 7.6.

A common denominator of the wells showing circumferentially bonded cement is liner rotation as shown in Fig. 7.2. Rotating the liner at 30-35 rpm is considered good industry practice, and the data clearly confirms the positive effect of liner rotation in terms of displacement efficiency. The effect of displacement rates is not as pronounced. 2/8-N-1 B was cemented with the highest displacement rate of 420 gpm, but also included the worst centralization. On the other hand, 2/8-N-9 T4 was cemented with the lowest displacement rate, but with a clear improvement in terms of stand-off as compared to well 2/8-N-1 B. Poor cement bonding was seen in both well 2/8-N-1 B and well 2/8-N-9 T4. The four wells constituting circumferentially bonded cement were cemented with a displacement rate of approximately 8 bpm. However, well 2/11-S-9 was underreamed to 13" which effectively reduced the annular velocity from 0.73 m/s to 0.55 m/s. The 2/11-S-9 SBT log showed in excess of 80 mTVD of circumferentially bonded cement, but the long interval of essentially free pipe is not fully understood. Creating a microannulus when pressure testing the liner string, or failing to remove a thin oil layer at the casing/formation given the decreased annular velocities are two viable theories. On the other hand, it is documented that the average hole size in well 2/8-N-9 T6 was in the region of 13". Circumferential cement was identfied from the SBT log throughout the entire interval in wellbore 2/8-N-9 T6. As a result there is reason to believe that the annular velocities of 0.55 m/s are sufficient to obtain GP-10-60 compliant primary cement jobs if the liner is rotated and sufficiently centralized.

One of the main, yet not answered, questions regarding cement displacement rates on Valhall is how low one can go if the required stand-off and liner rotation are achieved. Any reduction in displacement rate provide a significant ECD reduction, but on the other hand one do not want to compromise annular velocities and displacement efficiency. Decreasing the displacement rates when liner rotation has been achieved

has not been performed in any of the wells presented in the case histories. The main reason for not going down on the displacement rates is the fear of cement channeling along the wellpath (similar to what was seen in well 2/8-N-9 T4 where no rotation was applied). If TOC were to be found close to DPZ 7 with severe channeling it may be impossible to open and operate the port collars installed for remedial purposes. Hence, the only viable option is to cut and pull the liner above the TOC which is a costly and time consuming operation. In the wells cemented with no returns it has been impossible to establish a loss-free circulation rate prior to the cement job. As a result one may argue that the loss zone would have been at the same depth regardless of the displacement rate. Any reduction in displacement rate would possibly alter the cement status below the TOC.

After the UROS centralizers were installed in the lower part of the liner string both log results from 2/8-N-9 T6, 2/8-G-1 and 2/11-S-9 showed circumferentially bonded cement (although a deep loss zone was present in well 2/8-G-1). Liner rotation is thought to be the main displacement contributor, but any improvement made in stand-off reduces the risk of cement channeling and reduces the required displacement rate needed for proper displacement efficiency.

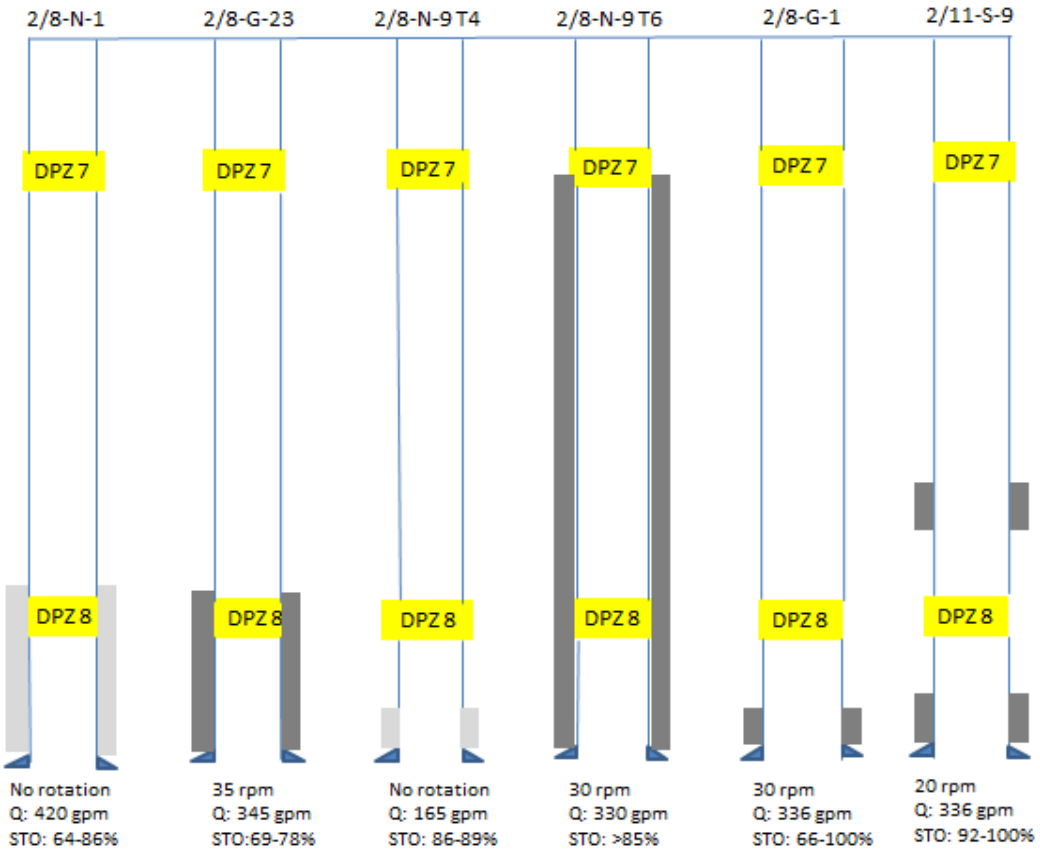

Figure 7.2: Illustrative overview of the 9 5/8" cement jobs across Valhall with both DPZ 7 and DPZ 8 exposed. Dark grey indicate well bonded cement whereas light grey indicate poorly bonded/channelized cement. The color index is meant to indicate the general cement status behind the liner. For accurate information see Chapter 6. Under each well the actual liner rotation, displacement rate and stand-off (STO) are listed.

No correlation between the wellbore inclination and intervals of circumferentially bonded cement has been identified from the case histories. The results are presented in Fig. 7.3. Taking the volumes pumped, as detailed in Chapter 6, into consideration it is apparant that the areas of circumferentially bonded cement corresponds to tail cement. This would also be expected due to the fact that the tail is of higher density (density hierarchy) and as deep losses has been experienced in the majority of the wells.

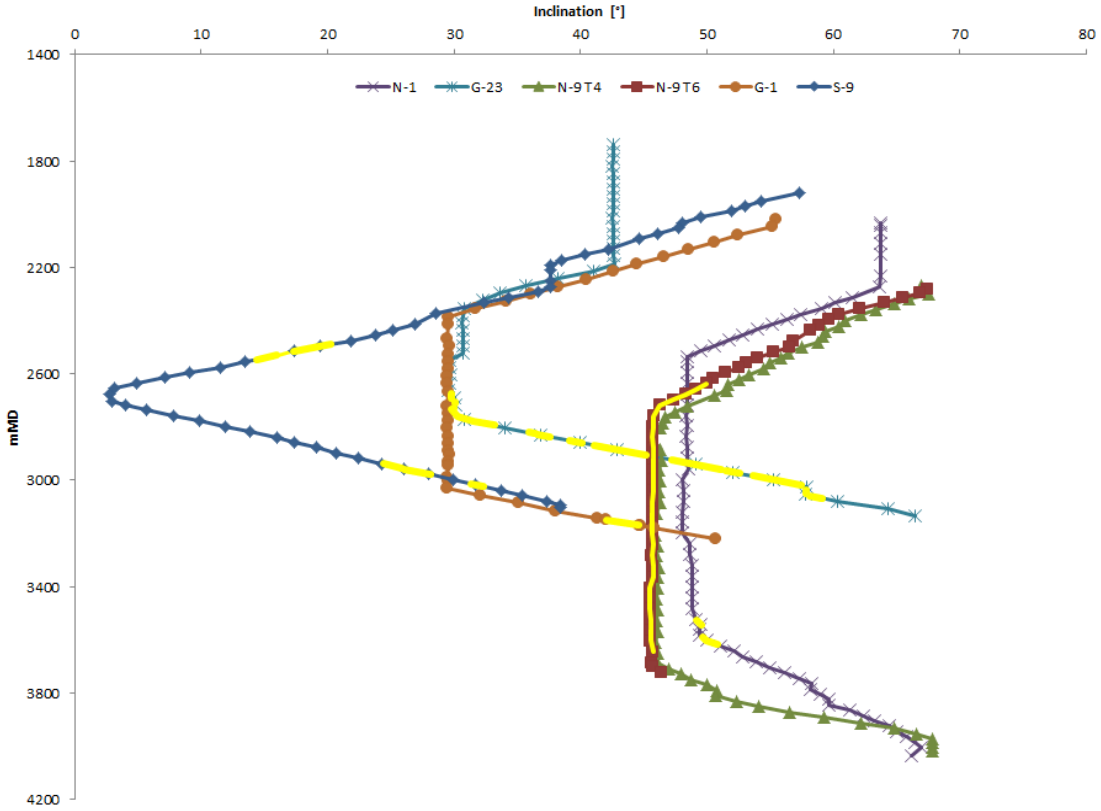

Figure 7.3: The wellbore inclination is plotted against the wellbore position [mMD] for all wells discussed in Chapter 6. Intervals of logged circumferential cement from the primary cement jobs are marked in yellow.

During any cement job the Halliburton recommendation to maximize the probability of an efficient displacement is to be within a turbulent flow regime. As stated in Section 5.4.5 the current 9 5/8" cement jobs are performed within a laminar flow regime. Assuming power-law fluid behaviour and the fluid rheology at 50°C as proposed for well 2/8-G-3 T3 it is possible to quantify how fast one would need to pump to get the mud, spacer and lead cement into turbulence. The results are presented in Fig. 7.4. It is observed that a displacement rate of approximately 13 bpm, 15 bpm and 24 bpm is required to get the Innovert mud, spacer and lead slurry into the transition zone between laminar and turbulent flow ($Re > 2000$). A 12 1/4" hole size has been assumed. Applying the planned wellpath of 2/8-G-3 T3 and assuming mud circulation with the liner on bottom the ECDs can be calculated as shown in Fig. 7.5. If MPD (managed pressure drilling) is introduced on the Valhall field it could be possible to have a mud weight in the hole corresponding to the pore pressure and control the bottomhole pressure from surface. Hence, the allowable annular frictional pressure

drop would be higher and one could manage to cement the 9 5/8" liner with a higher displacement rate. It is observed from Fig. 7.5 that if the mud weight was to be reduced to 14.0 ppg one could possibly displace the cement at 15 bpm.

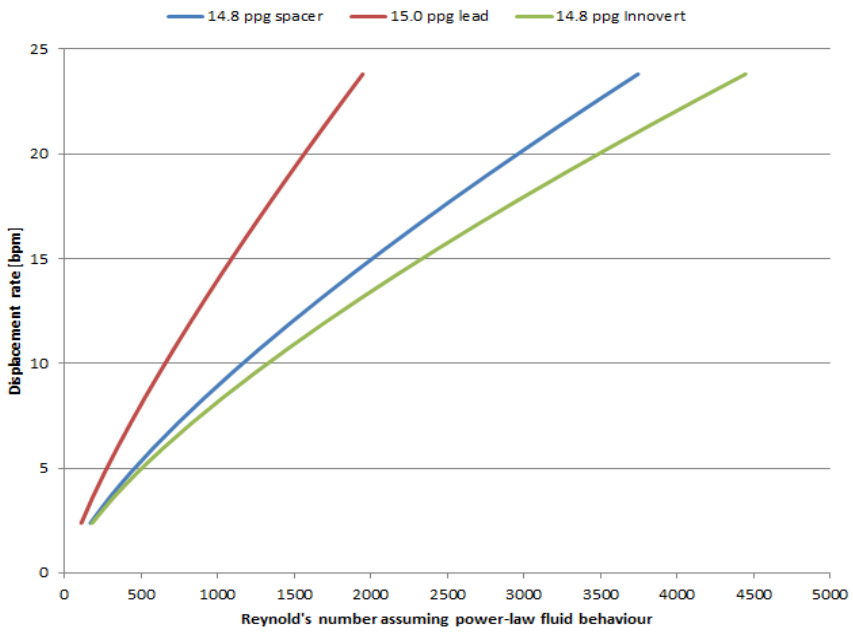

Figure 7.4: Reynold's numbers calculated for the spacer, lead slurry and Innovert OBM. The calculations have been performed under the assumption of a concentric 9 5/8" x 12 1/4" hole and power-law fluid behaviour of all fluids.

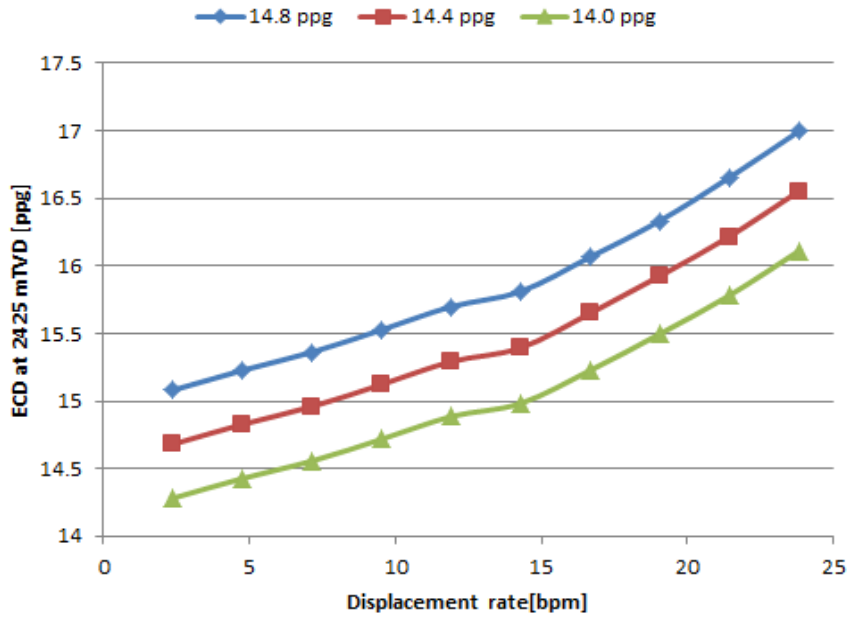

Figure 7.5: ECD calculations when circulating at 2425 mTVD (section TD well 2/8-G-3 T3) for three different mud weights. It is observed that for a MW of 14.0 ppg one could possibly displace the cement at 15 bpm (630 gpm) without fracturing the formation. The calculations have been performed under the assumption of a concentric 9 5/8" x 12 1/4" hole, Innovert OBM and power-law fluid behaviour of all fluids. Note: No hydrostatic nor frictional pressure from the cement is included in the calculations.

7.3 Measures to reduce ECD

During the learning process from 2/8-N-1 B to 2/11-S-9 a number of different measures to reduce the ECD have been evaluated. Some of the measures have been implemented, while some is still under evaluation. The calculations or simulations which support and describe the different alternatives are presented and discussed in this section. As the majority of the wells described in the case histories suffered from deep thief zones it is in many cases difficult to quantify the effect of the ECD reducing measures. However, some of the initiatives are explainable through mathematical expressions and the concepts of flow described in Chapter 4.

7.3.1 Low density pre-flush

In well 2/8-N-9 T4, 2/8-N-9 T6 and 2/8-G-1 a low density pre-flush (mud or base-oil) was pumped ahead of the spacer to reduce the weight of the annular fluid column. The volume of pre-flush is limited by the collapse gradient at all depths along the wellpath. The reduction in hydrostatic bottomhole pressure is a function of where the pre-flush is located in the annulus. As the pre-flush enters the annular space between the ID of the 13 5/8" casing and the 5 7/8" DP the pressure reduction diminishes quickly. The theoretical hydrostatic pressure and ECD decrease of the 30 bbl 6.8 ppg base-oil pre-flush applied in well 2/8-G-1 is presented in Fig. 7.6.

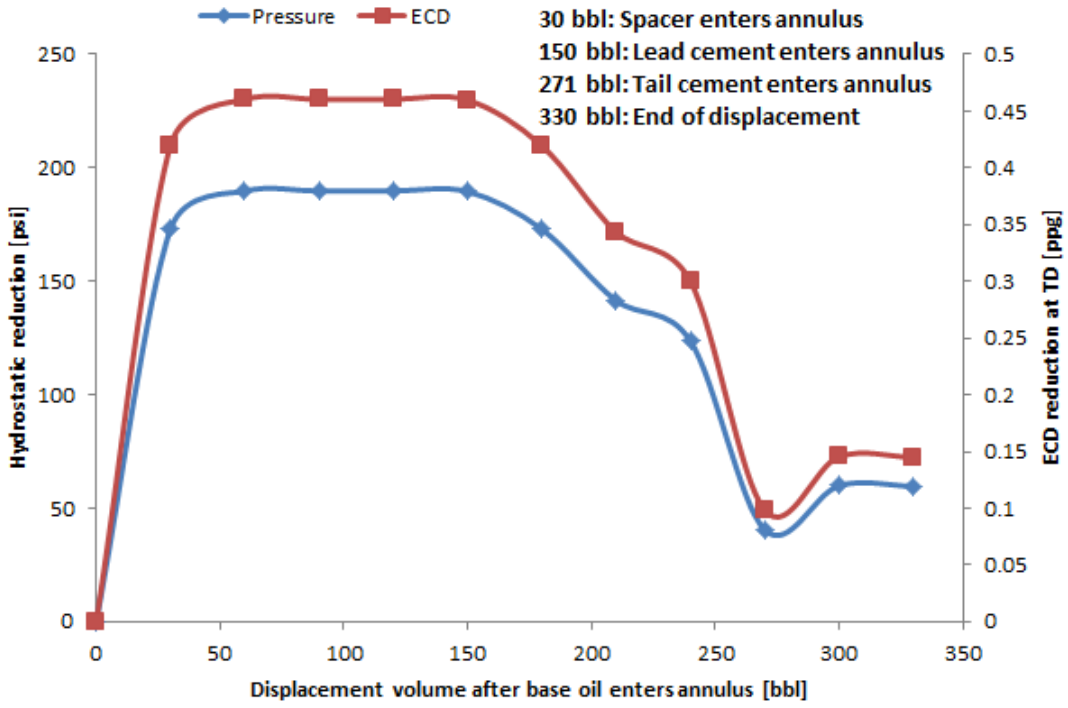

Figure 7.6: A simple model applied for the wellpath in 2/8-G-1 to calculate the effective hydrostatic pressure and ECD reduction at TD of a 30 bbl 6.8 ppg base oil pre-flush. The displacement volumes were nullified when the baseoil entered the annulus for simplicity. In-gauge hole and plug displacement have been assumed.

Fig. 7.6 is meant as an illustration. Each well needs to be treated separately as planned TOC, hole sizes, wellbore trajectory and volumes will affect the pre-flush pressure contribution. Even though the pre-flush is efficient in theory, some clear limitations are observed. Firstly, the preflush provide the highest ECD contribution when it is least needed (i.e. when displacing spacer), while the effect is dramatically reduced at a later stage of the displacement (i.e. when displacing tail cement). Secondly, if the pumps shut down during the displacement sequence hole stability issues may occur if the circulating presssure (ECD) has been held against the collapse pressure to determine the pre-flush volume. Finally, whether or not a base oil pre-flush can properly displace a 14.6 ppg mud is highly uncertain. 2/8-G-1 probably saw little or no effect of the pre-flush during cement displacement as a thief zone was present just above section TD. Nevertheless, some rare returns (7 bbl) were observed just after the spacer entered the annulus which may indicate that the pre-flush was effectively providing an ECD reduction.

7.3.2 IKM pump

Prior to drilling well 2/8-G-3 an IKM centrifugal pump was installed and connected to the riser. The intention of the pump is to lower the liquid level inside the riser to effectively reduce the hydrostatic bottomhole pressure component. In the 9 5/8" liner case the pump is hooked up to the riser drain valve located approximately 25 mTVD below the drill floor on Valhall IP. With a 20% safety factor the pump can draw down the annulus liquid height by 20 mTVD (as compared to the normal point of mud return). With a MW of 14.6 ppg a 50 psi hydrostatic pressure reduction is achieved. In terms of EMW this corresponds to 0.12 ppg reduction at 2500 mTVD, and 0.20 ppg reduction at 1450 mTVD (previous shoe). The shallower 18 5/8" and 13 5/8" casing strings benefit to a higher degree from the pump than the relatively deep 9 5/8" liner. Nevertheless, any reduction in ECD contributes to the overall goal of cementing the liner with no losses.

The major advantage with the IKM pump as opposed to minor mud weight reductions or pumping a low density pre-flush is that in case of circulation stops or downhole losses the riser liquid level is automatically correlated to maintain a pre-defined constant pressure. Hence, the risk of dropping the pressure below the collapse or pore pressure is reduced.

7.3.3 Underream 12 1/4" section

Ever since the 2/8-N-9 T6 success story constant discussions have been ongoing regarding whether or not the 12 1/4" hole section should be opened up to a larger hole size. Whereas the Valhall IP engineering team concluded that the ECD effect was neglegible it was included in the DOP to open the hole to 13" on the South Flank (well 2/11-S-9). Decreased ECD while cementing and decreased surge pressures when running the liner were the main arguments for an underreamed hole section. The introduction of the UROS centralizers has reduced some of the issues concerning centralization in case of a larger than 12 1/4" hole section.

Assuming laminar flow, concentric annuli, constant flow rate and power-law fluid behaviour the annular frictional pressure drop is given by Eq. (4.33). The ratio of the frictional pressure drop in a 12 1/4" and a 13 1/2" hole section is presented in Eq. (7.1).

$$\frac{P_{13.5''}}{P_{12.25''}} = \frac{(12.25 - 9.625)^{2n+1} (12.25 + 9.625)^n}{(13.5 - 9.625)^{2n+1} (13.5 + 9.625)^n} \tag{7.1}$$

Similarly the frictional pressure drop ratio of hole sizes ranging from 13.0" to 14.0" is plotted against the power-law index in Fig. 7.7. The effect of opening the hole section is apparantly of high value. Underreaming the hole section from 12 1/4" to 13 1/2" will reduce the open hole frictional pressure drop by approximately 40-70% (at a constant flow rate). Pressure drop across the liner hanger etc. will, of course, not be affected. An important contributor to the frictional pressure drop reduction is the fact that the annular velocity is reduced if the flow rate is assumed constant. If the flow rate is made a variable a more realistic expression of the annular pressure drop can be derived from Eq. (4.33). The result is shown in Eq. (7.2).

$$\frac{P_{13.5''}}{P_{12.25''}} = \left(\frac{Q_{13.5''}}{Q_{12.25''}}\right)^n \frac{(12.25 - 9.625)^{2n+1} (12.25 + 9.625)^n}{(13.5 - 9.625)^{2n+1} (13.5 + 9.625)^n} \tag{7.2}$$

A flow rate of 336 gpm in a 9 5/8" x 12 1/4" annulus corresponds to an annular velocity of 0.73 m/s. The equivalent flow rate in a 9 5/8" x 13 1/2" annulus is 524 gpm. What is interesting is that the effect of drilling an enlarged hole is reducing the frictional pressure drop even though the annular velocity is maintained constant rather than the flow rate. This is illustrated in Fig. 7.8. The simplified explanation is that the flow area increases to a higher degree than the annular circumference where the friction actually takes place. It should however be noted that the pressure drop across the hanger and PBR will increase if the flow rate is increased. Hence, to minimize ECD it is not optimal to increase the flow rate.

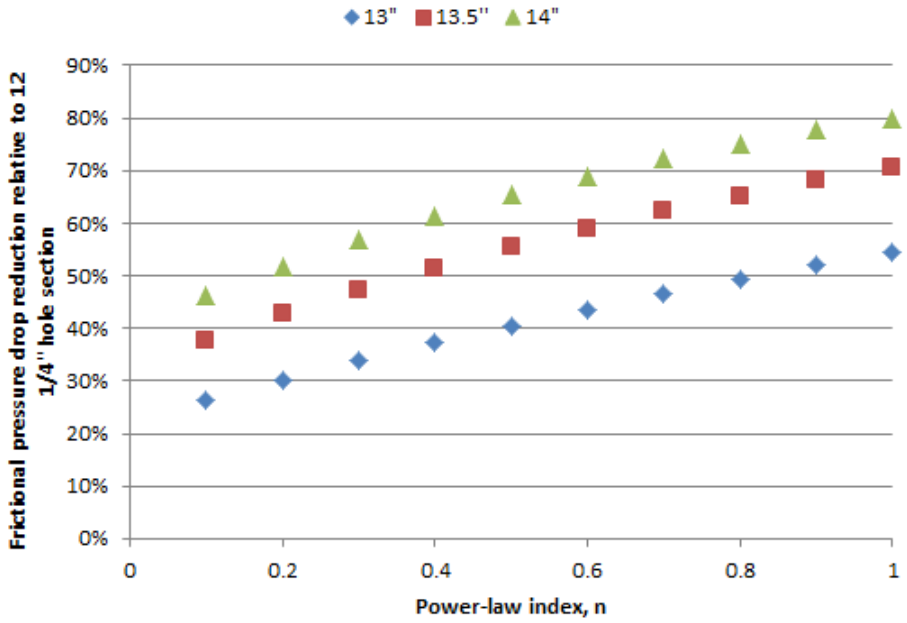

Figure 7.7: Open hole annular frictional pressure drop reduction (%) of different hole sizes relative to a 12 1/4" hole section (9 5/8" liner in hole). Laminar flow, concentric annuli, constant flow rate and power-law fluid behaviour has been assumed. The pressure ratio is plotted against the power-law index, n (n=1 corresponds to a Newtonian fluid).

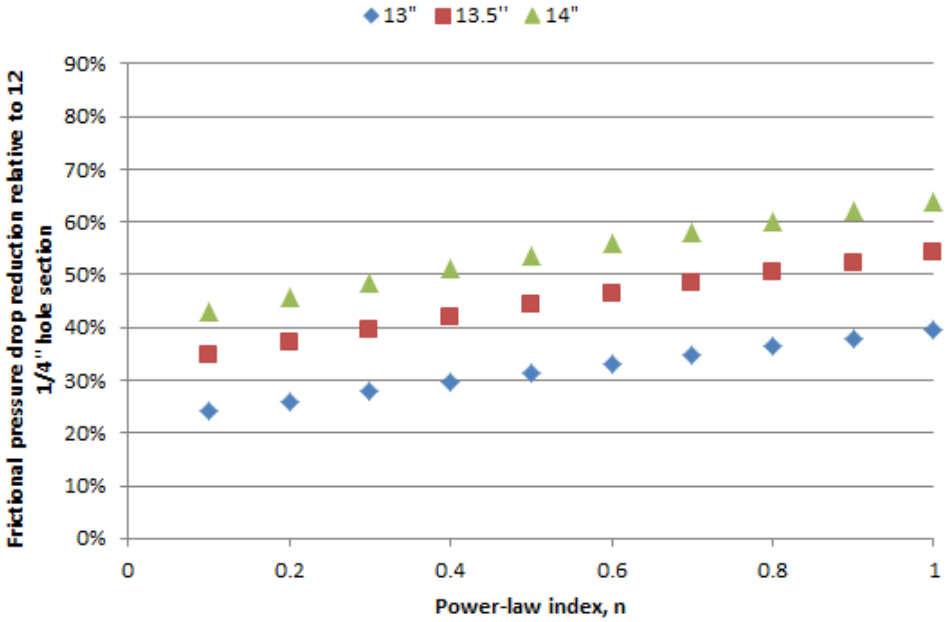

Figure 7.8: Open hole annular frictional pressure drop reduction (%) of different hole sizes relative to a 12 1/4" hole section (9 5/8" liner in hole). Laminar flow, concentric annuli, constant annular velocity and power-law fluid behaviour has been assumed. The pressure ratio is plotted against the power-law index, n (n=1 corresponds to a Newtonian fluid).

The theory applied to create Fig. 7.7 and Fig. 7.8 provide a simplified solution. Actual wellbore conditions such as temperature and pressure affect the fluid properties along the wellpath. The Halliburton simulation algorithm provide a more realistic calculation. Prior to drilling 2/11-S-9 a number of different simulations were performed for different scenarios including different hole sizes. Unfortunately, the OptiCem software does not provide the open hole frictional pressure drop. However, the ECD at different points across the wellpath is easily achieved. To estimate the open hole frictional pressure drop a situation of 14.6 ppg CarboSea OBM, TOC at 2580 mMD and the 9 5/8" shoe at 3090 mMD was assumed. ECD readings were programmed at TD and at the 13 5/8" shoe. As the flow conduit consists of fluids of different densities the ECD is composed of both a hydrostatic and a frictional component. The hydrostatic component is estimated to approximately 0.08 ppg at the liner shoe depth. Subtracting the hydrostatic component from the total open hole annular pressure drop yields the open hole annular frictional pressure drop. A summary of the simulations is given in Table 7.1.

Table 7.1: Comparison of the ECD simulations for different hole sizes. The flow rate is kept constant at 336 gpm. A mud system of 14.6 ppg CarboSea OBM has been assumed in the simulations.

Hole size	Max ECD at 13 5/8" shoe [ppg]	Max ECD at TD [ppg]	OH pressure drop [ppg]	OH frictional pressure drop [ppg]
12 1/4"	14.97	15.38	0.41	0.33
13"	14.97	15.21	0.24	0.16
13 1/2"	14.97	15.14	0.17	0.09

Opening the hole section to 13" yields a 52% open hole frictional pressure drop reduction as compared to the 12 1/4" base case. The 14.6 ppg CarboSea rheology data applied correspond to a power-law index of 0.4. In addition, the rheology of the spacer, lead and tail cement correspond to power-law indexes of 0.4, 0.8 and 0.6, respectively. Comparison of the simulated values with the theoretical calculations in Fig. 7.7 shows a fairly good correlation. One should always keep in mind that some of the pressure reduction is due to the fact that the annular velocity is reduced from 0.73 m/s to 0.55 m/s when opening the hole to 13" and maintaining a constant flow rate of 336 gpm. As a result the required flow rate necessary to obtain a rheological hierarchy increases when underreaming the 12 1/4" section. The SBT log from 2/11-S-9 indicate that circumferentially bonded cement can be achieved at the reduced annular velocity. A low-rheology mud system would yield a similar percentage pressure drop reduction, but the magnitude would be of less impact.

7.3.4 Low rheology mud systems

A low rheology mud system is beneficial due to a significant ECD reduction, but also in terms of increased displacement efficiency. The different mud systems evaluated at Valhall are discussed in Section 7.6. The rheology profile at 50°C of the Innovert, Warp and CarboSea mud systems are illustrated in Fig. 7.9a. Considering the viscosity definition and pressure drop calculations described in Chapter 4 it is apparant that the Warp mud yield the lowest frictional pressure drop. Furthermore, assuming power-law fluid behaviour, concentric annulus, the planned wellpath of 2/8-G-3 T3 and circulation with the liner on bottom it is possible to estimate the frictional pressure drop of the different mud systems. The results are presented in Fig. 7.9b. Simulations have confirmed that the Innovert mud provide a somewhat ECD midpoint, although skewed towards the Carbosea, between Warp and Carbosea.

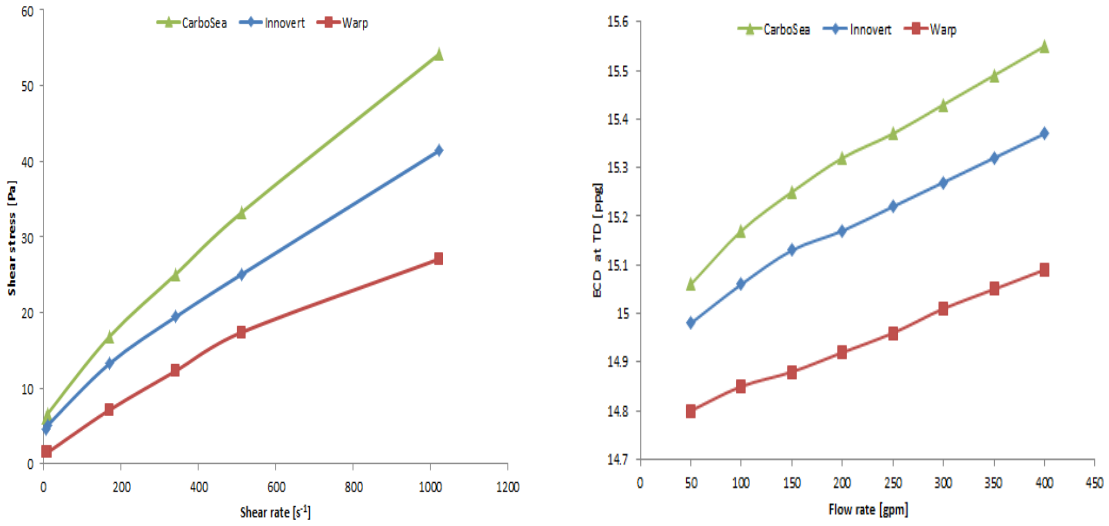

(a) Rheology comparison

(b) ECD comparison (power-law)

Figure 7.9: The Fann viscometer readings taken at 50°C for the Innovert, Warp and Carbosea mud systems (a). The simplified ECD calculations at TD for various flow rates (b) provide an indication of the ECD characteristics of the different mud systems. A mud weight of 14.7 ppg and a hole size of 12 1/4" have been assumed in the calculations.

7.3.5 Cement tweaks

Minor adjustments have been made in terms of cement characteristics and placement. Prior to drilling 2/8-G-3 T2 it was decided to design both the lead and tail cement at the same density to reduce the ECD. Traditionally the tail cement is of higher density than the lead cement. Density is positively correlated with the cement compressive strength. Hence, by pumping the tail slurry at the same density as the lead slurry the cement compressive strength at the bottom interval of the wellbore is decreased. The planned 2/8-G-3 T2 cement job included an interval of 882 mMD/570 mTVD of tail cement. Reducing the tail slurry density from 15.8 ppg to 15.0 ppg yield a net hydrostatic pressure reduction at TD of 78 psi or 0.18 ppg EMW.

Similarly, the 9 5/8" liner cement jobs have normally been planned with a TOC at the base of DPZ 7. Well 2/11-S-9 was cemented with a planned TOC approximately 330 mTVD below the base of DPZ 7. As a result, both the hydrostatic and frictional pressure components were decreased. In addition, it is desirable to avoid displacing the spacer fluid into the tight clearance between the ID of the 13 5/8" casing and the liner hanger/PBR. As the frictional pressure drop of the spacer is higher than of the mud (rheological hierarchy) the ECD will increase as the spacer fluid is displaced into the liner hanger area.

7.4 Liner setting depth

Due to reservoir compaction the stress state just above the reservoir is highly complex, especially in the crestal part of the field. To avoid potential loss zones, caused by stress changes due to subsidence, it was decided after the failure in well 2/8-N-9 T4 to set the 9 5/8" production liner shallower. The following cement job in well 2/8-N-9 T6 showed excellent zonal isolation and no losses as illustrated in Fig. 7.10. However, in well 2/8-G-1 the practice of setting the liner in the middle Eocene was continued, but the results were not as positive.

Major discussions have been ongoing regarding the optimal 9 5/8" liner setting depth. Whereas the Valhall IP engineering team chose to go back to the original design of setting the liner just above the reservoir (approx. 20 mTVD) prior to drilling 2/8-G-3, the Valhall Flank team decided to continue with the practice of setting the liner in the middle Eocene in well 2/11-S-9. A thorough review prior to drilling 2/11-S-9 highlighted that each well needs to treated separately, and at this stage a general field applicable solution in terms of 9 5/8" setting depth does not exist [66]. Nevertheless, the two most recent flank wells, 2/8-N-9 T6 and 2/11-S-9, have been cemented without losses when the liner has been set in the middle Eocene.

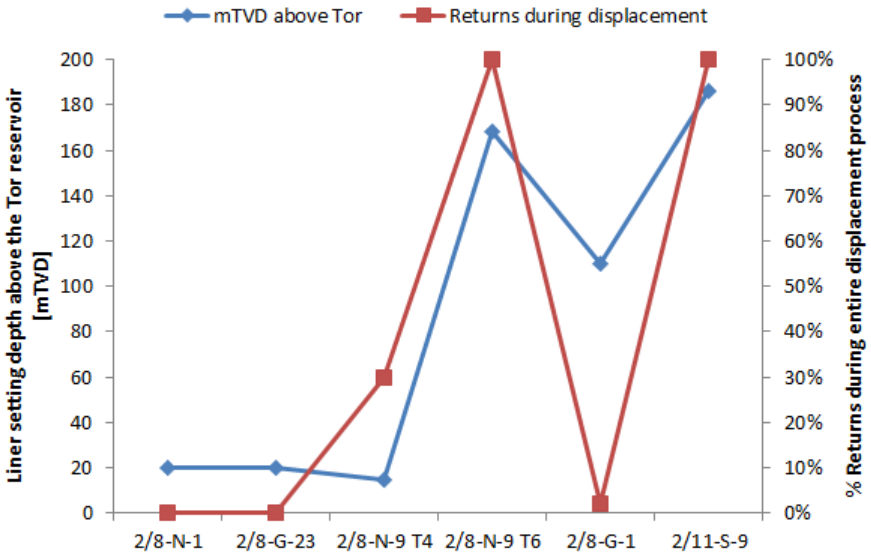

Figure 7.10: The vertical depth from the 9 5/8" liner setting depth to the top of Tor reservoir (blue) and percentage returns during displacement (red) plotted for each of the wells described in Chapter 6.

The main argument for a deep setting depth in the Sele formation is restoring the natural seal between DPZ 8 and the Tor reservoir. Future P&A operations will clearly benefit from a deep setting depth. As the 7 5/8" liner is drilled into the reservoir any reduction in the 9 5/8" liner setting depth will result in a correspondingly long uncemented interval. Furthermore, the shoe strength is stronger if the liner is set deep. Finally, by positioning the 9 5/8" liner shallower the 7 5/8" liner length will consequently increase. Hence, a deep setting depth minimize the ECD while drilling the reservoir section. Any reduction in ECD while drilling the reservoir section can result in an increased pay zone.

A shallow liner setting depth in the middle Eocene will decrease the 9 5/8" cementing ECD and reduce the risk of penetrating low stress zones near the reservoir. The formation strength at the shoe is also thought to be sufficiently high in the middle Eocene. In addition, a shorter liner string will decrease the torque required to initiate liner rotation. On the other hand, an increased risk of hydrocarbon migration due to less annular cement needs to be accounted for. As the distance between the 9 5/8" shoe and DPZ 8 is reduced, the length available to achieve 30 mTVD of circumferentially bonded cement is decreased.

No obvious correlation exists between the liner setting depth and returns during the cement job. Hence, it is difficult to determine the optimal 9 5/8" liner setting depth. It should be noted that a shallow setting depth proved successfull in well 2/8-N-9 T6 and 2/11-S-9. None of the 9 5/8" liners with a deep setting depth have been cemented without losses. However, as too few wells have been drilled and logged the data set carries a great uncertainty. Generally, many of the arguments for a deep liner setting depth quickly becomes invalid if a loss zone is penetrated near section TD. Hence, seismic and geological data should be thoroughly analysed to minimize the probability of penetrating faults, natural fractures and weak zones near the base of the section.

7.5 Centralization

The case histories show a gradual centralizer development from the rigid Weatherford Spiraglider centralizers to two different bow-type centralizers delivered by Centek. Firstly, 2/8-N-1 B and 2/8-G-23 were cemented using the rigid Spiraglider centralizers. Secondly, the liner in well 2/8-N-9 T4 was dressed with Slider II centralizers which improved standoff values as compared to the previous wells. Thirdly, well 2/8-N-9 T6 and 2/8-G-1 included a combination of the Slider II and UROS centralizers which showed perfect simulated centralization in some parts of the hole section. Finally, 2/11-S-9 was dressed only with UROS centralizers which showed close to perfect standoff in the entire interval of cement. It should be noted that the wellbore fluid assumptions have varied to some extent during the pre-job simulations. Cement outside and mud inside provide the most favourable situation due to maximum buoyance. Similarly, a situation of cement inside and mud outside provides the worst case scenario. In addition, a situation of mud both on the inside and outside of the liner has been applied. Which method is most correct is highly debatable. In all wells except for 2/8-N-1 B mud inside and outside were assumed to neglect any additional buoyance forces acting upon the liner string. The situation is not realistic, but as it

provides a midpoint between two extremes it has been granted acceptance. Unfortunately, the standoff simulation software cannot provide dynamic simulations as the different fluids enter the annulus.

From a general point of view the 9 5/8" liner centralization has been very good, especially after converting to the Slider II and UROS centralizers. There is no reason to believe that the centralization is a limitation in terms of cement quality and zonal isolation. However, if proper centralization is achieved one is less dependent upon high displacement rates to provide circumferentially bonded intervals of cement. The UROS centralizers also provide some safety margin in terms of centralizing over-gauged hole sections.

The centralizer concentration (i.e. number of centralizers per liner joint) has been varied as a result of the centralizer development. One centralizer per joint was installed in well 2/8-N-1 and 2/8-G-23, while two centralizers per joint was chosen in well 2/8-N-9 T4 and 2/8-N-9 T6. A combination of one and two centralizers were decided upon in well 2/8-G-1 and 2/11-S-9. Generally, if two centralizers are installed per joint one is less vulnerable if a centralizer is damaged while running in hole. Hence, one may benefit from installing two centralizers per joint in the bottom part of the liner string. On the other hand, the centralizers provide potential pack-off positions across the wellbore. No direct correlation between neither standoff nor centralizer concentration and cement quality is observed from the analysed data. As deep loss zones have been experienced in most of the wells any further analysis is difficult to perform. Probably the centralization across Valhall today is sufficient, and other parameters are more important for the outcome of the 9 5/8" liner cement jobs.

7.6 Mud systems

Mainly three different mud systems have been evaluated on Valhall, in addition to the traditional CarboSea OBM, to be able to deliver GP-10-60 compliant primary cement jobs. Synteq OBM was initially chosen, but due to increased torque and drag readings observed both in well 2/8-N-9 T4 and 2/8-N-9 T6 the choice of mud vendor was re-evaluated. Prior to drilling 2/8-G-1 the decision was taken to displace the wellbore to Warp OBM prior to running and cementing the 9 5/8" liner. Unfortunately, the displacement was aborted. After drilling the 12 1/4" section to TD in well 2/8-G-3 T2 the wellbore was successfully displaced from CarboSea to Warp. However, the 9 5/8" liner could not be run into the collapsed hole and the cement job was aborted.

Well 2/11-S-9 was drilled and cemented applying a Halliburton mud system in all hole sections, including the 12 1/4". The Innovert mud has very fragile gel-strengths which reduces the risk of cement channeling and excessive pressures when breaking circulation with the 9 5/8" liner in the hole. Rheology is managed through emulsifiers and fatty acids as opposed to the commonly used clay and lignite. The Innovert mud is a clay-free system and Halliburton reports this as the reason for the fragile, yet robust gel-strengths [67]. Although not as effective as Warp, the Innovert mud provide an ECD reduction as compared to CarboSea. The major advantage of the Innovert system is that it can be applied both during drilling and cementing. The time consuming displacement to a low rheology mud system is avoided. In addition,

spacer compatibility tests have shown that the Innovert mud system has desirable properties as compared to both Warp and CarboSea. A comparison of the CarboSea, Warp and Innovert mud systems is given in Table 7.2.

Table 7.2: Comparison of Carbosea, Warp and Innovert mud systems.

	CarboSea	Warp	Innovert
Hole cleaning	Good	Poor	Good
Gel-strengths	High	Low	High (fragile)
Displacement efficiency	Poor	Good	Average
ECD	High	Low	Average
Spacer compatibility	Poor	Average	Good
Good for drilling?	Yes	No	Yes
Good for cementing?	No	Yes	Yes

It should be noted that the best 9 5/8" liner primary cement job to date, 2/8-N-9 T6, was cemented in a thinned CarboSea OBM. In addition, the post-job stand-off simulations shown in Fig. 6.14 indicated a quite eccentric liner string. It is not fully understood why the cement job in well 2/8-N-9 T6 turned out as good as it did. If proper circulation prior to the cement job is achieved it may suggest that the CarboSea mud can be mobilized and applied without severe cement channeling. Nevertheless, both Warp and Innovert are beneficial from an ECD and displacement efficiency point of view.

7.7 Liner hangers

The liner hangers applied today on Valhall are delivered by Baker Oil Tools. A 12.8 m liner joint of varying outer diameters may at first sight seem like a neglectable source of pressure drop in the annulus, but due to the tight clearance between the ID of the 13 5/8" casing (12.375") and the OD of the PBR (12.01") the frictional pressure drop is significant. Kinetic pressure drops can be neglected. Assuming powerlaw fluid behaviour and that the smooth pipe turbulent friction factor is applicable one may calculate the frictional pressure drop applying the equations described in Section 4.4.5.

Equation (4.34) is solved iteratively and inputed in Eq. (4.24) taking the hydraulic diameter of the annulus into consideration. For simplicity the PBR is assumed to be 6m and the remaining 6.8m of the liner hanger joint is of an equivalent diameter of 11.7". The 14.7 ppg Innovert mud rheology at 50°C applied by Halliburton during the planning phase of well 2/8-G-3 T3 corresponds to a powerlaw index of 0.397 and a consistency index of 2.12 Pas^n. The frictional pressure drop across the liner hanger at a flow rate of 336 gpm is calculated to 52 psi (of which 42 psi is due to the PBR) or 0.12 ppg EMW at 2500 mTVD. It should be noted that the calculation is meant as an indication, proper simulations assuming a Herschel-Bulkley fluid should be performed for a more precise estimate.

To reduce the problem of high ECDs Halliburton delivers a low ECD expandable Versaflex hanger. The OD of the PBR is 11.91" during cementing. As a result, given the same assumptions as above, the pressure drop across the PBR is reduced from 7.0 psi/m to 3.8 psi/m. Due to some unsuccessful attempts of running the Versaflex liner hanger in well 2/8-N-16 the willingness to try the system again on Valhall has been reluctant. However, there are obvious advantages of trying to increase the flow area in terms of ECD reduction.

8 Lessons learned

The case histories described in Chapter 6 provide a valuable set of data, but the implemented initiatives to improve the 9 5/8" liner primary cement jobs are often observed to have both positive and negative effects. A gradual improvement has been observed from well 2/8-N-1 to the most recently cemented liner in well 2/11-S-9. However, a number of different possible solutions to the cementing challenges have been tested and evaluated. As several measures are tested at the same time it is difficult to quantify the effect of each element. The pros and cons of the main elements and the initiatives taken to improve the zonal isolation across Valhall are described in Chapter 7. A summary of the main parameters and results of the different 9 5/8" production liner cement jobs is given in Table 8.1.

Table 8.1: Summary of the main parameters affecting the six described 9 5/8" liner cement jobs. The gel-strengths (10sec/10min), YP and PV are given in $lb_f/100ft^2$, $lb_f/100ft^2$ and cP, respectively. The logged TOC and cumulative length of circumferential cement are used as indications of the success of the cement jobs. It is observed that deep losses have compromised the majority of the cement jobs.

Well	Mud system	Gel-strengths YP PV	Stand-off Rate Rotation	ECD reducing measures	TOC [mTVD]	Circumferential cement [mTVD]	Losses?	Failure mechanisms
2/8-N-1 B	CarboSea 14.8 ppg	15/27 27 54	64-86% 420 gpm No rotation	-	2330	27.3	Yes	- Channeling - Deep losses
2/8-G-23	CarboSea 14.6 ppg	18/27 24 38	69-80% 345 gpm 35 rpm	-	2184	250	Yes	- Deep losses
2/8-N-9 T4	Synteq 14.8 ppg	11/18 15 30	80% 165 gpm No rotation	- Low rheology mud - 14.4 ppg pre-flush	2490	0	Yes	- Channeling - Deep losses
2/8-N-9 T6	CarboSea 14.8 ppg	13/17 13 41	55-80% 330 gpm 30 rpm	- Shallow TD - Thinned mud - 14.4 ppg pre-flush	1674	587	No	-
2/8-G-1	CarboSea 14.6 ppg	14/18 21 37	60-100% 336 gpm 30 rpm	- Shallow TD - 6.8 ppg pre-flush	2389	15	Yes	- Deep losses
2/11-S-9	Innovert 14.7 ppg	11/26 16 31	60-100% 336 gpm 20 rpm	- Shallow TD - Underream to 13'' - IKM pump - Fragile gels - Deep TOC	1870	84	No	- Poor bonding (possibly microannulus)

From Table 8.1 it is observed that deep losses provide the most common failure mechanism. Furthermore, both wells in which initiation of liner rotation failed, 2/8-N-1 B and 2/8-N-9 T4, resulted in severe cement channeling. Liner rotation appears to be the main factor in terms of obtaining circumferential cement. The poor cement bonding seen in well 2/11-S-9 is not fully understood, but it may be due to the decreased annular velocities as a result of underreaming the hole section to 13". To reduce the probability of deep losses different measures, as described in Section 7.3, have been implemented. A quantification of the different ECD reducing measures are given in Table 8.2. It should be noted that the ECD reduction will vary from well to well, depending on its wellpath, well geometry and mud system. Table 8.2 provide an estimated ECD effect, and proper calculations given the available well data should be performed prior to each job. It is observed that cementing in Warp OBM is the option which yield the greatest ECD reduction. Applying the IKM pump, underreaming the section to 13" and cementing in Innovert are also important ECD reducing measures.

Table 8.2: Evaluation of the different ECD reducing measures discussed in Section 7.3. The ECD reduction from cementing in Warp and Innovert is compared to Carbosea. The data provide a rough estimate as the effect will vary from well to well. It should be noted that if one decides to cement in Warp mud, one would not get as high ECD reduction from underreaming or setting a shallow TD due to the low rheology characteristics of the mud.

Measure	**ECD reduction at TD [ppg]**
Pre-flush	0.1-0.4
IKM pump	0.1-0.2
Underream to 13"	0.2
Cement in Warp	0.3-0.5
Cement in Innovert	0.2
Shallow TD	0.1-0.2
Deep TOC	0.1
Low density tail cement	0.1-0.2
Versaflex liner hanger	< 0.1

Two matrixes are presented in Fig. 8.1 and Fig. 8.2 to classify and evaluate the main elements discussed throughout this thesis. The classification is a subjective, summarized interpretation of the case histories. The matrix shown in Fig. 8.1 shows the impact of each element evaluated against the contribution to a GP 10-60 compliant primary cement job. For example, displacing to Warp mud at TD provides a high impact and positive contribution due to its ECD and displacement efficiency characteristics. Similarly, losses prior to the cement job have proven to highly impact the outcome of the cement jobs in a negative direction.

Fig. 8.2 presents an evaluation of the probability of achieving the purpose of an element against its contribution to a GP 10-60 compliant cement job. For example, liner rotation has been successfully achieved in four out of the six case history wells which has mitigated the risk of cement channeling. Similarly, if total losses are encountered prior to the cement operations, the case histories clearly show that the probability of a successful cement job is low.

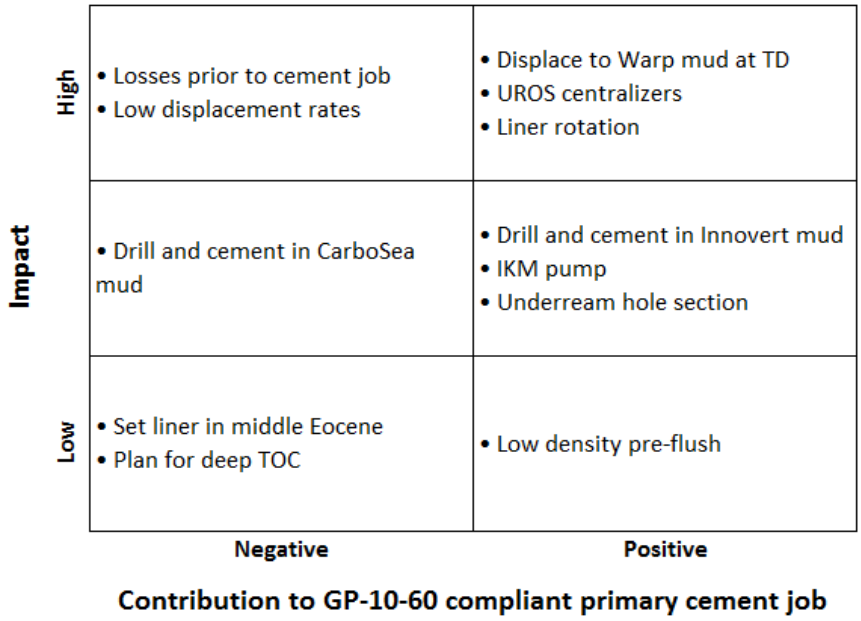

Figure 8.1: Matrix showing the main elements discussed in Chapter 7. Each element's contribution to a GP-10-60 compliant primary cement job is evaluated against its impact. Hence, for example to plan for a deep TOC is negative as the wellbore constitutes a significantly decreased interval of cement, but the impact is low as the planned TOC allows for a sufficient interval of cement above DPZ 8. The two upper right squares indicate the most desirable elements.

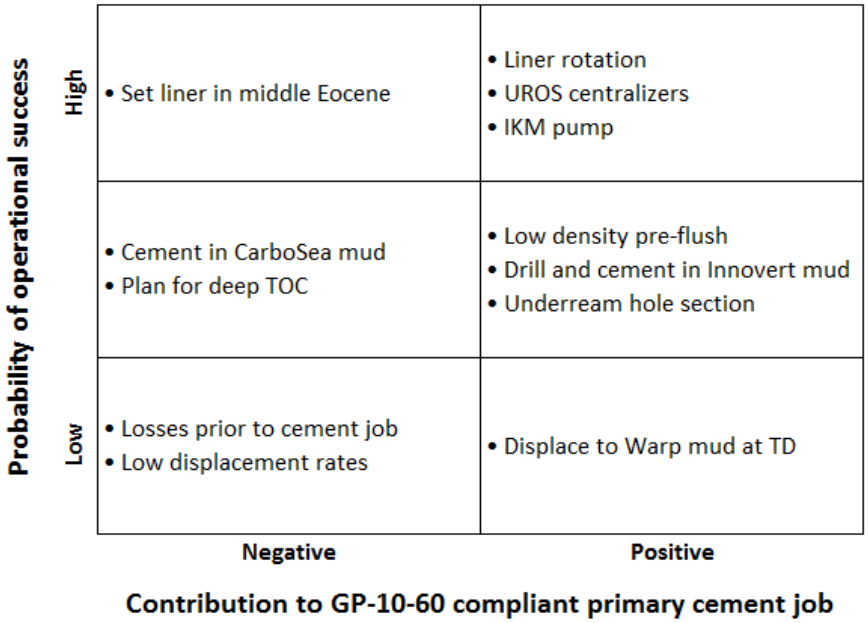

Figure 8.2: Matrix showing the main elements discussed in Chapter 7. Each element's contribution to a GP-10-60 compliant primary cement job is evaluated against the probability of actually achieving the purpose of the element. Hence, for example to set the liner in the middle Eocene is negative as the wellbore constitutes a significantly decreased interval of cement, but the probability of operational success is high given the outcome of the two latest flank wells. The two upper right squares indicate the most desirable elements.

Any decision taken provide a compromise between the two matrixes described in Fig. 8.1 and Fig. 8.2. One would ideally choose the elements which yield high impact and positive contribution to GP-10-60 compliant primary cement jobs. However, one needs to take the probability of actually achieving the purpose of the element into consideration. Displacing to a Warp OBM has proven unsuccessful in well 2/8-G-1 and 2/8-G-3, although the simulated impact is of very high value. Hence, the optimal elements in terms of obtaining a compliant primary cement job need to be present in the two upper right squares of both matrixes. As a result the most desirable elements in order to maximize the probability of a successful primary cement job are liner rotation, UROS centralisers, IKM pump, Innovert mud and underreaming the hole section to 13". If different options are, for any reason, needed one may evaluate the initiatives listed in the two upper left squares of the matrix described in Fig. 8.2.

Based upon the ECD simulations performed prior to each cement job one is lead to believe that one is well within the fracturing limits of the formations. However, whereas the formations tend to withstand the ECDs during drilling, running and cementing the liner often introduce losses. The surge pressure simulations when running the liner in hole could be too optimistic as it is difficult to determine the mud gel-strengths when it has been left static for a long period of time. It could also be beneficial to hold the cementing and liner running pressures against the minimum horizontal stress rather than the fracture gradient for more realistic estimates in faults, fractures and stringers. To reduce some of the uncertainties regarding the actual cementing pressures, it would be beneficial to apply a MPD system on Valhall. One would then be able to open up a larger hydraulic window which would reduce the risk of inducing downhole losses which could potentially compromise the entire cement job.

9 Conclusions

Cementing the 9 5/8" production liner on Valhall is highly complex, especially at the crestal part of the field. However, the six most recently drilled wells have indicated some key focal areas for future liner cement jobs.

- Currently the 9 5/8" liner cement jobs are performed within a laminar flow regime. If MPD is introduced to the Valhall field one could open up a hydraulic window which allows high enough displacement rates to get the spacer and mud into the transition zone between laminar and turbulent flow during the cement jobs.
- Liner rotation is the most important parameter in terms of obtaining circumferentially bonded cement given the available displacement rates.
- The ECD contribution from liner rotation at 30-40 rpm is negligible (<0.04 ppg as per Virtual Hydraulics simulations for well 2/8-G-3).
- If circulation cannot be established without total losses it is most likely that the loss zone is below, within or just above DPZ 8. No common loss zone has been identified from the case histories.
- The Warp mud provide the most desirable ECD characteristics, but Innovert also provide an ECD reduction as compared to CarboSea.
- Taking the outcome of the two collapsed wellbores in well 2/8-G-3 and the successful cement job on 2/11-S-9 into consideration it is at this point apparant that one should avoid a time consuming displacement to a low rheology mud at TD.
- Underreaming the hole section to 13" can be performed if the UROS centralizers are applied. At a displacement rate of 8 bpm the annular velocity is reduced from 0.73 m/s (144 ft/min) to 0.55 m/s (108 ft/min) if underreaming the hole section to 13". The liner hanger is a restriction in terms of increasing the displacement rates in an underreamed hole size.
- No correlation between centralization and intervals of circumferentially bonded cement has been identified. However, the centralization of the 9 5/8" production liner across Valhall today is in excess of the Halliburton cementing recommendations.
- No correlation between wellbore inclination and intervals of circumferentially bonded cement has been identified.

10 Recommendations

Based on the log results of the six cemented 9 5/8" liners described in Chapter 6 the following measures are recommended to maximize the probability of successful future production liner cement jobs:

- Liner rotation at 30-40 rpm should always be obtained prior to displacing the spacer and cement. If simulations indicate excessive torque values one should evaluate to set the liner in the middle Eocene to reduce the risk of stalling out.
- Underream hole section to 13" to reduce surge pressures, risk of getting stuck with liner and ECD during drilling and cementing.
- Displace the cement at a rate of 8 bpm (336 gpm). The displacement rate is a compromise between i) displacement efficiency and ii) formation fracture pressure.
- Apply a mud system which is designed both for drilling and cementing to avoid the time consuming displacement to a new, cold mud system at TD. Currently, the Innovert mud is the most viable option.
- Avoid excessive circulation at TD if the shakers and ECD trend indicate that the hole is clean. This will reduce the time it takes to get the liner in the hole and reduce the risk of washing out the wellbore.
- Draw down the riser liquid level applying the IKM centrifugal pump. If further ECD reduction is desired one should evaluate to pump a low density pre-flush. Hold the equivalent static density above the collapse curve if applying a pre-flush.
- Apply a combination of one and two UROS 13 1/2" centralizers per joint. Stand-off simulations in excess of 90% should be expected even when opening the hole to 13".
- If a very tight ECD window is encountered one should evaluate to pump lead/tail at same density and/or plan for a deeper TOC (similar to what was done in well 2/11-S-9).
- In case of lost circulation events, do not continue drilling until the fracture has been healed/properly evaluated. It may be difficult at a later stage to determine where the losses actually are occuring if several thief zones are penetrated.
- The mud LCM concentration should be maintained at a minimum of 5 ppb throughout the section to artifically strengthen the formation strength.
- For future 9 5/8" jobs on Valhall one should evaluate use a MPD technique to open up a hydraulic window which allows for signficantly higher displacement rates.

Nomenclature

Abbreviations

BHA	=	Bottom hole assembly
BOD	=	Basis of design
bpm	=	Barrels per minute
CBL	=	Cement bond log
CRT	=	Casing running tool
DDM	=	Derrick drilling machine
DDR	=	Daily drilling report
DOE	=	Drilling optimization engineer
DOP	=	Drilling operation plan
DP	=	Drill pipe
DPZ	=	Distinct permeable zone
ECD	=	Equivalent circulating density
EMW	=	Equivalent mud weight
EOWR	=	End of well report
FG	=	Fracture gradient
FIT	=	Formation integrity test
GC	=	Gas cloud
GP	=	Group practice
gpm	=	Gallon per minute
ID	=	Inner diameter
IMM	=	Intra middle Miocene
LCM	=	Lost circulation material
LOT	=	Leak-off test
MD	=	Measured depth
MMBOE	=	Million barrels oil equivalents
MPD	=	Managed pressure drilling
MW	=	Mud weight
NCS	=	Norwegian continental shelf
NMR	=	Nuclear magnetic resonance
NPD	=	Norwegian Petroleum Directorate
OBM	=	Oil based mud
OD	=	Outer diameter
P&A	=	Plug and abandonment
PBR	=	Polished bore receptacle
POOH	=	Pull out of hole
PPFG	=	Pore pressure - Fracture gradient
ppg	=	Pounds per gallon
PV	=	Plastic viscosity
PWD	=	Pressure while drilling
RAP	=	Rig action plan
RIH	=	Run in hole
rpm	=	Revolutions per minute
SBT	=	Segmented bond tool
TD	=	Total depth
TOC	=	Top of cement

Abbreviations

TVD	=	True vertical depth
TVDBRT	=	True vertical depth below rotary table
USIT	=	Ultra sonic imager tool
WBM	=	Water based mud
XLOT	=	Extended leak-off test
YP	=	Yield point

Symbols

A	=	Cross sectional pipe area
A_L	=	Fluid wetted cross sectional area
D_{avg}	=	Average hole diameter
D	=	Pipe diameter
D_i	=	Inner diameter
D_H	=	Hydraulic diameter
D_o	=	Outer diameter
$E(t)$	=	Displacement efficiency at a given time
F	=	Force
f_F	=	Fanning friction factor
K	=	Power-law consistency index
L	=	Wellbore length
L_{min}	=	Minimum distance between casing and formation wall
N	=	Rotating speed
n	=	Power-law index
R	=	Pipe radius
r	=	Distance r from the center of the pipe
P_{hydr}	=	Hydrostatic pressure component of dynamic fluid
P_{kin}	=	Kinetic pressure component of dynamic fluid
P_{fric}	=	Frictional pressure component of dynamic fluid
P_{tot}	=	Dynamic fluid pressure
P_0	=	Pore pressure
P_{wc}	=	Collapse pressure
P_{wf}	=	Fracture pressure
Q	=	Volumetric flow rate
Re	=	Reynold's number
Re_{pl}	=	Reynold's number in concentric annuli for power-law fluids
S	=	Pipe circumference
s	=	Stand-off ratio
S_L	=	Total fluid wetted circumference
U	=	Average fluid velocity
u_{max}	=	Maximum fluid velocity (centerline velocity)
$u(r)$	=	Velocity at a distance r away from the center of the pipe
V	=	Sound propagation velocity
x	=	Length of wellbore
y	=	Distance from pipe wall to point of interest (y=R-r)
Z	=	Acoustic impedance

Greek symbols

γ	=	Wellbore inclination
$\dot{\gamma}$	=	Shear rate
$\dot{\gamma}_w$	=	Wall shear rate
ϕ	=	Angle of internal friction
σ	=	Normal stress
$\sigma^{'}$	=	Effective stress
σ_h	=	Minimum horizontal in-situ stress
σ_H	=	Maximum horizontal in-situ stress
σ_v	=	Overburden in-situ stress
$\sigma_r, \sigma_\theta, \sigma_z$	=	Wellbore stresses cylindrical coordinates
$\sigma_x, \sigma_y, \sigma_z$	=	Wellbore stresses cartesian coordinates
τ	=	Shear stress
τ_0	=	Cohesive rock strength
τ_y	=	Yield shear stress
τ_w	=	Wall shear stress
μ	=	Viscosity
μ_p	=	Plastic viscosity
ρ	=	Fluid density

References

[1] B. Piot and G. Cuvillier, "Primary cementing techniques," in *Well Cementing: Second Edition*, E. B. Nelson and D. Guillot, Eds. Sugar Land, Texas, Schlumberger, 2006, ch. 13, pp. 459–500.

[2] *Zonal isolation*, BP Engineering Technical Standard GP 10-60, 2012.

[3] T. G. Kristiansen *et al.*, "Drilling wellbore stability in the compacting and subsiding Valhall field: A case study," *SPE Drilling & Completion*, vol. 22, no. 04, pp. 277–295, 2007.

[4] O. Barkved *et al.*, "Valhall field-still on plateau after 20 years of production," *Offshore Europe*, 2003.

[5] N. O. B. Njå, "P&A of Valhall DP wells," Master's thesis, University of Stavanger, Norway, 2012.

[6] *Valhall and Hod well history book*, BP internal, 2012.

[7] B. Rasen, *Valhall 25 år- og det er bare begynnelsen.* Wigestrand Forlag, Stavanger, 2007.

[8] J. Duncan, "Valhall stratigraphic framework," *BP Norge, Stavanger*, internal document, 2013.

[9] P. Heavey, "Valhall overburden and DPZ introduction," Personal communication, February 2014.

[10] L. T. Vika *et al.*, "Drilling Operation Plan 2/8-G-1," BP internal, 2013.

[11] E. Skaugen, "Introduction to Drilling," Lecture: Drilling, 2009.

[12] L. T. Vika *et al.*, "Basis of Design 2/8-G-1," BP internal, 2013.

[13] B. S. Aadnoy and R. Looyeh, *Petroleum Rock Mechanics: Drilling Operations and Well Design.* Elsevier, Amsterdam, 2011.

[14] R. Sant and J. Zhang, "Lost circulation mitigation class," BP internal, March 2014.

[15] S. Wilson and J. Zhang, "Wellbore stability handbook: A guide to assure a stable wellbore," BP America, Tech. Rep., 2008.

[16] B. S. Aadnoy *et al.*, "Quality assurance of wellbore stability analyses," in *SPE/IADC Drilling Conference and Exhibition.* Society of Petroleum Engineers, 2011.

[17] M. McLean, M. Addis *et al.*, "Wellbore stability: The effect of strength criteria on mud weight recommendations," in *SPE Annual Technical Conference and Exhibition.* Society of Petroleum Engineers, 1990.

[18] A. J. White, M. O. Traugott, and R. E. Swarbrick, "The use of leak-off tests as means of predicting minimum in-situ stress," *Petroleum Geoscience*, vol. 8, no. 2, pp. 189–193, 2002.

[19] D. Okland *et al.*, "The importance of extended leak-off test data for combatting lost circulation," in *SPE/ISRM Rock Mechanics Conference*. Society of Petroleum Engineers, 2002.

[20] T. G. Kristiansen, "Valhall rock mechanics," Personal communication, BP Norge, Stavanger, May 2014.

[21] J. E. Finnemore and F. J. B, *Fluid Mechanics with Engineering Applications*, 10th ed. McGraw Hill, New York, 2009.

[22] R. Time, *Two-phase flow in pipelines*. University of Stavanger, 2009, ch. 2: Definitions and basic quantities, pp. 11–39.

[23] O. Skjeggestad, *Boreslamteknologi: Teori og praksis*. Alma Mater, 1989.

[24] B. Dargaud and L. Boukhelifa, "App. B: Laboratory testing, evaluation and analysis of well cements," in *Well Cementing: Second Edition*, E. B. Nelson and D. Guillot, Eds. Sugar Land, Texas, Schlumberger, 2006, pp. 627–657.

[25] D. Guillot, "Rheology and flow of well cement slurries," in *Well Cementing: Second Edition*, E. B. Nelson and D. Guillot, Eds. Sugar Land, Texas, Schlumberger, 2006, ch. 4, pp. 93–142.

[26] R. Time, *Two-phase flow in pipelines*. University of Stavanger, 2009, ch. 3: Single phase flow hydrodynamics, pp. 41–64.

[27] Schlumberger. (Read: 24.02.2014) Oilfield Glossary. [Online]. Available: www.glossary.oilfield.slb.com/en

[28] (Read: 1.3.2014) Bernoulli's principle. [Online]. Available: http://avstop.com/ac/Aviation_Maintenance_Technician_Handbook_General/3-32.html

[29] UiS. (Read: 24.02.2014) Lecture notes petroleum drilling 411: Laminar flow. [Online]. Available: http://www1.uis.no/Fag/Learningspace_kurs/PetBachelor/webpage/tech%5Cdrilling%5CLamFlowSlotFlow.ppt

[30] K. Founargiotakis, V. Kelessidis, and R. Maglione, "Laminar, transitional and turbulent flow of Herschel–Bulkley fluids in concentric annulus," *The Canadian Journal of Chemical Engineering*, vol. 86, no. 4, pp. 676–683, 2008.

[31] A. W. Iyoho *et al.*, "An accurate slot-flow model for non-Newtonian fluid flow through eccentric annuli," *Society of Petroleum Engineers Journal*, vol. 21, no. 05, pp. 565–572, 1981.

[32] L. K. Moran *et al.*, "Fluid movement measurements through eccentric annuli: unique results uncovered," in *SPE Annual Technical Conference and Exhibition*. Society of Petroleum Engineers, 2007.

[33] M. A. Silva *et al.*, "Friction pressure correlations of Newtonian and non-Newtonian fluids through concentric and eccentric annuli," *SPE/ICoTA Coiled Tubing Roundtable*, 2000.

[34] E. B. Nelson and M. Michaux, "Chemistry and characterization of Portland cement," in *Well Cementing: Second Edition*, E. B. Nelson and D. Guillot, Eds. Sugar Land, Texas, Schlumberger, 2006, ch. 2, pp. 23–48.

[35] E. B. Nelson, M. Michaux, and B. Drochon, "Cement additives and mechanisms of action," in *Well Cementing: Second Edition*, E. B. Nelson and D. Guillot, Eds. Sugar Land, Texas, Schlumberger, 2006, ch. 3, pp. 49–91.

[36] Weatherford. (Read: 26.02.2014) Casing wiper plugs and darts. [Online]. Available: http://www.weatherford.com/dn/WFT235047

[37] I. Byberg, "Liner hanger systems," Personal communication, Baker Hughes, Stavanger, February 2014.

[38] C. Sauer *et al.*, "Mud displacement during cementing state of the art," *Journal of Petroleum Technology*, vol. 39, no. 09, pp. 1–091, 1987.

[39] A. Sanchez, C. F. Brown, and W. Adams, "Casing centralization in horizontal and extended reach wells," in *SPE/EAGE European Unconventional Resources Conference & Exhibition-From Potential to Production*, 2012.

[40] G. Liu *et al.*, "Centralizer selection and placement optimization," in *SPE Deepwater Drilling and Completions Conference*. Society of Petroleum Engineers, 2012.

[41] E. Leugemors *et al.*, "Cementing equipment and casing hardware," in *Well Cementing: Second Edition*, E. B. Nelson and D. Guillot, Eds. Sugar Land, Texas, Schlumberger, 2006, ch. 11, pp. 343–434.

[42] Schlumberger. (Read: 03.03.2014) Oilfield Glossary: Casing centralizer. [Online]. Available: www.glossary.oilfield.slb.com/en

[43] G. Daccord, D. Guillot, and F. Nilsson, "Mud removal," in *Well Cementing: Second Edition*, E. B. Nelson and D. Guillot, Eds. Sugar Land, Texas, Schlumberger, 2006, ch. 5, pp. 143–149.

[44] A. Tehrani *et al.*, "Laminar displacement in annuli: A combined experimental and theoretical study," in *SPE Annual Technical Conference and Exhibition*. Society of Petroleum Engineers, 1992.

[45] S. Bittleston, J. Ferguson, and I. Frigaard, "Mud removal and cement placement during primary cementing of an oil well–laminar non-newtonian displacements in an eccentric annular Hele-Shaw cell," *Journal of engineering mathematics*, vol. 43, no. 2-4, pp. 229–253, 2002.

[46] M. Couturler *et al.*, "Design rules and associated spacer properties for optimal mud removal in eccentric annuli," in *CIM/SPE International Technical Meeting*. Society of Petroleum Engineers, 1990.

[47] L. Delabroy, "Displacement mechanisms," Personal communication, BP Norge, Stavanger, May 2014.

[48] R. Van Zanten *et al.*, "Using surfactant nanotechnology to engineer displacement packages for cementing operations," in *IADC/SPE Drilling Conference and Exhibition*. Society of Petroleum Engineers, 2010.

[49] H. Gai *et al.*, "Zonal isolation and evaluation for cemented horizontal liners," in *International meeting on petroleum engineering*, 1995, pp. 287–296.

[50] N. Moroni *et al.*, "Pipe rotation improves hole cleaning and cement-slurry placement: Mathematical modeling and field validation," *Offshore Europe*, 2009.

[51] T. Hemphill *et al.*, "A simplified method for prediction of ECD increase with drillpipe rotation," in *SPE Annual Technical Conference and Exhibition*. Society of Petroleum Engineers, 2008.

[52] A. Asko, "Virtual Hydraulics software," Personal communication, MI Swaco, Stavanger, March 2014.

[53] Halliburton. (Read: 05.03.2014) Spacers and flushes. [Online]. Available: http://www.halliburton.com/en-US/ps/cementing/materials-chemicals-additives/spacers-and-flushes/default.page?node-id=hfqelagh

[54] G. Daccord, D. Guillot, and S. James, "Remedial cementing," in *Well Cementing: Second Edition*, E. B. Nelson and D. Guillot, Eds. Sugar Land, Texas, Schlumberger, 2006, ch. 14, pp. 503–548.

[55] G. Lende, "Advanced cementing series: Challenges for long term zonal isolation," Personal communication, Halliburton, Stavanger, May 2014.

[56] M. Allouche *et al.*, "Cement evaluation," in *Well Cementing: Second Edition*, E. B. Nelson and D. Guillot, Eds. Sugar Land, Texas, Schlumberger, 2006, ch. 15, pp. 549–612.

[57] E. L. Bigelow, *Cement evaluation guidelines*. Baker Hughes, Houston, 2006.

[58] G. J. Frisch *et al.*, "Advances in cement evaluation tools and processing methods allow improved interpretation of complex cements," in *SPE Annual Technical Conference and Exhibition*. Society of Petroleum Engineers, 2005.

[59] D. A. Boyd *et al.*, "Reliability of cement bond log interpretations compared to physical communication tests between formations," in *Abu Dhabi International Petroleum Exhibition and Conference*. Society of Petroleum Engineers, 2006.

[60] J. M. Ferkingstad *et al.*, "End of well report 2/8-N-1," BP internal, 2013.

[61] BP, "Daily drilling reports Valhall IP and Valhall Flank North," BP internal, 2012-2014.

[62] N. O. B. Njå *et al.*, "End of well report 2/8-G-23," BP internal, 2013.

[63] J. M. Ferkingstad *et al.*, "End of well report 2/8-N-9," BP internal, 2013.

[64] N. O. B. Njå *et al.*, "End of well report 2/8-G-1," BP internal, 2014.

[65] I. Cameron, “Fracture gradient and LCM strategy,” Personal communication, BP Norge, Stavanger, April 2014.

[66] D. Meyer, “9 5/8” liner setting depth recommendation,” BP internal, 2014.

[67] Halliburton. (Read: 28.04.2014) Innovert high performance paraffin/mineral oil-based fluids from Baroid. [Online]. Available: http://www.halliburton.com/public/bar/contents/Data_Sheets/web/Sales_Data_Sheets/H06024.pdf